

# User's Guide: Estimation of Key PCC, Base, Subbase, and Pavement Engineering Properties from Routine Tests and Physical Characteristics

PUBLICATION NO. FHWA-HRT-12-031

AUGUST 2012



U.S. Department of Transportation  
**Federal Highway Administration**

Research, Development, and Technology  
Turner-Fairbank Highway Research Center  
6300 Georgetown Pike  
McLean, VA 22101-2296



## FOREWORD

Material characterization is a basic aspect of pavement engineering and is critical for analysis, performance prediction, design, construction, quality control/quality assurance, pavement management, and rehabilitation. Advanced tools like the American Association of State Highway and Transportation Officials *Mechanistic-Empirical Pavement Design Guide, Interim Edition: A Manual of Practice*, commonly known as the MEPDG, can be used to estimate the influence of several fundamental engineering material parameters on the long-term performance of a pavement.<sup>(1)</sup> Consequently, there is a great need for more information about material properties, which are addressed only to a limited extent with currently available resources for performing laboratory and field testing. Reliable correlations between material parameters and index properties offer a cost-effective alternative, and the derived material property values are equivalent to the level 2 inputs in the MEPDG. This study initially verified data adequacy in the Long-Term Pavement Performance (LTPP) database and also involved retrieving needed data.<sup>(2)</sup> In the next phase of the study, prediction models were developed to help practicing engineers estimate proper MEPDG inputs. This report describes the basis for selecting material parameters that need predictive models, provides a review of current LTPP program data, and proposes several statistically derived models to predict material properties. The models developed under this effort have been incorporated into a simple software program compatible with current versions of Microsoft Windows<sup>®</sup> operating system.

Jorge E. Pagán-Ortiz  
Director, Office of Infrastructure  
Research and Development

### Notice

This document is disseminated under the sponsorship of the U.S. Department of Transportation in the interest of information exchange. The U.S. Government assumes no liability for the use of the information contained in this document. This report does not constitute a standard, specification, or regulation.

The U.S. Government does not endorse products or manufacturers. Trademarks or manufacturers' names appear in this report only because they are considered essential to the objective of the document.

### Quality Assurance Statement

The Federal Highway Administration (FHWA) provides high-quality information to serve Government, industry, and the public in a manner that promotes public understanding. FHWA uses standards and policies are used to ensure and maximize the quality, objectivity, utility, and integrity of its information. It also periodically reviews quality issues and adjusts its programs and processes to ensure continuous quality improvement.

## TECHNICAL REPORT DOCUMENTATION PAGE

1. Report No. FHWA-HRT-12-031	2. Government Accession No.	3. Recipient's Catalog No.	
4. Title and Subtitle User's Guide: Estimation of Key PCC, Base, Subbase, and Pavement Engineering Properties from Routine Tests and Physical Characteristics		5. Report Date August 2012	
		6. Performing Organization Code	
7. Author(s) C. Rao, L. Titus-Glover, B. Bhattacharya, and M.I. Darter		8. Performing Organization Report No.	
9. Performing Organization Name and Address Applied Research Associates, Inc. 100 Trade Centre Drive, Suite 200 Champaign, IL 61820		10. Work Unit No. (TRAIS)	
		11. Contract or Grant No. DTFH61-02-C-00138	
12. Sponsoring Agency Name and Address Office of Infrastructure Research and Development Federal Highway Administration 6300 Georgetown Pike McLean, VA 22101-2296		13. Type of Report and Period Covered Interim Report	
		14. Sponsoring Agency Code	
15. Supplementary Notes The Contracting Officer's Technical Representative (COTR) was Larry Wiser, HRDI LTPP data analysis contract.			
16. Abstract Material characterization is a critical component of modern day pavement analysis, design, construction, quality control/quality assurance, management, and rehabilitation. At each stage during the life of a project, the influence of several fundamental engineering material parameters on the long-term performance of the pavement can be predicted using advanced tools like the American Association of State Highway and Transportation Officials <i>Mechanistic-Empirical Pavement Design Guide</i> (MEPDG). Consequently, there is a need for more information about material properties, which are addressed only to a limited extent with currently available resources for performing laboratory and field testing. Reliable correlations between material parameters and index properties offer a cost-effective alternative and are equivalent to the level 2 MEPDG inputs. The Long-Term Pavement Performance (LTPP) database provides data suitable for developing predictive models for Portland cement concrete (PCC) materials, stabilized materials, and unbound materials, as well as other design-related inputs for the MEPDG. This user's guide provides a summary of the models developed, describes their applications for specific project conditions, and lists their limitations. The following models are included: <ul style="list-style-type: none"> <li>• PCC materials: Compressive strength, flexural strength, elastic modulus, tensile strength, and coefficient of thermal expansion.</li> <li>• Stabilized materials: Elastic modulus of lean concrete base.</li> <li>• Unbound materials: Resilient modulus of fine-grained and coarse-grained materials.</li> <li>• Rigid pavement design features: Pavement curl/wrap effective temperature difference for jointed plain concrete pavement and continuously reinforced concrete pavement designs.</li> </ul>			
17. Key Words Pavements, LTPP, material properties, MEPDG, prediction model, Index properties		18. Distribution Statement No restrictions. This document is available to the public through the National Technical Information Service, Springfield, VA 22161.	
19. Security Classification (of this report) Unclassified	20. Security Classification (of this page) Unclassified	21. No. of Pages 86	22. Price

# SI\* (MODERN METRIC) CONVERSION FACTORS

## APPROXIMATE CONVERSIONS TO SI UNITS

Symbol	When You Know	Multiply By	To Find	Symbol
<b>LENGTH</b>				
in	inches	25.4	millimeters	mm
ft	feet	0.305	meters	m
yd	yards	0.914	meters	m
mi	miles	1.61	kilometers	km
<b>AREA</b>				
in <sup>2</sup>	square inches	645.2	square millimeters	mm <sup>2</sup>
ft <sup>2</sup>	square feet	0.093	square meters	m <sup>2</sup>
yd <sup>2</sup>	square yard	0.836	square meters	m <sup>2</sup>
ac	acres	0.405	hectares	ha
mi <sup>2</sup>	square miles	2.59	square kilometers	km <sup>2</sup>
<b>VOLUME</b>				
fl oz	fluid ounces	29.57	milliliters	mL
gal	gallons	3.785	liters	L
ft <sup>3</sup>	cubic feet	0.028	cubic meters	m <sup>3</sup>
yd <sup>3</sup>	cubic yards	0.765	cubic meters	m <sup>3</sup>
NOTE: volumes greater than 1000 L shall be shown in m <sup>3</sup>				
<b>MASS</b>				
oz	ounces	28.35	grams	g
lb	pounds	0.454	kilograms	kg
T	short tons (2000 lb)	0.907	megagrams (or "metric ton")	Mg (or "t")
<b>TEMPERATURE (exact degrees)</b>				
°F	Fahrenheit	5 (F-32)/9 or (F-32)/1.8	Celsius	°C
<b>ILLUMINATION</b>				
fc	foot-candles	10.76	lux	lx
fl	foot-Lamberts	3.426	candela/m <sup>2</sup>	cd/m <sup>2</sup>
<b>FORCE and PRESSURE or STRESS</b>				
lbf	poundforce	4.45	newtons	N
lbf/in <sup>2</sup>	poundforce per square inch	6.89	kilopascals	kPa

## APPROXIMATE CONVERSIONS FROM SI UNITS

Symbol	When You Know	Multiply By	To Find	Symbol
<b>LENGTH</b>				
mm	millimeters	0.039	inches	in
m	meters	3.28	feet	ft
m	meters	1.09	yards	yd
km	kilometers	0.621	miles	mi
<b>AREA</b>				
mm <sup>2</sup>	square millimeters	0.0016	square inches	in <sup>2</sup>
m <sup>2</sup>	square meters	10.764	square feet	ft <sup>2</sup>
m <sup>2</sup>	square meters	1.195	square yards	yd <sup>2</sup>
ha	hectares	2.47	acres	ac
km <sup>2</sup>	square kilometers	0.386	square miles	mi <sup>2</sup>
<b>VOLUME</b>				
mL	milliliters	0.034	fluid ounces	fl oz
L	liters	0.264	gallons	gal
m <sup>3</sup>	cubic meters	35.314	cubic feet	ft <sup>3</sup>
m <sup>3</sup>	cubic meters	1.307	cubic yards	yd <sup>3</sup>
<b>MASS</b>				
g	grams	0.035	ounces	oz
kg	kilograms	2.202	pounds	lb
Mg (or "t")	megagrams (or "metric ton")	1.103	short tons (2000 lb)	T
<b>TEMPERATURE (exact degrees)</b>				
°C	Celsius	1.8C+32	Fahrenheit	°F
<b>ILLUMINATION</b>				
lx	lux	0.0929	foot-candles	fc
cd/m <sup>2</sup>	candela/m <sup>2</sup>	0.2919	foot-Lamberts	fl
<b>FORCE and PRESSURE or STRESS</b>				
N	newtons	0.225	poundforce	lbf
kPa	kilopascals	0.145	poundforce per square inch	lbf/in <sup>2</sup>

\*SI is the symbol for the International System of Units. Appropriate rounding should be made to comply with Section 4 of ASTM E380.  
(Revised March 2003)

## TABLE OF CONTENTS

<b>CHAPTER 1. INTRODUCTION</b> .....	<b>1</b>
<b>BACKGROUND</b> .....	<b>1</b>
<b>DATA NEEDS</b> .....	<b>1</b>
Design .....	2
Construction.....	2
Pavement Management.....	4
<b>SCOPE</b> .....	<b>4</b>
<b>CHAPTER 2. MODEL DEVELOPMENT</b> .....	<b>7</b>
<b>LIST OF MODELS</b> .....	<b>8</b>
<b>PRACTICAL GUIDE AND SOFTWARE PROGRAM</b> .....	<b>10</b>
<b>CHAPTER 3. PCC MODELS</b> .....	<b>11</b>
<b>PCC COMPRESSIVE STRENGTH MODELS</b> .....	<b>11</b>
Compressive Strength Model 1: 28-day Cylinder Strength Model .....	12
Compressive Strength Model 2: Short-Term Cylinder Strength Model.....	14
Compressive Strength Model 3: Short-Term Core Strength Model .....	17
Compressive Strength Model 4: All Ages Core Strength Model .....	21
Compressive Strength Model 5: Long-Term Core Strength Model .....	24
Relative Comparison of All Compressive Strength Models.....	25
<b>PCC FLEXURAL STRENGTH MODELS</b> .....	<b>29</b>
Validation of Existing Models .....	29
Flexural Strength Model 1: Flexural Strength Based on Compressive Strength.....	30
Flexural Strength Model 2: Flexural Strength Based on Age, Unit Weight, and w/c Ratio .....	33
Flexural Strength Model 3: Flexural Strength Based on Age, Unit Weight, and CMC ...	35
<b>PCC ELASTIC MODULUS MODELS</b> .....	<b>38</b>
Validation of Existing Models .....	38
Elastic Modulus Model 1: Model Based on Aggregate Type.....	40
Elastic Modulus Model 2: Model Based on Age and Compressive Strength.....	42
Elastic Modulus Model 3: Model Based on Age and 28-Day Compressive Strength.....	43
Limitations of Elastic Modulus Models.....	45
<b>PCC TENSILE STRENGTH MODELS</b> .....	<b>45</b>
PCC Tensile Strength Model Based on Compressive Strength .....	45
<b>PCC CTE MODELS</b> .....	<b>47</b>
Current Issue with CTE Overestimation in LTPP Data.....	47
CTE Model 1: CTE Based on Aggregate Type (Level 3 Equation for MEPDG) .....	48
CTE Model 2: CTE Based on Mix Volumetrics (Level 2 Equation for MEPDG).....	49
<b>CHAPTER 4. RIGID PAVEMENT DESIGN FEATURES MODELS</b> .....	<b>53</b>
<b>DELTA T—JPCP DESIGN</b> .....	<b>53</b>
Using the JPCP <i>deltaT</i> Model.....	59
<b>DELTA T—CRCP DESIGN</b> .....	<b>60</b>
Using the CRCP <i>deltaT</i> Model .....	64

<b>CHAPTER 5. STABILIZED MATERIALS MODELS .....</b>	<b>65</b>
<b>LCB ELASTIC MODULUS MODEL .....</b>	<b>65</b>
<b>CHAPTER 6. UNBOUND MATERIALS MODELS .....</b>	<b>67</b>
<b>RESILIENT MODULUS OF UNBOUND MATERIALS .....</b>	<b>67</b>
Constitutive Model Parameter $k_1$ .....	67
Constitutive Model Parameter $k_2$ .....	67
Constitutive Model Parameter $k_3$ .....	68
<b>REFERENCES.....</b>	<b>75</b>

## LIST OF FIGURES

Figure 1. Illustration. MEPDG performance prediction during the design and construction stage .....	3
Figure 2. Screenshot. View of <i>Correlations</i> user interface .....	10
Figure 3. Equation. Prediction model 1 for $f_{c,28d}$ .....	12
Figure 4. Graph. Predicted versus measured for 28-day cylinder compressive strength model...	13
Figure 5. Graph. Residual error plot for 28-day cylinder compressive strength model .....	13
Figure 6. Graph. 28-day compressive strength model sensitivity to w/c ratio .....	14
Figure 7. Graph. 28-day compressive strength model sensitivity to CMC.....	14
Figure 8. Equation. Prediction model 2 for $f_{c,t}$ .....	14
Figure 9. Graph. Predicted versus measured for short-term cylinder compressive strength model.....	15
Figure 10. Graph. Residual errors for short-term cylinder compressive strength model .....	16
Figure 11. Graph. Short-term cylinder compressive strength sensitivity to CMC .....	16
Figure 12. Graph. Short-term cylinder compressive strength sensitivity to w/c ratio .....	16
Figure 13. Graph. Short-term cylinder compressive strength sensitivity to age.....	17
Figure 14. Equation. Prediction model 3 for $f_{c,t}$ .....	17
Figure 15. Graph. Predicted versus measured for short-term core compressive strength model.....	18
Figure 16. Graph. Residual errors for short-term core compressive strength model.....	18
Figure 17. Graph. Short-term core compressive strength sensitivity to CMC.....	19
Figure 18. Graph. Short-term core compressive strength sensitivity to unit weight .....	19
Figure 19. Graph. Short-term core compressive strength sensitivity to MAS .....	19
Figure 20. Graph. Short-term core compressive strength sensitivity to w/c ratio .....	20
Figure 21. Graph. Short-term core compressive strength sensitivity to fine aggregate FM.....	20
Figure 22. Graph. Short-term core compressive strength sensitivity to age .....	20
Figure 23. Equation. Prediction model 4 for $f_{c,t}$ .....	21
Figure 24. Graph. Predicted versus measured for all ages core compressive strength model .....	22
Figure 25. Graph. Residual errors for all ages core compressive strength model .....	22
Figure 26. Graph. All ages core compressive strength sensitivity to w/c ratio .....	23
Figure 27. Graph. All ages core compressive strength sensitivity to CMC.....	23
Figure 28. Graph. All ages core compressive strength sensitivity to unit weight .....	23
Figure 29. Graph. All ages core compressive strength sensitivity to age .....	24
Figure 30. Equation. Prediction model 5 for $f_{c,LT}$ .....	24
Figure 31. Graph. Predicted versus measured for long-term core compressive strength model ..	25
Figure 32. Graph. Residual errors for long-term core compressive strength model.....	25
Figure 33. Graph. Model compressive strength prediction for varying CMC.....	26
Figure 34. Graph. Model compressive strength prediction for varying w/c ratio.....	26
Figure 35. Graph. Model compressive strength prediction for varying unit weights .....	27
Figure 36. Graph. Strength gain in the short-term predicted by three models.....	27
Figure 37. Graph. Long-term strength gain predicted by the models .....	28
Figure 38. Equation. $M_r$ .....	29
Figure 39. Graph. Predicted versus measured for validating 0.5 power flexural strength model.....	30

Figure 40. Graph. Predicted versus measured for validating 0.667 power flexural strength model.....	30
Figure 41. Equation. Prediction model 6 for $MR_t$ .....	30
Figure 42. Graph. Predicted versus measured values for flexural strength model based on compressive strength.....	31
Figure 43. Graph. Residual errors for flexural strength model based on compressive strength...	32
Figure 44. Graph. Comparison of flexural strength models based on compressive strength .....	33
Figure 45. Equation. Prediction model 7 for $MR_t$ .....	33
Figure 46. Graph. Predicted versus measured values for flexural strength model based on age, unit weight, and w/c ratio .....	34
Figure 47. Graph. Residual errors for flexural strength model based on age, unit weight, and w/c ratio.....	35
Figure 48. Equation. Prediction model 8 for $MR_t$ .....	35
Figure 49. Graph. Predicted versus measured values for flexural strength model based on age, unit weight, and CMC .....	36
Figure 50. Graph. Residual errors for flexural strength model based on age, unit weight, and CMC.....	36
Figure 51. Graph. Sensitivity of flexural strength predictions to CMC.....	37
Figure 52. Graph. Sensitivity of flexural strength predictions to w/c ratio .....	37
Figure 53. Graph. Sensitivity of flexural strength predictions to unit weight .....	38
Figure 54. Graph. Sensitivity of flexural strength predictions to age.....	38
Figure 55. Equation. $E_c$ as a function of square root of compressive strength .....	38
Figure 56. Equation. Model form for $E$ as a function of compressive strength with slope and intercept.....	39
Figure 57. Equation. $E_c$ .....	39
Figure 58. Equation. $E$ as function of unit weight and compressive strength .....	39
Figure 59. Equation. Prediction model 9 for $E_c$ .....	40
Figure 60. Graph. Predicted versus measured for elastic modulus model based on aggregate type .....	41
Figure 61. Graph. Residual errors for elastic modulus model based on aggregate type.....	41
Figure 62. Equation. Prediction model 10 for $E_{c,t}$ .....	42
Figure 63. Graph. Predicted versus measured for elastic modulus model based on age and compressive strength.....	43
Figure 64. Graph. Residual errors for elastic modulus model based on age and compressive strength.....	43
Figure 65. Equation. Prediction model 11 for $E_{c,t}$ .....	43
Figure 66. Graph. Predicted versus measured for elastic modulus model based on age and 28-day compressive strength.....	44
Figure 67. Graph. Residual errors for elastic modulus model based on age and 28-day compressive strength.....	45
Figure 68. Equation. Prediction model 12 for $f_t$ .....	45
Figure 69. Graph. Predicted versus measured for tensile strength model .....	46
Figure 70. Graph. Residual errors plot for tensile strength model.....	46
Figure 71. Graph. Sensitivity of tensile strength prediction model to change compressive strength.....	47

Figure 72. Graph. Comparison of average values from other sources and recommended CTE values based on aggregate type from LTPP data .....	49
Figure 73. Equation. Prediction model 14 for $CTE_{PCC}$ .....	49
Figure 74. Graph. Predicted versus measured for CTE model based on mix volumetrics .....	50
Figure 75. Graph. Residual errors for CTE model based on mix volumetrics .....	50
Figure 76. Graph. Comparison of CTE model prediction with average values reported in literature for each aggregate rock type.....	51
Figure 77. Graph. CTE model prediction versus average values reported in literature for each aggregate rock type .....	51
Figure 78. Graph. Sensitivity of the CTE model to coarse aggregate content.....	52
Figure 79. Equation. Prediction model 15 for $\delta T/\text{inch}$ .....	53
Figure 80. Graph. Predicted versus measured for JPCP $\delta T$ gradient model.....	54
Figure 81. Graph. Residual errors for JPCP $\delta T$ gradient model .....	55
Figure 82. Graph. Predicted versus measured $\delta T$ based on the JPCP $\delta T$ gradient model.....	55
Figure 83. Graph. Sensitivity of predicted $\delta T$ to temperature range during month of construction.....	56
Figure 84. Graph. Sensitivity of predicted $\delta T$ to slab width.....	56
Figure 85. Graph. Sensitivity of predicted $\delta T$ to slab thickness .....	56
Figure 86. Graph. Sensitivity of predicted $\delta T$ to PCC slab unit weight .....	57
Figure 87. Graph. Sensitivity of predicted $\delta T$ to PCC w/c ratio.....	57
Figure 88. Graph. Sensitivity of predicted $\delta T$ to latitude of the project location .....	57
Figure 89. Graph. Predicted $\delta T$ for different locations in the United States .....	58
Figure 90. Equation. Prediction model 16 for $\delta T/\text{inch}$ .....	60
Figure 91. Graph. Predicted versus measured for CRCP $\delta T$ model .....	61
Figure 92. Graph. Residual errors for CRCP $\delta T$ model.....	62
Figure 93. Graph. Effect of maximum temperature on CRCP $\delta T$ prediction model .....	62
Figure 94. Graph. Effect of temperature range on CRCP $\delta T$ prediction model .....	63
Figure 95. Graph. Effect of slab thickness on CRCP $\delta T$ prediction model.....	63
Figure 96. Graph. Effect of geographic location on CRCP $\delta T$ prediction model.....	63
Figure 97. Equation. Prediction model 17 for $E_{LCB}$ .....	65
Figure 98. Graph. Predicted versus measured for the LCB elastic modulus model .....	65
Figure 99. Graph. Residual errors for the LCB elastic modulus model .....	66
Figure 100. Equation. $M_r$ .....	67
Figure 101. Equation. Prediction model 18 for $k_1$ .....	67
Figure 102. Equation. Prediction model 19 for $k_2$ .....	67
Figure 103. Equation. Prediction model 20 for $k_3$ .....	68
Figure 104. Graph. Resilient modulus parameter $k_1$ for unbound material types included in the model development database .....	68
Figure 105. Graph. Resilient modulus parameter $k_2$ for unbound material types included in the model development database .....	69
Figure 106. Graph. Resilient modulus parameter $k_3$ for unbound material types included in the model development database .....	69
Figure 107. Graph. Plot of measured versus predicted resilient modulus (using $k_1$ , $k_2$ , and $k_3$ derived from figure 101 through figure 103).....	70

Figure 108. Graph. Plot showing predicted and measured resilient modulus versus bulk stress for fine- and coarse-grained soils.....	70
Figure 109. Graph. Effect of material type (AASHTO soil class) on predicted resilient modulus.....	71
Figure 110. Graph. Effect of percent passing $\frac{1}{2}$ -inch sieve on predicted resilient modulus .....	72
Figure 111. Graph. Effect of liquid limit on predicted resilient modulus.....	72
Figure 112. Graph. Effect of optimum moisture content on predicted resilient modulus .....	73
Figure 113. Graph. Effect of No. 80 sieve on predicted resilient modulus .....	73
Figure 114. Graph. Effect of gravel content on predicted resilient modulus.....	74
Figure 115. Graph. Effect of effective size on predicted resilient modulus .....	74

## LIST OF TABLES

Table 1. Regression statistics for selected prediction model for 28-day PCC cylinder strength.....	12
Table 2. Range of data used for 28-day PCC cylinder strength.....	12
Table 3. Regression statistics for short-term cylinder strength model.....	15
Table 4. Range of data used for short-term cylinder strength model.....	15
Table 5. Regression statistics for short-term core strength model.....	17
Table 6. Range of data used for short-term core strength model.....	18
Table 7. Regression statistics for all ages core strength model .....	21
Table 8. Range of data used for all ages core strength model .....	21
Table 9. Regression statistics for long-term core strength model.....	24
Table 10. Range of data used for long-term core strength model.....	24
Table 11. Power models developed for flexural strength prediction using LTPP data for validation.....	29
Table 12. Regression statistics for flexural strength model based on compressive strength.....	31
Table 13. Range of data used for flexural strength model based on compressive strength.....	31
Table 14. Regression statistics for flexural strength model based on age, unit weight, and w/c ratio.....	34
Table 15. Range of data used for flexural strength model based on age, unit weight, and w/c ratio.....	34
Table 16. Regression statistics for flexural strength model based on age, unit weight, and CMC.....	35
Table 17. Range of data used for flexural strength model based on age, unit weight, and CMC.....	36
Table 18. Range of data used for elastic modulus model based on aggregate type.....	41
Table 19. Regression statistics for elastic modulus model based on age and compressive strength.....	42
Table 20. Range of data used for elastic modulus model based on age and compressive strength.....	42
Table 21. Regression statistics for elastic modulus model based on age and 28-day compressive strength.....	44
Table 22. Range of data used for elastic modulus model based on age and 28-day compressive strength.....	44
Table 23. Model statistics for tensile strength prediction model .....	46
Table 24. Range of data used for tensile strength prediction model.....	46
Table 25. Prediction model 13 for PCC CTE based on aggregate type, $\times 10^{-6}$ inch/inch/ $^{\circ}$ F.....	48
Table 26. Statistical analysis results for CTE model based on mix volumetrics .....	49
Table 27. Range of data used for CTE model based on mix volumetrics .....	50
Table 28. Regression statistics for JPCP <i>deltaT</i> model .....	54
Table 29. Range of data used for JPCP <i>deltaT</i> model .....	54
Table 30. Regression statistics for CRCP <i>deltaT</i> model.....	60
Table 31. Range of data used for CRCP <i>deltaT</i> model.....	61



## CHAPTER 1. INTRODUCTION

### BACKGROUND

Material characterization is vital to pavement analyses and has received increasing focus as it forms a critical component in recent improvements to engineering practices. This pertains to all aspects of pavement engineering—analysis, design, construction, quality control/quality assurance (QC/QA), pavement management, and rehabilitation. At each stage during the life of a project, the influence of several fundamental engineering material parameters on the long-term performance of the pavement has been recognized. There is a greater emphasis for optimizing the performance of concrete pavements, which involves a detailed understanding of the variables that affect pavement behavior and the properties of concrete that correspond to the desired performance.

Consequently, there is a need for more information about material properties so that they can be characterized accurately for predicting performance or for verifying their quality during the construction phase. With limited resources for performing laboratory and field tests to determine material properties, the need for a secondary means to obtain these material property values (i.e., through correlations or predictive models based on data from routine or less expensive tests) is obvious. Additionally, the American Association of State Highway and Transportation Officials (AASHTO) *Mechanistic-Empirical Pavement Design Guide, Interim Edition: A Manual of Practice* (MEPDG) offers users the option of using inputs obtained through correlations.<sup>(1)</sup> The MEPDG defines level 2 inputs as those obtained from correlations between the primary inputs (level 1 measured) and other parameters that are material-specific or are measured through simpler tests. The Long-Term Pavement Performance (LTPP) database provides an excellent source of information to develop these correlations using material properties of field sections.<sup>(2)</sup>

The current report addresses critical data needs for design, construction, and pavement management operations under the LTPP Data Analysis Technical Support contract. This project focuses on developing predictive models to estimate Portland cement concrete (PCC) and unbound material properties using LTPP data.

### DATA NEEDS

Material property data needs in the context of this study are grouped into the following three categories:

- Inputs during the design stage.
- QC/QA during construction.
- Scheduling maintenance and rehabilitation in a pavement management program.

## Design

In both empirical and mechanistic-empirical design systems, material property inputs are essential to characterize pavement behavior and to predict pavement responses, such as the magnitudes of stress, strain, and displacement when subjected to applied traffic loads and environmental conditions. Furthermore, major pavement distresses are associated directly with the material properties of a component (or layer) of the pavement structure. For example, in jointed plain concrete pavements (JPCPs), transverse cracking is influenced by PCC flexural strength. Faulting can be related to the erodibility of the underlying base/subbase material. Punchout development in continuously reinforced concrete pavements (CRCs) can be related to PCC tensile strength.

The MEPDG, developed under National Cooperative Highway Research Program (NCHRP) Project 1-37A and subsequently improved under NCHRP 1-40D, allows users to model the effects of project-specific climate, traffic loads, materials, design features, and construction practices mechanistically to predict pavement performance based on distress models calibrated with LTPP field sections.<sup>(3,4)</sup> The MEPDG is considered a significant improvement over current pavement design procedures, and it received the status of an AASHTO interim standard in November 2007. The publication *User Manual and Local Calibration Guide for the Mechanistic-Empirical Pavement Design Guide and Software* developed under NCHRP Project 1-40B provides guidance to State highway agencies (SHAs) that are considering implementing the MEPDG.<sup>(5)</sup> It is expected that SHAs will adopt locally calibrated distress models that are representative of their specific materials and design conditions.

The need for a variety of material inputs is being recognized as agencies evaluate the MEPDG and streamline efforts for implementation. They continue to face challenges in estimating material parameter inputs and understanding their impact on pavement performance. For example, agencies do not have measured test data or access to databases and the necessary engineering expertise to develop correlations for their needs. Furthermore, due to a lack of familiarity with several input categories, they have come to rely on default values to characterize their typical materials. These default parameters are often a gross approximation of the true value, which may lead to erroneous distress and International Roughness Index (IRI) predictions. As another example, the permanent curl/warp gradient in the national calibration was set at -10 °F through the slab because it was not possible to obtain an accurate value for this parameter, which depends on construction-related conditions. Analysis of selected LTPP data made it possible to derive an improved way to estimate this important input for design.

This study provides much needed procedures to obtain several inputs and provide correlations to determine the range of material properties based on routine test results and physical characteristics. These correlations will supplement the *User Manual and Local Calibration Guide for the Mechanistic-Empirical Pavement Design Guide and Software* to support MEPDG implementation efforts.<sup>(5)</sup>

## Construction

Pavement construction practices are being continually enhanced for faster and more efficient processes. In addition, new materials and material types are being introduced. For example,

cement compositions and cement types have changed considerably over the years, resulting in PCC properties and durability characteristics different from the past.

The current focus of QC/QA procedures is on identifying more reliable and faster QC/QA tests and determining material properties that are related directly to performance. The MEPDG enables performance prediction of the as-built pavement in addition to that of the as-designed pavement as long as deviations from design assumptions (i.e., material properties or construction practices such as curing or temperature during construction) are identified during the construction process (see figure 1). For example, although the density of an unbound material is a good indicator of construction quality, the more fundamental resilient modulus is an indicator of performance and is a key input to the MEPDG. The ability to predict resilient modulus from index properties measured during construction will make the QA process address both construction quality and pavement performance issues. Note that in figure 1, material properties measured during construction can be used to predict performance in the field and may be different from the design/target performance.

Also, performance-related specifications (PRSs) for concrete pavements have been developed in recent years. Irick et al., under a Federal Highway Administration (FHWA) study to demonstrate a PRS system for rigid pavement construction, considered three key performance indicators: PCC strength, PCC slab thickness, and initial serviceability.<sup>(6)</sup> Several relationships for the prediction of PCC properties were evaluated under this study. PRSs have also been implemented on several projects that required many correlations between pavement properties and performance.<sup>(7,8)</sup>

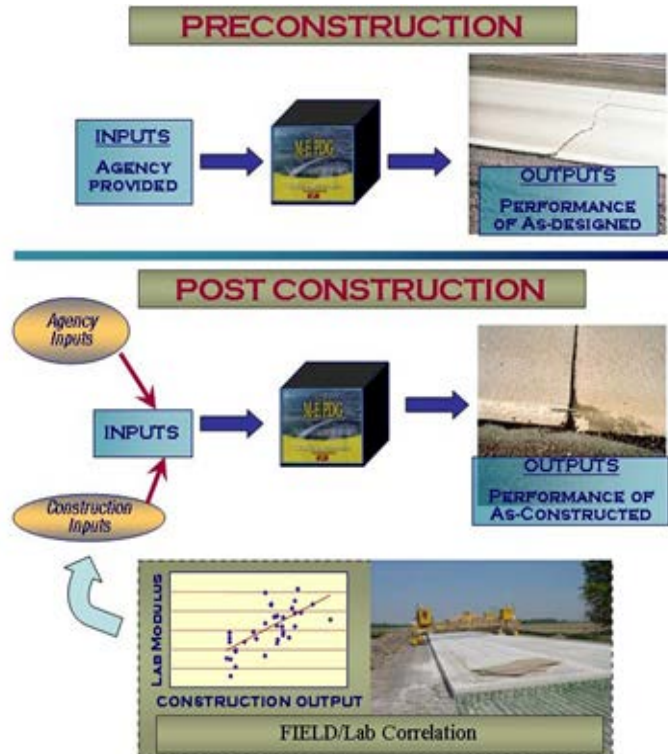


**Figure 1. Illustration. MEPDG performance prediction during the design and construction stage.**

This study will bridge the gaps in current knowledge regarding the estimation of more fundamental material parameters that influence performance-based index properties or other commonly measured properties during construction.

## **Pavement Management**

One of the key needs in managing pavements is an estimation of remaining life. Several SHAs use this parameter to program rehabilitation treatments. Various models (including the MEPDG models) are useful here in that they can be utilized to predict the remaining life until critical levels of each distress and IRI are reached. Also, agencies are now considering the integration of construction quality databases with pavement management databases to track the effect of design and construction quality on long-term performance. Such efforts lend themselves to more accurate performance predictions, whereby the performance of the as-constructed pavement can be used for scheduling maintenance and rehabilitation programs (see figure 1). However, many model inputs are needed related to the existing pavement, including inputs to characterize materials accurately. Index properties from construction QA data can be used to predict fundamental material properties that are related to performance.

In summary, the MEPDG provides a tool to specify material characteristics during the design and construction processes to achieve desired performance. The same models used in the MEPDG for design and construction analyses can be used in the future management of the pavement to estimate its remaining structural and functional life. For example, the inputs for a 10-year-old pavement could be measured from the existing pavement and estimated from the MEPDG models to project future slab cracking. The curve can be adjusted to match today's actual performance to improve the prediction. The slab cracking curve can be projected into the future to determine when it reaches a critical value to estimate its remaining life. The same could be done with joint faulting and IRI.

Therefore, the design, construction, and pavement management stages share a common need for determining a variety of material properties based on correlations from index properties and/or properties determined from more routine test procedures. This practice has been used in past AASHTO pavement design procedures and likely will increase in the future due to the more complex fundamental inputs required for the MEPDG procedure.

## **SCOPE**

This user's guide provides a summary of the material property relationships that were developed through correlations to index properties. Also included are relationships for the prediction of the permanent curl/warp equivalent temperature difference, commonly referred to as  $\Delta T$ , in rigid pavement design. A detailed research report prepared under this study is available as a separate publication.<sup>(9)</sup>

SHAs can use these correlations to characterize material and design parameters as necessary for design, QC/QA, and pavement management. Most of the data used in the development of prediction models to estimate material properties were obtained from the LTPP *Long-Term Pavement Performance Standard Data Release 23.0*.<sup>(10)</sup> Since these correlations are based on actual data from LTPP and field calibration sections used in the development of MEPDG distress

prediction models, they are more reliable than default or typical values currently being used. This full potential of the MEPDG to predict performance accurately can be realized by providing more accurate input values to the procedure. These models can also help improve material specifications for use in pavement construction, particularly for PRSs.

Chapter 2 of this user's guide provides general comments on the analyses performed in developing the models so that users understand the validity of the models presented in this guide. Each material type is then discussed in a separate chapter. Models for PCC materials, MEPDG design features, stabilized materials, and unbound materials are included in chapters 3 through 6, respectively. For each predictive model, the following are included:

- The mathematical relationship.
- Model statistics.
- Plots showing the quality of prediction (predicted versus measured and residual error plots).
- Plots showing the sensitivity of each model parameter.



## CHAPTER 2. MODEL DEVELOPMENT

The LTPP study database, *Long-Term Pavement Performance Standard Data Release Version 23.0*, was used to develop the models.<sup>(10)</sup> Material properties and pavement engineering properties for which develop predictive models were developed were selected based on the following:

- Material inputs requirements for the MEPDG design procedure and the sensitivity of the specific parameter for performance prediction.
- Typical agency needs for determining material properties during QA.
- Typical agency needs for determining material properties during routine pavement management functions.
- Data availability in the LTPP database.

Predictive models were developed for PCC compressive strength, PCC flexural strength, PCC elastic modulus, PCC tensile strength, lean concrete base (LCB) modulus, and unbound materials resilient modulus. In addition, rigid pavement design feature inputs properties were developed using the MEPDG calibration data. These include the JPCP and CRCP *deltaT* parameters. For all PCC material properties, multiple models were developed for use in different project situations and to provide user prediction model alternatives depending on the extent of mix design information available.

In developing the models, a uniform set of statistical criteria were used to select independent parameters to define a relationship as well as to mathematically formulate prediction functions. The analyses examined several statistical parameters in choosing the optimal model and in determining the predictive ability of the model. In general, the optimal set of independent variables (Mallows coefficient,  $C_p$ ), the interaction effects (variance inflation factor (VIF)), the significance of the variable ( $p$ -value), and the goodness of fit ( $R^2$ ) were verified. Additionally, the study validated or refined existing models and developed new relationships. In the analyses, the following general observations were made:

- PCC compressive strength could be correlated to several index properties. It was found to increase with decreasing water/cementitious (w/c) ratio, increasing cementitious materials content (CMC), increasing curing time, increasing unit weight, decreasing maximum aggregate size (MAS) for a given level of w/c ratio, and decreasing fineness modulus (FM) of the sand.
- PCC flexural strength could be correlated to the compressive strength using a power model. These relationships were validated and refined using the LTPP data. It also could be correlated to the w/c ratio, unit weight, CMC, and curing time. The correlation was improved significantly in the new models with the additional parameters. The flexural strength increased proportionally with all parameters listed except w/c ratio, with which it had an inverse relationship.

- PCC elastic modulus could be correlated to the compressive strength and unit weight using a power model, as has been done in past studies. These relationships were validated and verified with the data used in this study. Predictions could be made based on aggregate type, unit weight, compressive strength, and age with improved correlation. The elastic modulus increases with an increase in magnitude of all parameters listed.
- PCC tensile strength was found to correlate well with the compressive strength using a power relationship.
- The coefficient of thermal expansion (CTE) of PCC was most sensitive to the coarse aggregate type and the volumetrics of the mix design.
- JPCP  $\Delta T$  negative gradient was found to increase with an increase in temperature range at the project location for the month of construction and slab width and with a decrease in PCC thickness, unit weight, w/c ratio, and latitude of the project location.
- CRCP  $\Delta T$  negative gradient was found to increase with an increase in maximum temperature at the project location for the month of construction and maximum temperature range and decrease with the use of chert, granite, limestone, and quartzite.
- The modulus of LCB was found to correlate well with its 28-day compressive strength based on a power model.
- The prediction of resilient modulus was possible using parameters  $k_1$ ,  $k_2$ , and  $k_3$  of the constitutive model as follows:
  - The parameter  $k_1$  was found to increase with a decrease in percent passing the  $\frac{1}{2}$ -inch sieve, an increase in liquid limit, and a decrease in optimum moisture content.
  - The parameter  $k_2$  was found to increase with a decrease in percent passing the No. 80 sieve, liquid limit, and percent gravel and an increase in the maximum particle size of the smallest 10 percent of the soil sample.
  - The parameter  $k_3$  was dependent on the soil classification (coarse-grained versus fine-grained materials).

## LIST OF MODELS

The following models have been developed under this study.

PCC compressive strength models include the following:

- Compressive strength model 1: 28-day cylinder strength model.
- Compressive strength model 2: Short-term cylinder strength model.
- Compressive strength model 3: Short-term core strength model.

- Compressive strength model 4: All ages core strength model.
- Compressive strength model 5: Long-term core strength model.

PCC flexural strength models include the following:

- Flexural strength model 1: Flexural strength based on compressive strength.
- Flexural strength model 2: Flexural strength based on age, unit weight, and w/c ratio.
- Flexural strength model 3: Flexural strength based on age, unit weight, and CMC.

PCC elastic modulus models include the following:

- Elastic modulus model 1: Model based on aggregate type.
- Elastic modulus model 2: Model based on age and compressive strength.
- Elastic modulus model 3: Model based on age and 28-day compressive strength.

The PCC indirect tensile strength model is as follows:

- PCC indirect tensile strength model: Model based on compressive strength.

PCC CTE models include the following:

- CTE model 1: CTE based on aggregate type (level 3 equation for MEPDG).
- CTE model 2: CTE based on mix volumetrics (level 2 equation for MEPDG).

The JPCP design  $\Delta T$  model is as follows:

- JPCP  $\Delta T$  model: JPCP  $\Delta T$  gradient based on temperature range, slab width, slab thickness, PCC unit weight, w/c ratio, and latitude.

The CRCP design  $\Delta T$  model is as follows:

- CRCP  $\Delta T$  model: CRCP  $\Delta T$  gradient based on maximum temperature, maximum temperature range, and aggregate type.

The LCB elastic modulus model is as follows:

- Elastic modulus model: Elastic modulus based on 28-day compressive strength.

The unbound materials resilient modulus is as follows:

- Resilient modulus model: Resilient modulus using constitutive model based on gradation, Atterberg limits, optimum moisture content, and soil classification.

## PRACTICAL GUIDE AND SOFTWARE PROGRAM

The models described in this user's guide have been incorporated into a user friendly software program, *Correlations*, which was developed under this study and can be used independently from the MEPDG. The software was developed on the Microsoft.NET platform to be compatible with the latest versions of the Microsoft Windows® operating systems. It uses a modern user interface library to provide a familiar look and feel. It features multiple windows on the user interface that are initially docked inside the main window. These windows can be moved separately from the main window for better viewing of the inputs or results.

The program interface features tabs for PCC, design features, stabilized materials, and unbound materials. Models that belong to each of these categories are made available through a series of radio button selections placed in an accordion control. This placement not only provides the ability to make multiple selections, but it also conserves screen space so that the results of the calculations can be placed for easy viewing. Once a model is selected, the entry area adds controls for the available inputs of the model. Figure 2 shows a screenshot of the program and displays the various tabs and general layout of the user interface.

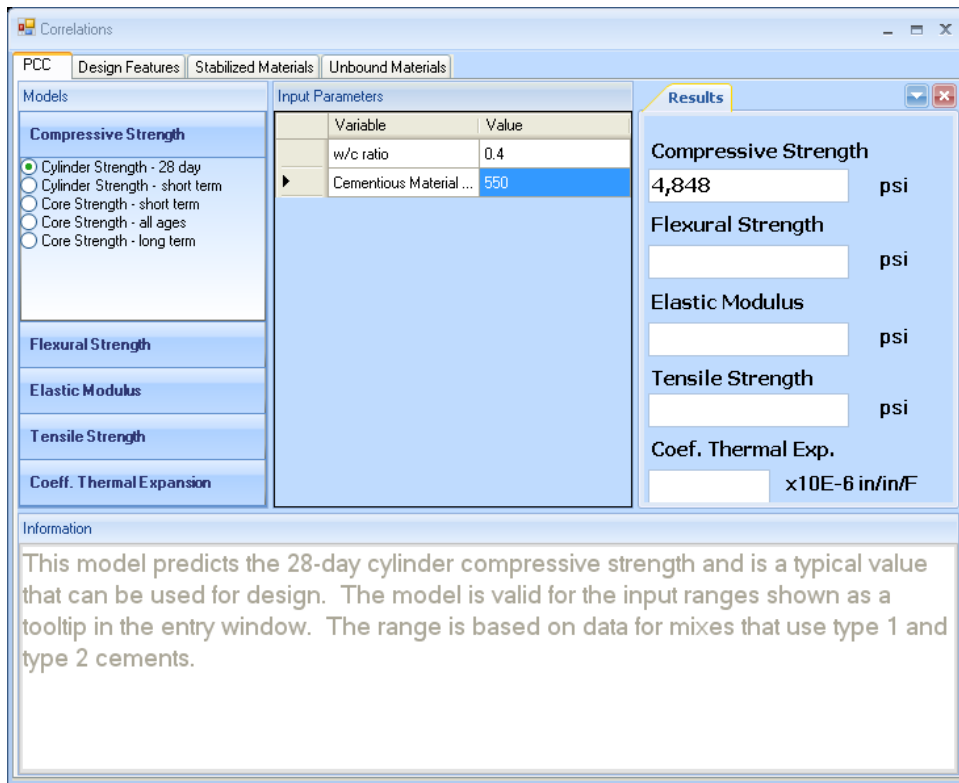


**Figure 2. Screenshot. View of *Correlations* user interface.**

On all screens of the software, tooltips are provided for feedback on input range. Calculations occur after all necessary values have been input. Information about each model is available in an information window initially located at the bottom of the screen. This information is context-sensitive to the specific selections that the software user has made. Results of each calculation are displayed prominently in the results area window initially placed on the right side of the main window.

## CHAPTER 3. PCC MODELS

Prediction models were developed for PCC compressive strength, PCC flexural strength, PCC elastic modulus, PCC tensile strength, and CTE. The following limitations apply to all PCC models:

- A fundamental limitation for any model is that the relationship that exists between the predicted parameter and the regressors is only valid for the range of data that has been included in the dataset. Furthermore, the statistical modeling procedures for the most part assume that the variables are normally distributed within the dataset. For example, the relationships developed for PCC properties, (e.g., compressive strength prediction model) are applicable only for mixes with cement types 1 and 2. While one data point with type 3 cement exists in the database (a JRCP section) compared to 500 data sets with type 1 and type 2 cements, the strength gain pattern of a type 3 cement is clearly outcompeted by the other 2 cement types in the database. As a result, it might not be evident within this dataset that type 3 cements produce higher strengths, especially in the early ages.
- The model will reflect the intrinsic trends of the dataset used. For example, the data used for prediction of the 28-day compressive strength contains target low-strength and high-strength mix designs. If the primary means of achieving higher strengths for the States was to increase the cement content, the model will show a high correlation between the CMC and strength. However, there are multiple ways to enhance mix compressive strength, such as the use of lower w/c ratios, water-reducing agents, higher-strength aggregates, curing at higher temperatures and insulation, and use of type 3 cements. This is critical when the prediction models are implemented for estimating material properties.

### PCC COMPRESSIVE STRENGTH MODELS

Compressive strength is considered a fundamental strength parameter and is used at different stages of a project—design, QA, opening time, rehabilitation design, etc. The following models are offered for PCC compressive strength, each of which is discussed in subsections to follow:

- Compressive strength model 1: 28-day cylinder strength model (suitable for estimating design strength).
- Compressive strength model 2: Short-term cylinder strength model (suitable for estimating opening time).
- Compressive strength model 3: Short-term core strength model (suitable for in situ strength and opening time).
- Compressive strength model 4: All ages core strength model (suitable for estimating in situ strength at any age).
- Compressive strength model 5: Long-term core strength model (suitable for estimating long-term strength for rehabilitation design).

### Compressive Strength Model 1: 28-day Cylinder Strength Model

The 28-day compressive strength model developed for cylinder strength is as follows:

$$f_{c,28d} = 4028.41841 - 3486.3501 * w/c + 4.02511 * CMC$$

**Figure 3. Equation. Prediction model 1 for  $f_{c,28d}$ .**

Where:

- $f_{c,28d}$  = 28-day compressive strength, psi.
- $w/c$  = Water to cementitious materials ratio.
- $CMC$  = Cementitious materials content, lb/yd<sup>3</sup>.

The model statistics are shown in table 1. The model was developed using 42 data points, and the prediction has an  $R^2$  value of 54.44 percent and a root mean square error (RMSE) of 871 psi. Although it was compromised relative to the models discussed above, it provides a more meaningful model with a superior predictive ability. Table 2 provides details of the range of data used to develop the model.

**Table 1. Regression statistics for selected prediction model for 28-day PCC cylinder strength.**

Variable	Degrees of Freedom (DF)	Estimate	Standard Error	t-Value	$P_r >  t $	VIF
Intercept	1	4,028.41841	1,681.71576	2.4	0.0215	0
w/c ratio	1	-3486.3501	2,152.99857	-1.62	0.1134	2.40903
CMC	1	4.02511	1.32664	3.03	0.0043	2.40903

**Table 2. Range of data used for 28-day PCC cylinder strength.**

Parameter	Minimum	Maximum	Average
w/c ratio	0.27	0.71	0.42
Cementitious content	376	936	664
Compressive strength	3,034	7,611	5,239

Figure 4 and figure 5 show the predicted versus measured values and the residuals plot for the model, respectively. Figure 6 and figure 7 show the sensitivity of this model to w/c ratio and CMC. The change in compressive strength appears reasonable for both of the parameters for the range of values evaluated. They are also consistent with the data in the database. Within practical ranges, a change in CMC from 500 to 650 lb/ft<sup>3</sup> increases the 28-day strength from approximately 4,700 to 5,300 psi for a w/c ratio of 0.4. Likewise, a decrease in w/c ratio from 0.5 to 0.35 increases the strength from 4,700 to 5,200 psi.

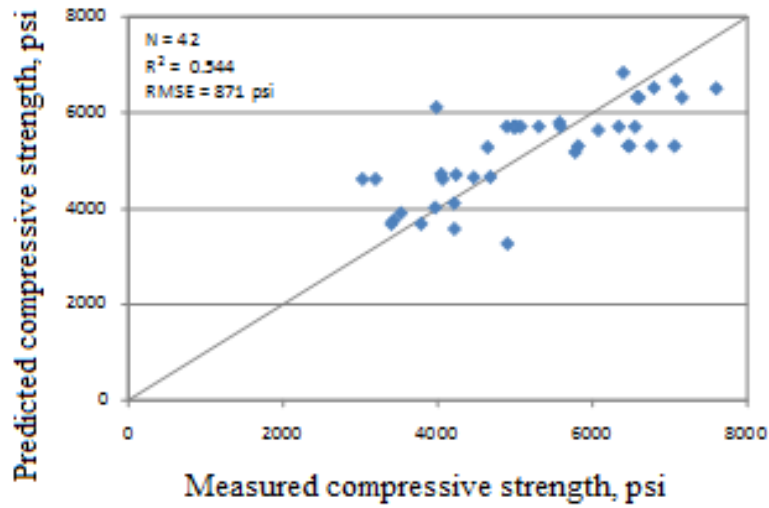


Figure 4. Graph. Predicted versus measured for 28-day cylinder compressive strength model.

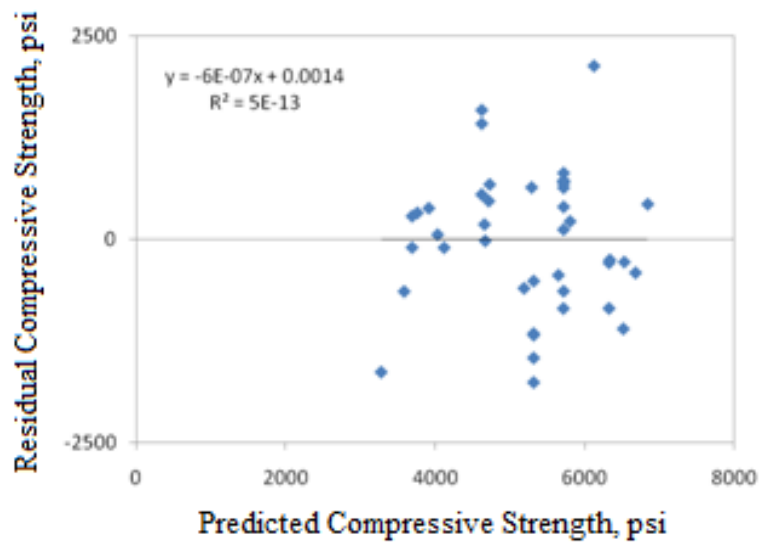


Figure 5. Graph. Residual error plot for 28-day cylinder compressive strength model.

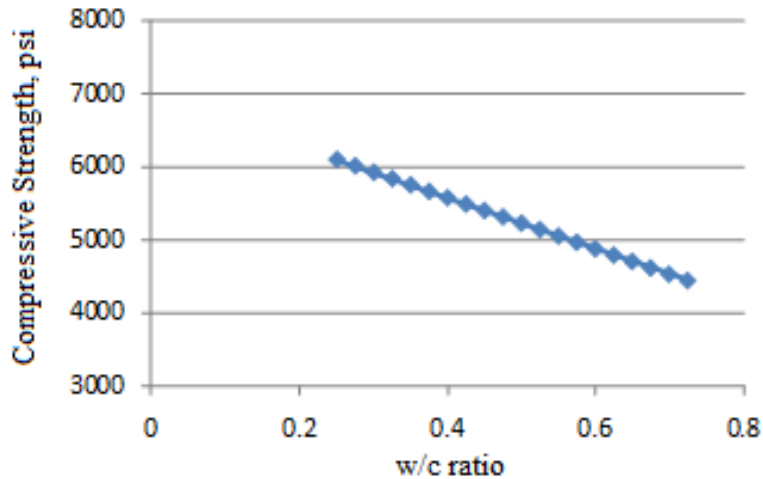


Figure 6. Graph. 28-day compressive strength model sensitivity to w/c ratio.

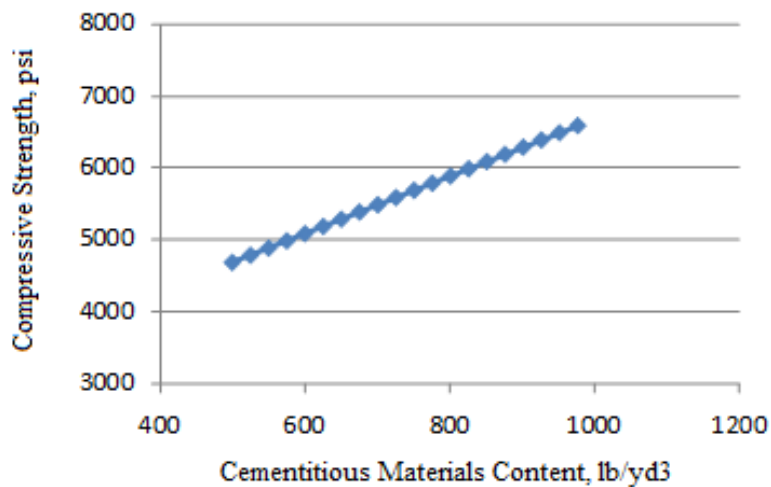


Figure 7. Graph. 28-day compressive strength model sensitivity to CMC.

### Compressive Strength Model 2: Short-Term Cylinder Strength Model

The short-term cylinder compressive strength is expressed as follows:

$$f_{c,t} = 6358.60655 + 3.53012 * CMC - 34.24312 * w/c * uw + 633.3489 * \ln(t)$$

Figure 8. Equation. Prediction model 2 for  $f_{c,t}$ .

Where:

$f_{c,t}$  = Compressive strength at age  $t$  years, psi.

$CMC$  = Cementitious materials content, lb/yd<sup>3</sup>.

$w/c$  = Water to cementitious materials ratio.

$uw$  = Unit weight, lb/ft<sup>3</sup>.

$t$  = Short-term age up to 1 year.

The regression statistics for this model are presented in table 3, and details of the range of data used to develop the model are presented in table 4. The model was developed using 79 data points, and the prediction has an  $R^2$  value of 66.6 percent and an RMSE of 789 psi. The reason for an improved  $R^2$  compared to the 28-day strength model is not clear from these analyses.

**Table 3. Regression statistics for short-term cylinder strength model.**

Variable	DF	Estimate	Standard Error	t-Value	$P_r >  t $	VIF
Intercept	1	6,358.60655	1,213.09762	5.24	< 0.0001	0
CMC	1	3.53012	0.90968	3.88	0.0002	2.15941
w/c × unit weight	1	-34.24312	11.00358	-3.11	0.0026	2.152
Ln(age)	1	633.3489	87.49625	7.24	< 0.0001	1.00604

**Table 4. Range of data used for short-term cylinder strength model.**

Parameter	Minimum	Maximum	Average
w/c ratio	0.27	0.69	0.43
Cementitious content	376	936	660
Unit weight	124	151	143
Pavement age	0.0384	1.0000	0.3081
Compressive strength	2,480	10,032	5,256

Figure 9 and figure 10 show the predicted versus measured plot and the residual plot, respectively. Figure 11 through figure 13 show the sensitivity of this model to CMC, w/c ratio, and age, respectively. The trends are all reasonable. Figure 11 and figure 12 show the change in compressive strength at two ages, 28 days and 1 year, which are almost at the lower and upper bounds of ages included in this model. The plot in figure 13 can be considered a strength gain curve for typical unit weight and w/c ratios used in mix designs.

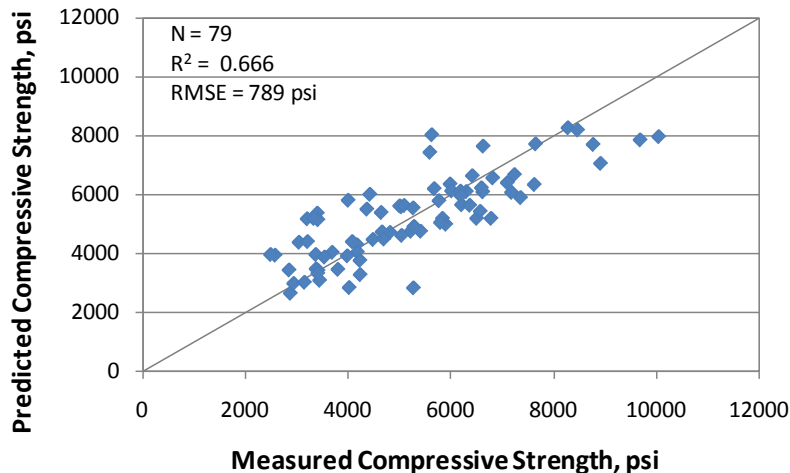


**Figure 9. Graph. Predicted versus measured for short-term cylinder compressive strength model.**

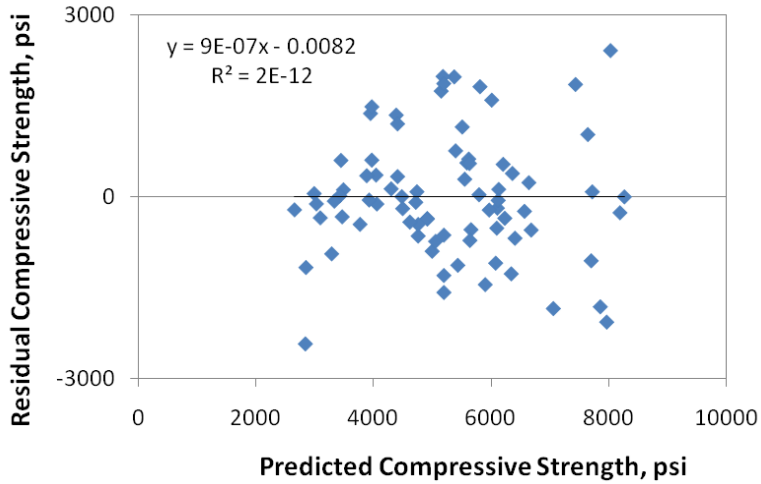


Figure 10. Graph. Residual errors for short-term cylinder compressive strength model.

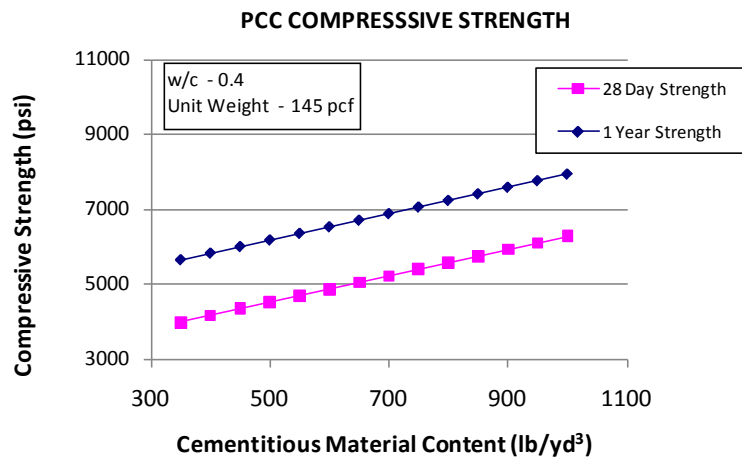


Figure 11. Graph. Short-term cylinder compressive strength sensitivity to CMC.

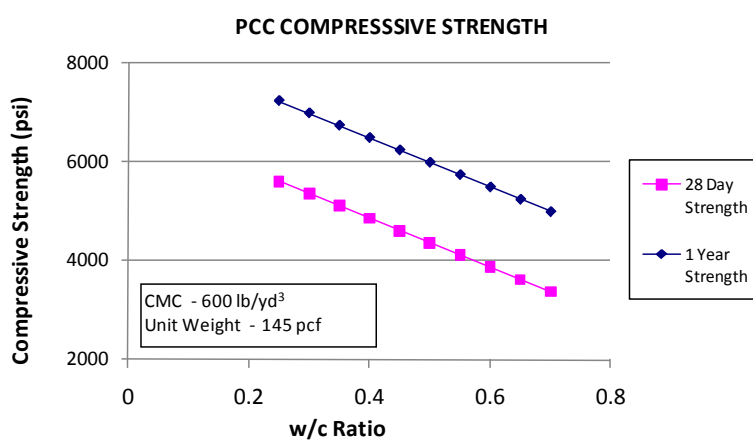
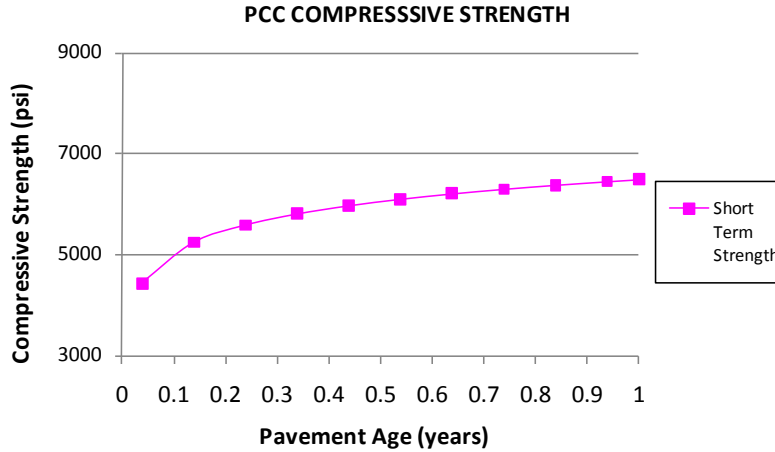


Figure 12. Graph. Short-term cylinder compressive strength sensitivity to w/c ratio.



**Figure 13. Graph. Short-term cylinder compressive strength sensitivity to age.**

### Compressive Strength Model 3: Short-Term Core Strength Model

The short-term core compressive strength model is as follows:

$$f_{c,t} = 98.92962 + 5.70412 * CMC + 28.48527 * uw + 2570.13151 * MAS * w/c - 199.84664 * FM + 611.30879 * \ln(t)$$

**Figure 14. Equation. Prediction model 3 for  $f_{c,t}$ .**

Where:

- $f_{c,t}$  = Compressive strength at age  $t$  years, psi.
- $CMC$  = Cementitious materials content, lb/yd<sup>3</sup>.
- $uw$  = Unit weight, lb/ft<sup>3</sup>.
- $MAS$  = Maximum aggregate size, inch.
- $w/c$  = Water to cementitious materials ratio.
- $FM$  = Fineness modulus of fine aggregate.
- $t$  = Short-term age up to 1 year.

The regression statistics for this model are presented in table 5. The model was developed using 294 points, and the prediction has an  $R^2$  value of 67.61 percent and an RMSE of 1,122 psi. Table 6 provides details of the range of data used to develop the model.

**Table 5. Regression statistics for short-term core strength model.**

Variable	DF	Estimate	Standard Error	t-Value	$P_r >  t $	VIF
Intercept	1	98.92962	1,544.34064	0.06	0.949	0
CMC	1	5.70412	0.36589	15.59	< 0.0001	1.23548
Unit weight	1	28.48527	10.59672	2.69	0.0076	1.0182
MAS × w/c ratio	1	2,570.13151	538.267	-4.77	< 0.0001	1.2201
FM	1	-199.84664	120.68288	-1.66	0.0988	1.01426
Ln(age)	1	611.30879	45.08962	13.56	< 0.0001	1.00026

**Table 6. Range of data used for short-term core strength model.**

Parameter	Minimum	Maximum	Average
w/c ratio	0.27	0.69	0.42
Cementitious content	376	999	670
Unit weight	120	163	144
MAS	0.375	1.000	0.683
FM	2.50	4.37	3.05
Pavement age	0.0380	2.2160	0.4230
Compressive strength	1990	11,350	5,596

Figure 15 and figure 16 show the predicted versus measured plot and the residual plot, respectively. Figure 17 through figure 22 show the sensitivity of this model to CMC, unit weight, MAS, w/c ratio, FM, and age, respectively.

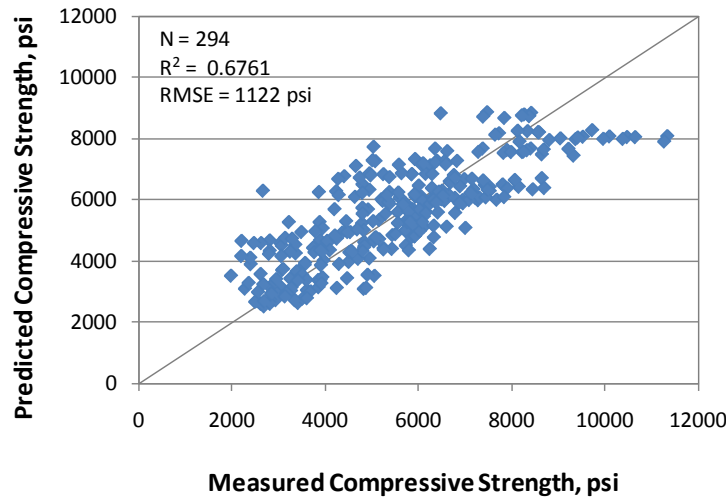


**Figure 15. Graph. Predicted versus measured for short-term core compressive strength model.**

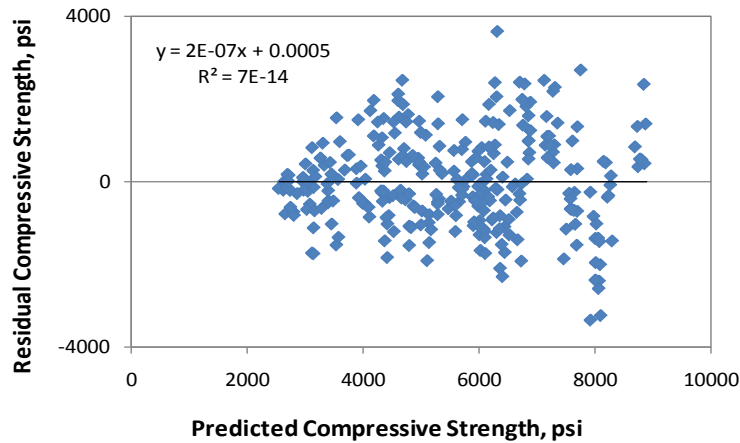


**Figure 16. Graph. Residual errors for short-term core compressive strength model.**

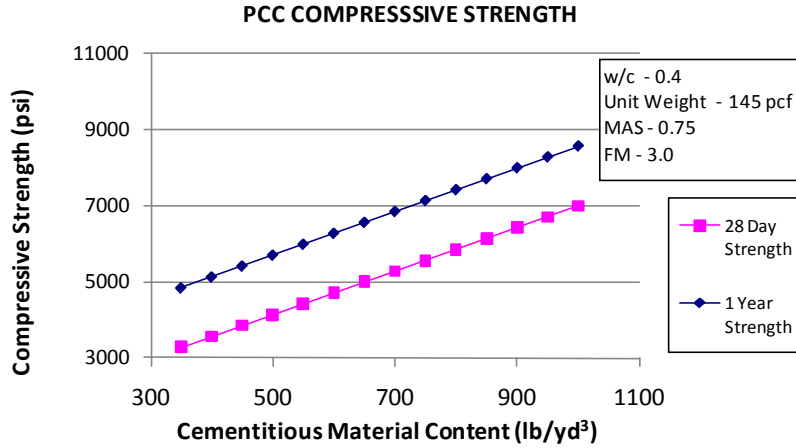


Figure 17. Graph. Short-term core compressive strength sensitivity to CMC.

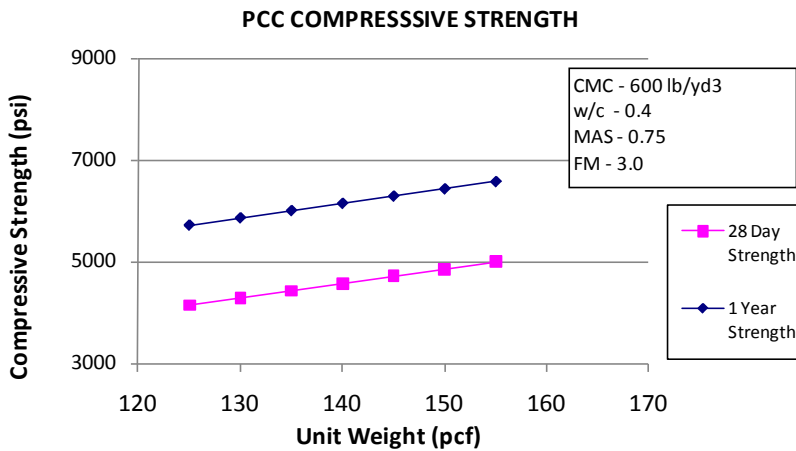


Figure 18. Graph. Short-term core compressive strength sensitivity to unit weight.

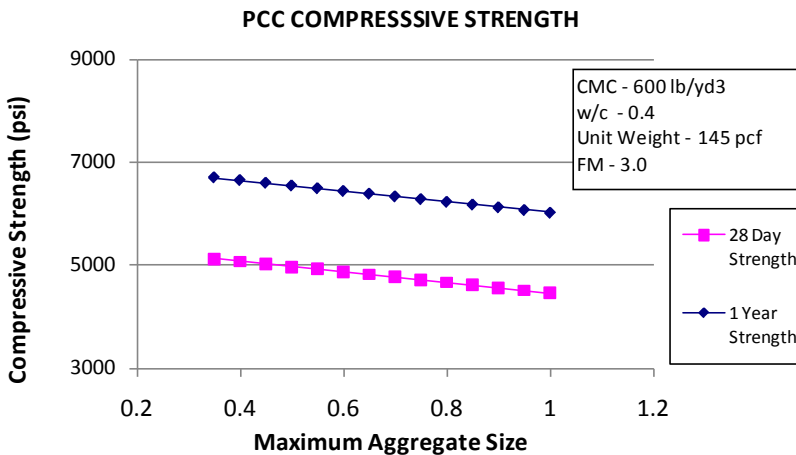


Figure 19. Graph. Short-term core compressive strength sensitivity to MAS.

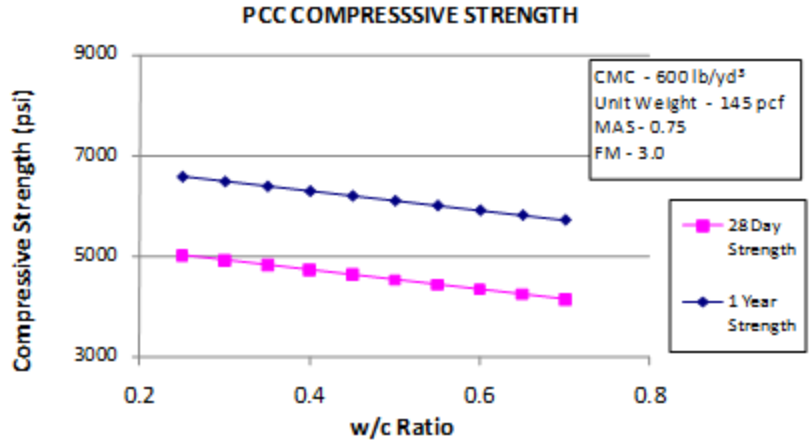


Figure 20. Graph. Short-term core compressive strength sensitivity to w/c ratio.

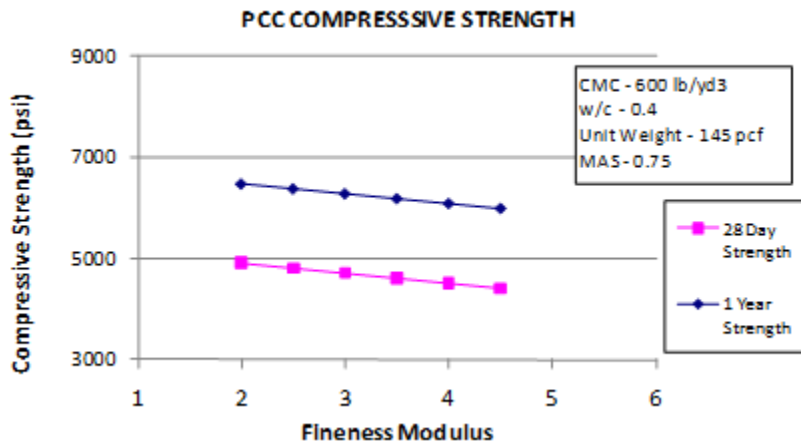


Figure 21. Graph. Short-term core compressive strength sensitivity to fine aggregate FM.

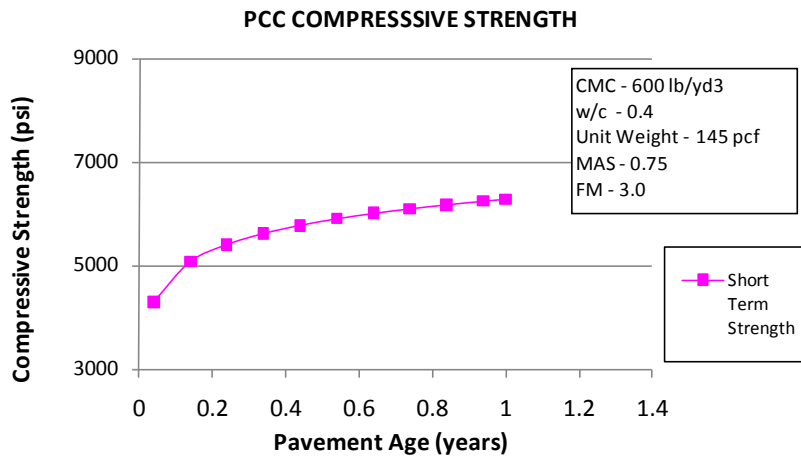


Figure 22. Graph. Short-term core compressive strength sensitivity to age.

### Compressive Strength Model 4: All Ages Core Strength Model

The compressive strength for cores at all ages is estimated as follows:

$$f_{c,t} = -6022.44 - 854.46 * w/c + 4.8656 * CMC + 68.5337 * uw + 533.15 * \ln(t)$$

**Figure 23. Equation. Prediction model 4 for  $f_{c,t}$ .**

Where:

$f_{c,t}$  = Compressive strength at age  $t$  years, psi.

$w/c$  = Water to cementitious materials ratio.

$CMC$  = Cementitious materials content, lb/yd<sup>3</sup>.

$uw$  = Unit weight, lb/ft<sup>3</sup>.

$t$  = Short-term age in years.

The regression statistics for this model are presented in table 7. The model was developed using 580 data points, and the prediction has an  $R^2$  value of 55.38 percent and an RMSE of 992 psi. Table 8 provides details of the range of data used to develop the model.

**Table 7. Regression statistics for all ages core strength model.**

Variable	Estimate	Standard Error	$t$ -Value	$P_r >  t $	VIF
Intercept	-6,022.44	2,028.37	-2.97	0.0032	0
w/c ratio	-854.46	675.86	-1.26	0.2069	2.15941
CMC	4.8656	0.5737	8.48	< 0.0001	2.152
Unit weight	68.5337	13.4368	5.1	< 0.0001	1.00604
Ln(age)	533.15	22.3343	23.87	< 0.0001	1.00026

**Table 8. Range of data used for all ages core strength model.**

Parameter	Minimum	Maximum	Average
w/c ratio	0.00	0.72	0.43
Cementitious content	354	999	615
Unit weight	120	163	145
Pavement age	0.0380	45.3840	6.4320
Compressive strength	1,990	11,750	6,430

Figure 24 and figure 25 show the predicted versus measured plot and the residual plot, respectively.

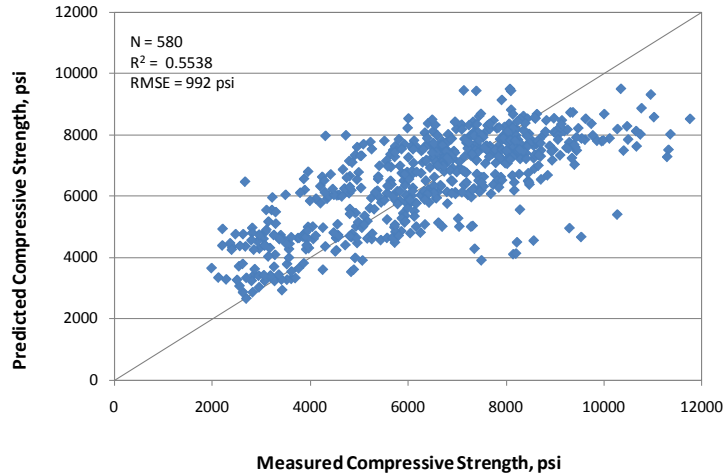


**Figure 24. Graph. Predicted versus measured for all ages core compressive strength model.**

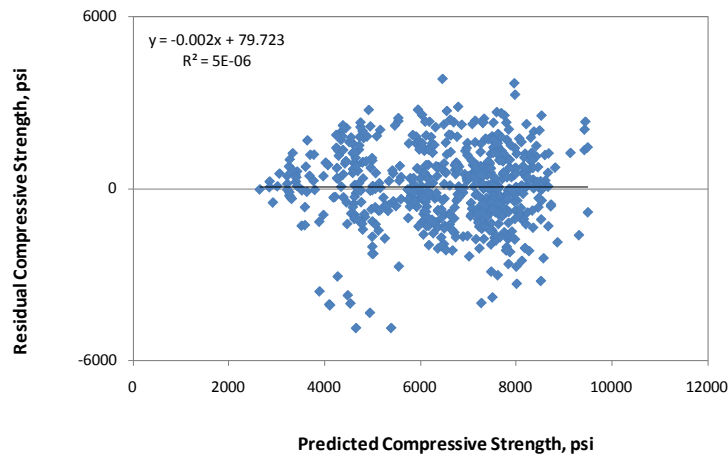


**Figure 25. Graph. Residual errors for all ages core compressive strength model.**

Figure 26 through figure 29 show the sensitivity of this model to w/c ratio, CMC, unit weight, and age, respectively. Again, the sensitivity plots showing the variation in core compressive strength with changes in w/c ratio, CMC, and unit weight are presented for 28 days, 1 year, and 20 years. The rate of strength gain clearly is much higher in the short term (28 days to 1 year) than during the next 19 years. Figure 29 can be treated as the strength gain relationship representative of a typical mix (w/c of 0.4, CMC of 600 lb/yd<sup>3</sup>, and unit weight of 145 lb/ft<sup>3</sup>).

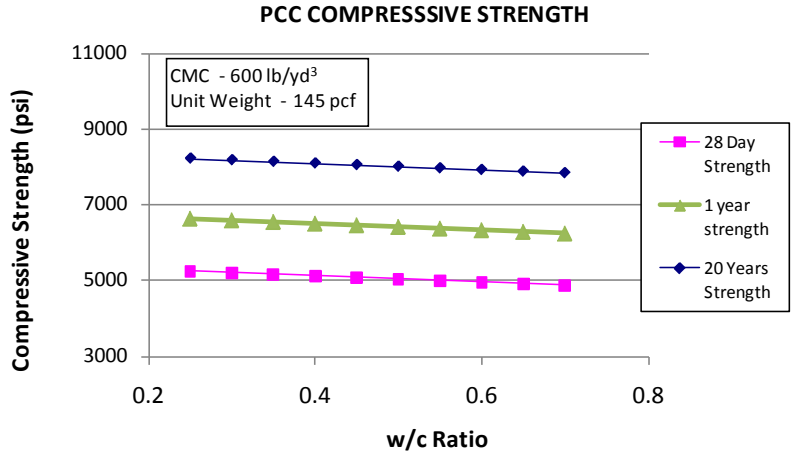


Figure 26. Graph. All ages core compressive strength sensitivity to w/c ratio.

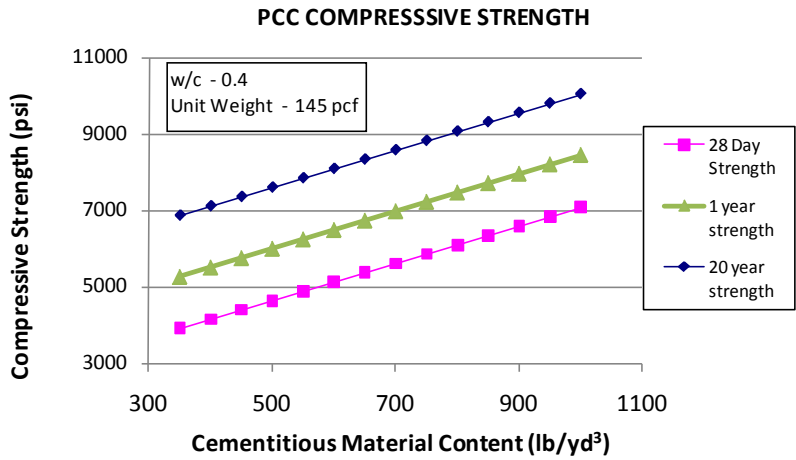


Figure 27. Graph. All ages core compressive strength sensitivity to CMC.

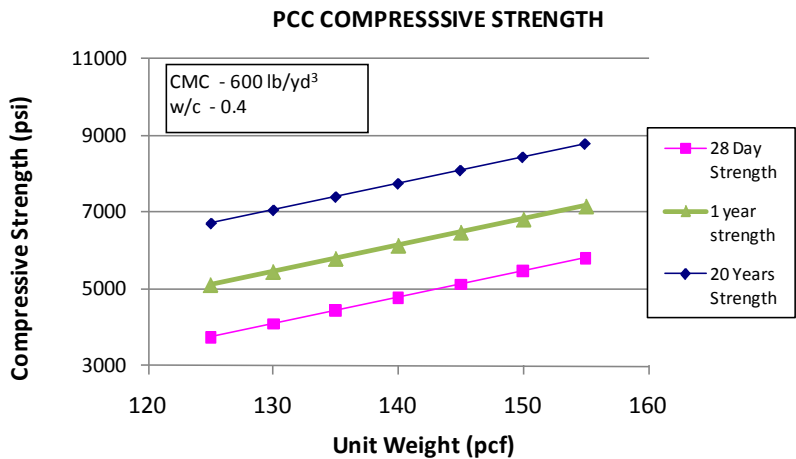
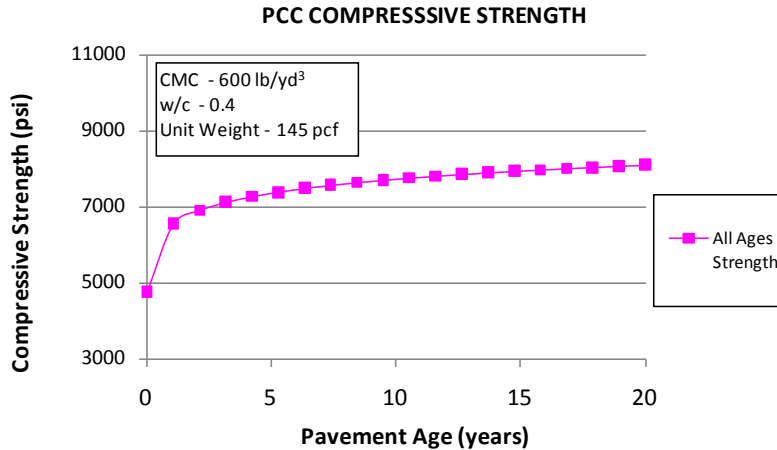


Figure 28. Graph. All ages core compressive strength sensitivity to unit weight.



**Figure 29. Graph. All ages core compressive strength sensitivity to age.**

**Compressive Strength Model 5: Long-Term Core Strength Model**

The model developed for the long-term strength is expressed as follows:

$$f_{c,LT} = -3467.3508 + 3.63452 * CMC + 0.42362 * uw^2$$

**Figure 30. Equation. Prediction model 5 for  $f_{c,LT}$ .**

Where:

- $f_{c,LT}$  = Long-term compressive strength, psi.
- $CMC$  = Cementitious materials content, lb/yd<sup>3</sup>.
- $uw$  = Unit weight, lb/ft<sup>3</sup>.

The regression statistics for this model are presented in table 9. The model was developed using 201 data points, and the prediction has an  $R^2$  value of 18.03 percent and an RMSE of 1,179 psi. Table 10 provides details of the range of data used to develop the model.

**Table 9. Regression statistics for long-term core strength model.**

Variable	DF	Estimate	Standard Error	t-Value	$P_r >  t $	VIF
Intercept	1	-3,467.3508	1,720.49637	-2.02	0.0452	0
Cementitious	1	3.63452	1.38354	2.63	0.0093	1.024
(Unit weight) <sup>2</sup>	1	0.42362	0.06634	6.39	< 0.0001	1.024

**Table 10. Range of data used for long-term core strength model.**

Parameter	Minimum	Maximum	Average
Cementitious content	354	781	550
Unit weight	134	156	147
Compressive strength	4,315	11,750	7,655

Figure 31 and figure 32 show the predicted versus measured plot and the residual plot, respectively. This model does not have a good predictive ability (see figure 31). While there is no significant bias, the error in prediction is fairly high (see figure 32). This model needs to be used with caution. Additionally, other means to verify the value would be necessary, such as core tests.

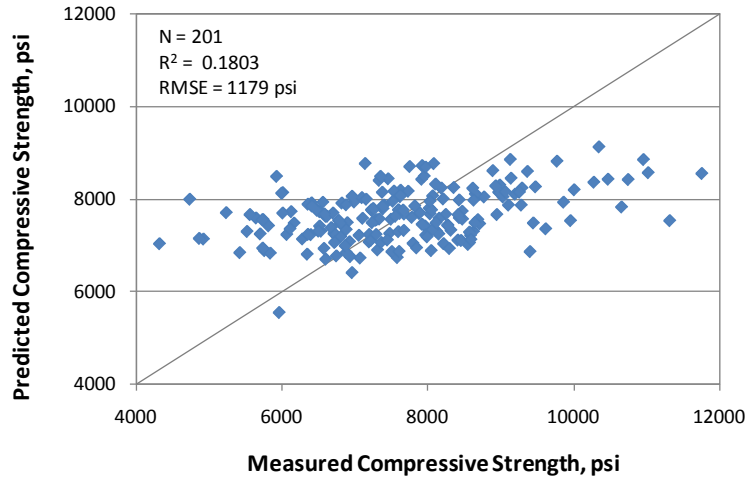


**Figure 31. Graph. Predicted versus measured for long-term core compressive strength model.**

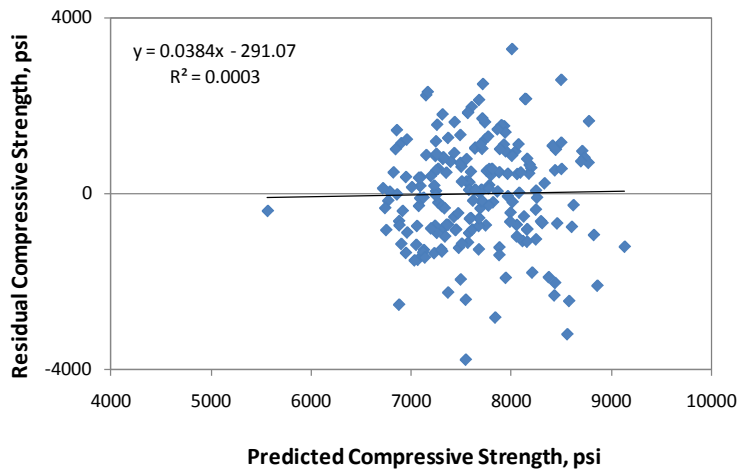


**Figure 32. Graph. Residual errors for long-term core compressive strength model.**

### Relative Comparison of All Compressive Strength Models

The compressive strength models, like any other empirical model, reproduce the trends present in the datasets used for each correlation. It is highly recommended that a user estimate the strength based on as many models as possible with the information available at the time of analysis. This might provide a fair assessment of the ranges of compressive strength likely for the project and at different ages.

Figure 33 through figure 37 show the relationship between compressive strength and CMC, w/c ratio, and unit weight, respectively. Figure 36 and figure 37 show the strength gain at short- and long-term ages, respectively. Note that relationships have been plotted for typical values for all variables, and the raw data used in the models do not necessarily lie on the plots.

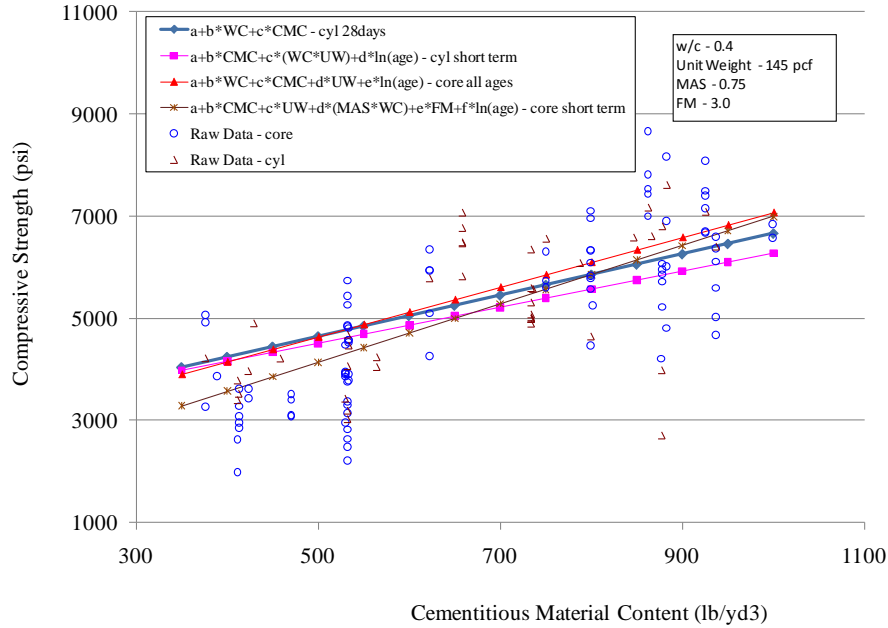


**Figure 33. Graph. Model compressive strength prediction for varying CMC.**

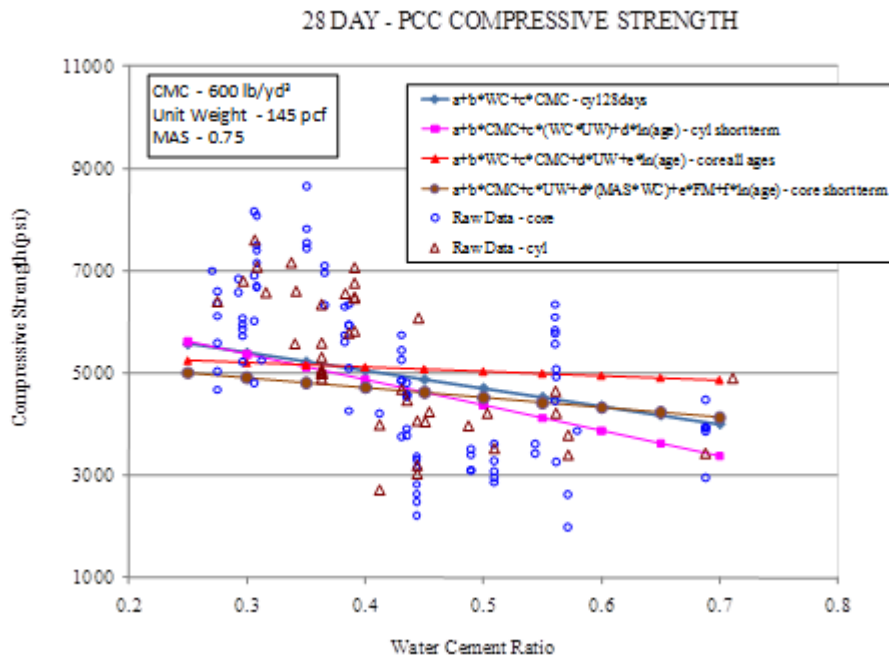


**Figure 34. Graph. Model compressive strength prediction for varying w/c ratio.**

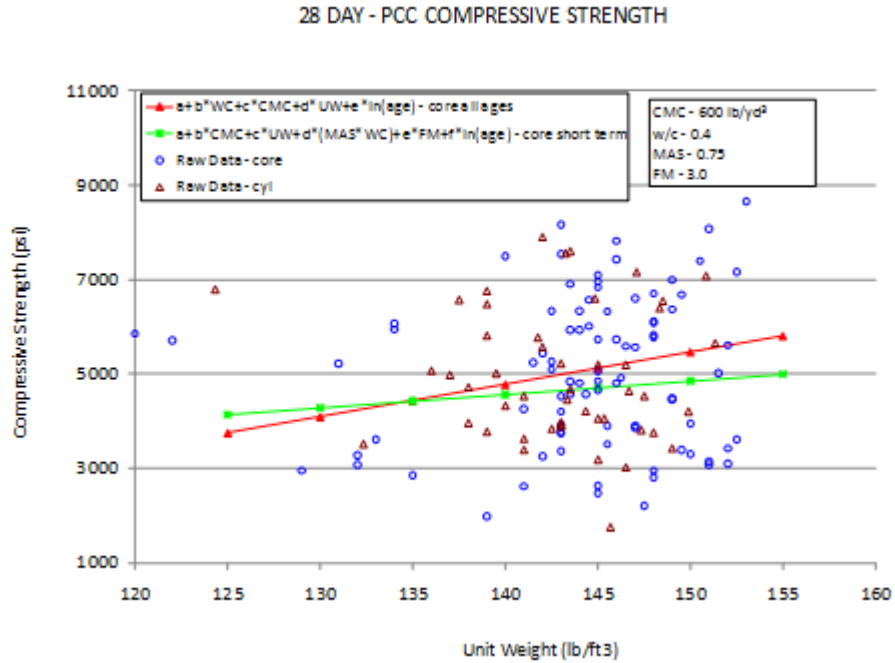


Figure 35. Graph. Model compressive strength prediction for varying unit weights.

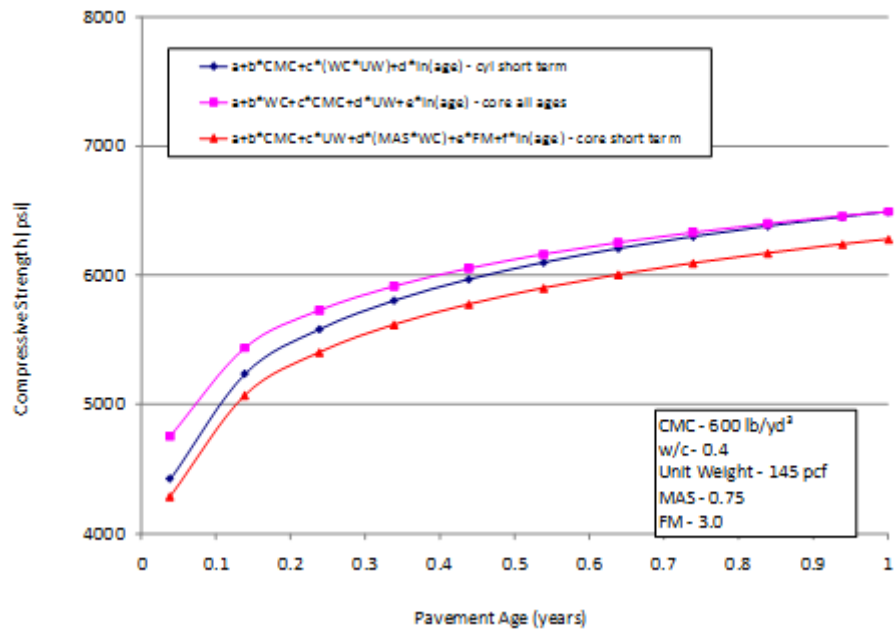
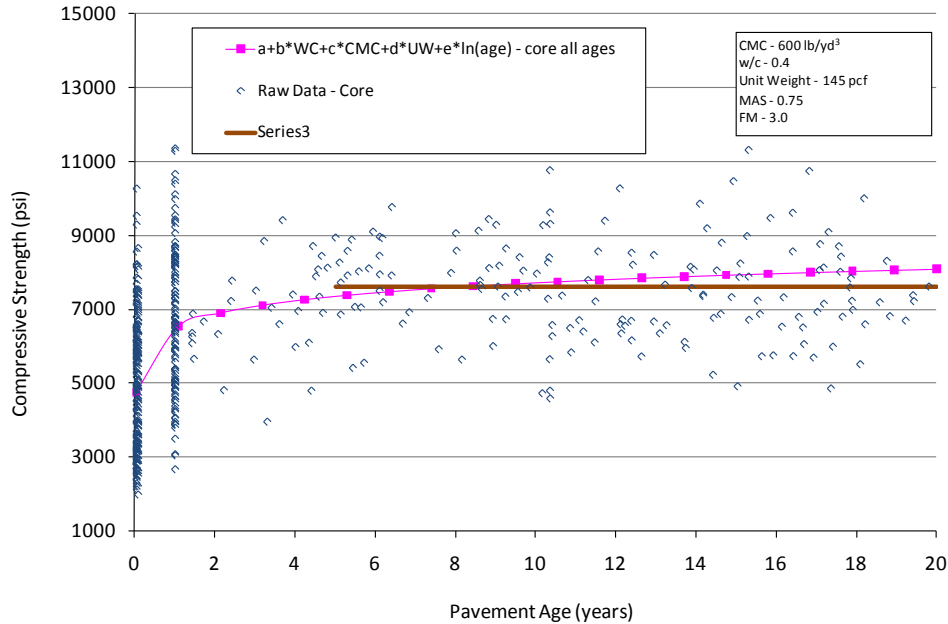


Figure 36. Graph. Strength gain in the short-term predicted by three models.



**Figure 37. Graph. Long-term strength gain predicted by the models.**

The following observations can be made:

- The predictions are within 700 psi of each other for a given CMC (see figure 33). However, for more typical ranges of cement contents, the predictions are within 300 to 400 psi of each other. The short-term core compressive model has the steepest slope for this relationship.
- Figure 34 suggests that the predictions have a range as high as 1,500 psi for a given w/c ratio, especially at very high w/c ratios. However, within typical ranges (0.3 to 0.5), the models predict within a range of 250 to 800 psi. The range slightly increases at lower w/c ratios. The short-term cylinder strength has the highest slope in this case.
- Based on the trend presented in figure 35, for a given level of unit weight, the compressive strength predictions are within 200 to 300 psi for typical ranges of unit weight (140 to 145 lb/ft<sup>3</sup>). The prediction can vary by about 800 psi for very high unit weight values. Note that the short-term cylinder compressive strength model has not been included in this plot, as the variable appears as a transformed variable in the model and its effect cannot be isolated.
- Short-term strength predictions by all models that are relevant to short-term strengths show predictions within 200 to 400 psi of each other. The predictions are closer in value at as the age increases from 14 days to 1 year (see figure 36).
- Figure 37 suggests that the long-term strength predicted by the core all ages model is close to the strength predicted by the long-term model. This is essentially because the data used in this range are common to both models.

These observations illustrate the benefit of comparing predictions made by the various models available to obtain the range of strength that each project or observation could develop. Any other information to substantiate or validate the strength predictions should be utilized whenever possible, such as strength values from other projects that have used similar materials and mix design.

## PCC FLEXURAL STRENGTH MODELS

### Validation of Existing Models

Previous models correlating flexural strength to compressive strength have generally used a power model of the following form:

$$M_r = a * f'_c{}^b$$

**Figure 38. Equation.  $M_r$ .**

Where:

$a = 7.5$  to  $11.7$  for  $b = 0.5$ .

$a = 2$  to  $2.7$  for  $b = 0.67$ .

Table 11 shows a summary of the models developed. The regressed constants,  $a$  and  $b$ , were found to be within the range of values reported by the other studies. This validation not only provides feasible models, but it also confirms that the data used reasonably represent the broad range considered in the various studies. The correlations are presented in figure 39 and figure 40 for the power models with exponents of 0.5 and 0.67, respectively.

**Table 11. Power models developed for flexural strength prediction using LTPP data for validation.**

Model	$a$	$b$	$R^2$	$N$
$M_r = a * f'_c{}^b$	10.3022	0.50	0.446	185
	2.4277	0.67	0.449	185

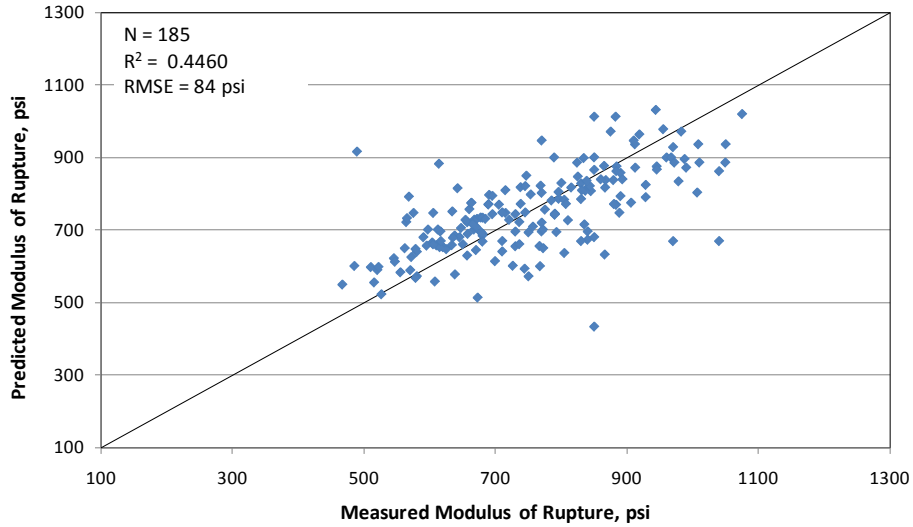


**Figure 39. Graph. Predicted versus measured for validating 0.5 power flexural strength model.**

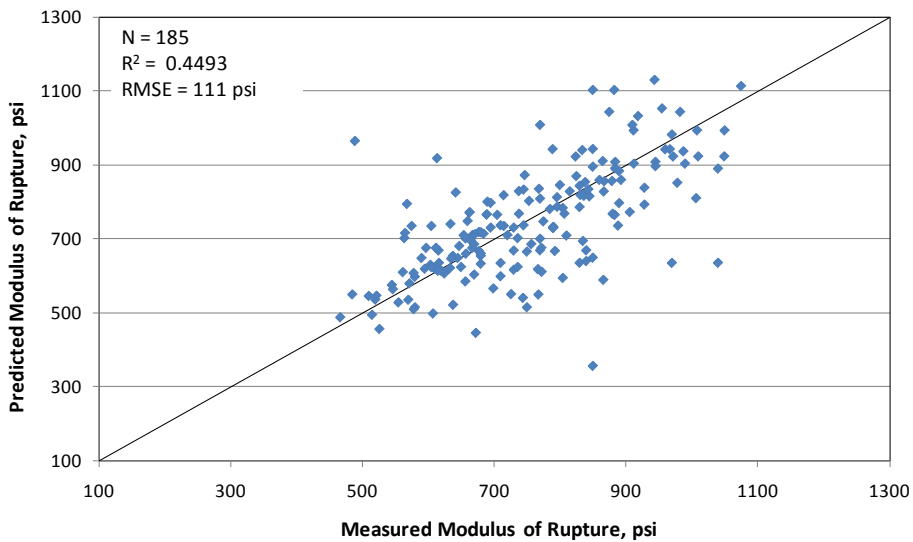


**Figure 40. Graph. Predicted versus measured for validating 0.667 power flexural strength model.**

**Flexural Strength Model 1: Flexural Strength Based on Compressive Strength**

This model provides the best correlation between compressive strength and flexural strength with the LTPP data. The model form utilizes the power equation. This model will be most useful for cases when the compressive strength of the PCC has been determined through a routine cylinder break. This model can be expressed as follows:

$$MR = 22.7741 * f'_c^{0.4082}$$

**Figure 41. Equation. Prediction model 6 for MR.**

Where:

$MR$  = Flexural strength, psi.

$f'_c$  = Compressive strength determined at the same age, psi.

The regression statistics for this model are presented in table 12. The model was developed using 185 data points, and the prediction has an  $R^2$  value of 45.2 percent and an RMSE of 69 psi. Table 13 provides details of the range of data used to develop the model.

**Table 12. Regression statistics for flexural strength model based on compressive strength.**

Parameter	Estimate	Standard Error	Approximate 95 Percent Confidence Limits
$a$	22.7741	6.6362	9.6807 to 35.8674
$b$	0.4082	0.0338	0.3416 to 0.4748

**Table 13. Range of data used for flexural strength model based on compressive strength.**

Parameter	Minimum	Maximum	Average
Compressive strength	1,770	10,032	5,431
Flexural strength	467	1,075	754

Figure 42 and figure 43 show the predicted versus measured plot and the residual plot, respectively.

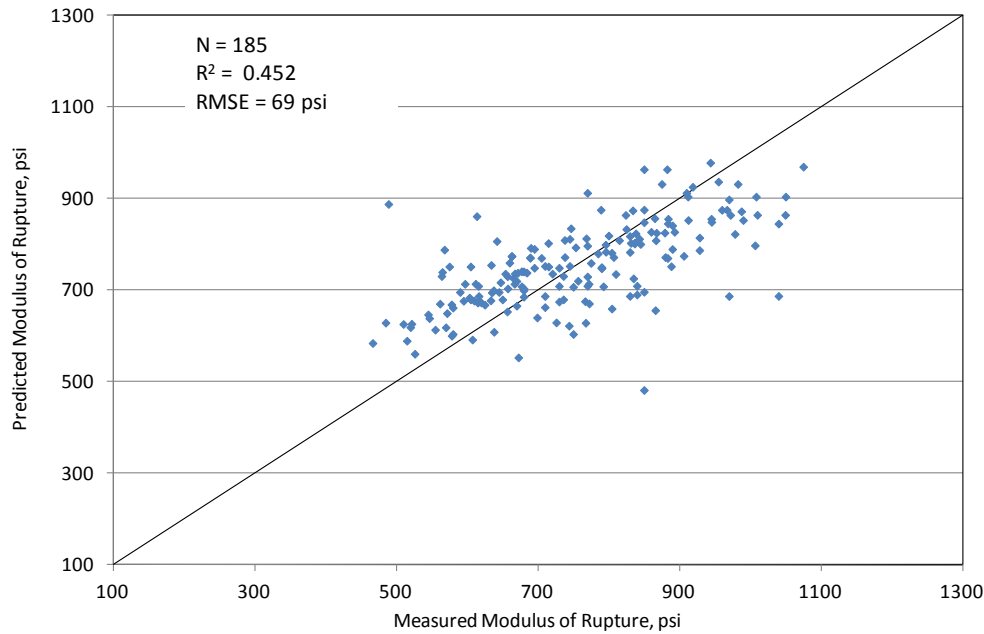


**Figure 42. Graph. Predicted versus measured values for flexural strength model based on compressive strength.**

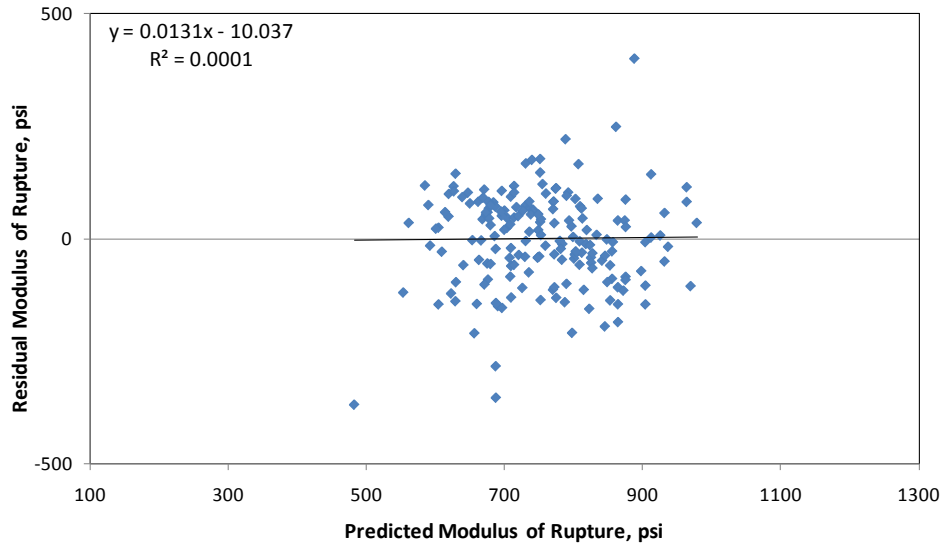


**Figure 43. Graph. Residual errors for flexural strength model based on compressive strength.**

Figure 44 shows a comparison of the power models used to validate the data and develop a new correlation. Note that the three power models (the new equation developed for this study as well as the validation models) provide close estimates (within 50 psi) in the 4,500- to 5,500-psi compressive strength range.

The American Concrete Institute (ACI) and Portland Cement Association (PCA) models are plotted for comparison. Also plotted are the raw data that were used in the model. Clearly, the ACI equation is conservative for this data. It has also been found to give a conservative estimate for several large datasets that have been used in flexural strength model prediction. Conversely, the PCA model fits the LTPP data more closely. The reasons for this lack of fit of the current data with the previous models may be too many to fully explain. The data used in models from prior studies often came from mixes batched under controlled laboratory experiments and were typical of paving and structural concrete. The mixes used in the current model developed from LTPP data relies on only mixes proportioned for typical paving operations. Furthermore, the LTPP data used are from many projects widely dispersed around the United States. This in itself makes the models more robust than any previous data used to make similar correlations.

The spread in the raw data about the prediction model in figure 44 clearly indicates that there are factors other than compressive strength that influence the flexural strength of PCC. Among the various factors influencing flexural strength are the mix design parameters and age of the concrete. These variables are considered in the other models developed in this study.

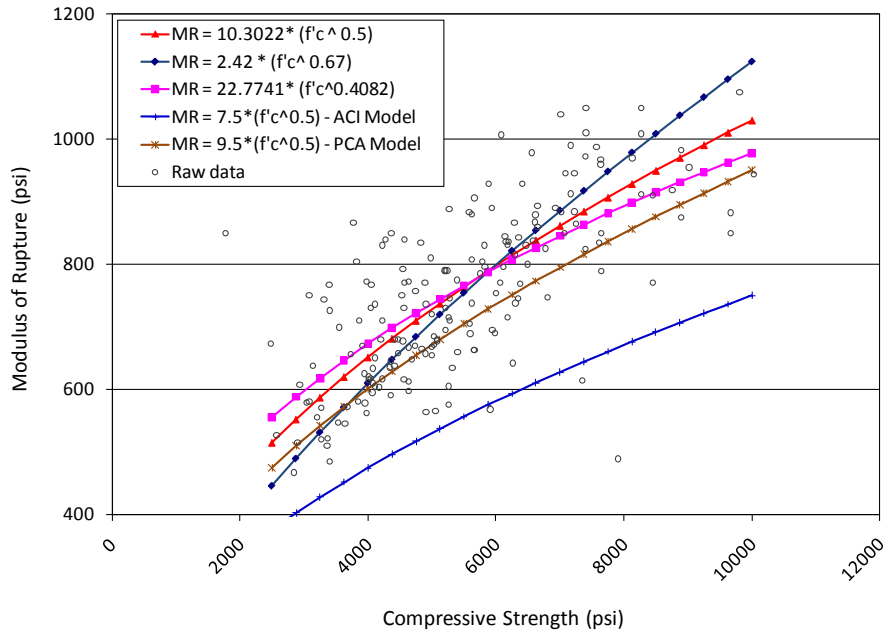


**Figure 44. Graph. Comparison of flexural strength models based on compressive strength.**

### **Flexural Strength Model 2: Flexural Strength Based on Age, Unit Weight, and w/c Ratio**

Flexural strength model 2 provides a correlation between flexural strength and mix design parameters, specifically the unit weight and w/c ratio. Age is also a parameter in this model, which helps reduce some of the variability seen in the prediction relative to the predictions shown in figure 44. This model will be most useful for cases when the compressive strength of PCC is not determined but mix design information is available. Also, the user has the option of predicting the 28-day strength value for design or estimating the strength at traffic opening time.

This model can be expressed as follows:

$$MR_t = 676.0159 - 1120.31 * w/c + 4.1304 * uw + 35.74627 * \ln(t)$$

**Figure 45. Equation. Prediction model 7 for  $MR_t$ .**

Where:

$MR_t$  = Flexural strength at age  $t$  years, psi.

$w/c$  = w/c ratio.

$uw$  = Unit weight, lb/ft<sup>3</sup>.

$t$  = Pavement age, years.

The regression statistics for this model are presented in table 14. The model was developed using 62 data points, and the prediction has an  $R^2$  value of 61.11 percent and an RMSE of 91 psi. Table 15 provides details of the range of data used to develop the model.

**Table 14. Regression statistics for flexural strength model based on age, unit weight, and w/c ratio.**

Variable	DF	Estimate	Standard Error	t-Value	$P_r >  t $	VIF
Intercept	1	676.0159	277.7887	2.43	0.0181	0
w/c	1	-1,120.31	141.3573	-7.93	< 0.0001	1.00591
Unit weight	1	4.1304	1.88934	2.19	0.0329	1.00311
Ln(age)	1	35.74627	8.78516	4.07	0.0001	1.00619

**Table 15. Range of data used for flexural strength model based on age, unit weight, and w/c ratio.**

Parameter	Minimum	Maximum	Average
w/c ratio	0.27	0.58	0.40
Unit weight	124	151	142
Pavement age	0.0384	1.0000	0.3169
Flexural strength	467	978	742

Figure 46 and figure 47 show the predicted versus measured plot and the residual plot, respectively.

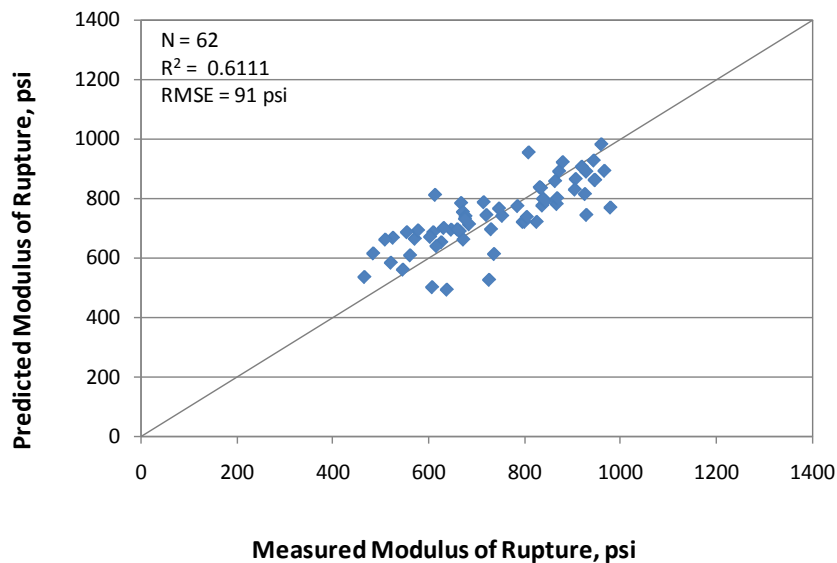


**Figure 46. Graph. Predicted versus measured values for flexural strength model based on age, unit weight, and w/c ratio.**

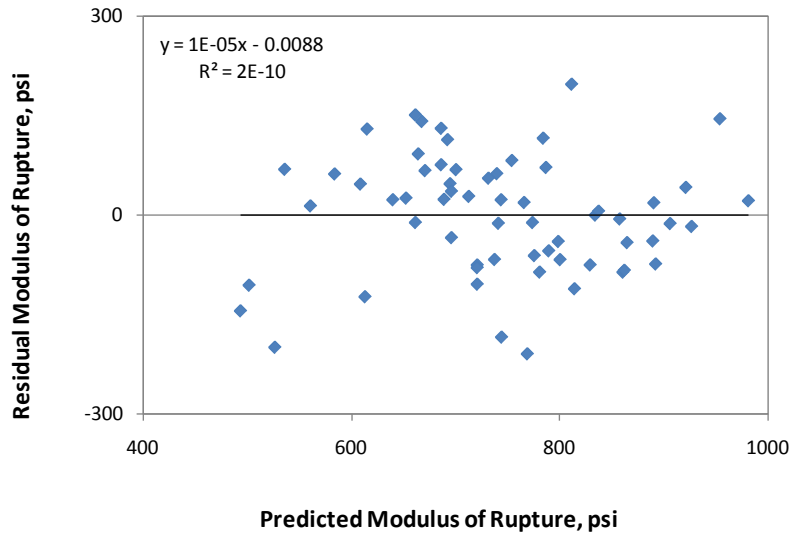


**Figure 47. Graph. Residual errors for flexural strength model based on age, unit weight, and w/c ratio.**

**Flexural Strength Model 3: Flexural Strength Based on Age, Unit Weight, and CMC**

The model is expressed as follows:

$$MR_t = 24.15063 + 0.55579 * CMC + 2.96376 * uw + 35.54463 * \ln(t)$$

**Figure 48. Equation. Prediction model 8 for  $MR_t$ .**

Where:

$MR_t$  = Flexural strength at age  $t$  years, psi.

$CMC$  = Cementitious materials content, lb/yd<sup>3</sup>.

$uw$  = Unit weight, lb/ft<sup>3</sup>.

$t$  = Pavement age, years.

The regression statistics for this model are presented in table 16. The model was developed using 62 data points, and the prediction has an  $R^2$  value of 70.23 percent and RMSE of 80 psi. Table 17 provides details of the range of data used to develop the model.

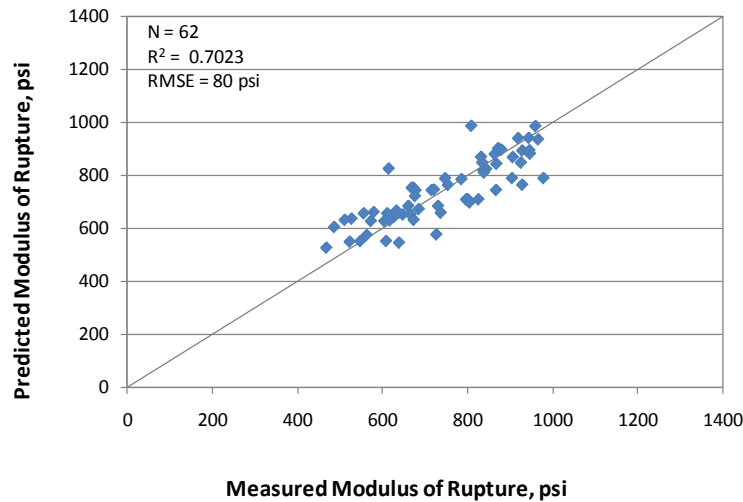
**Table 16. Regression statistics for flexural strength model based on age, unit weight, and CMC.**

Variable	DF	Estimate	Standard Error	t-Value	$P_r >  t $	VIF
Intercept	1	24.15063	236.7606	0.1	0.9191	0
CMC	1	0.55579	0.05563	9.99	< 0.0001	1.01522
Unit weight	1	2.96376	1.66087	1.78	0.0796	1.01253
Ln(age)	1	35.54463	7.68504	4.63	< 0.0001	1.00573

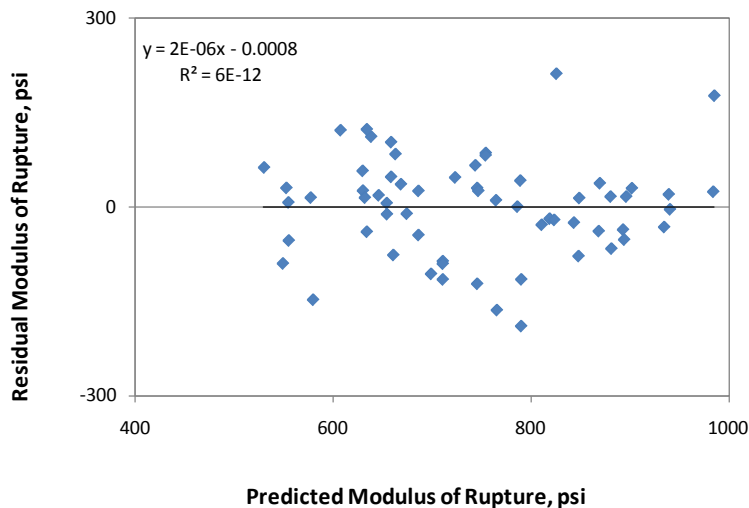
**Table 17. Range of data used for flexural strength model based on age, unit weight, and CMC.**

Parameter	Minimum	Maximum	Average
CMC	388	936	668
Unit weight	124	151	142
Pavement age	0.0384	1.0000	0.3169
Flexural strength	467	978	742

Figure 49 and figure 50 show the predicted versus measured plot and the residual plot, respectively.



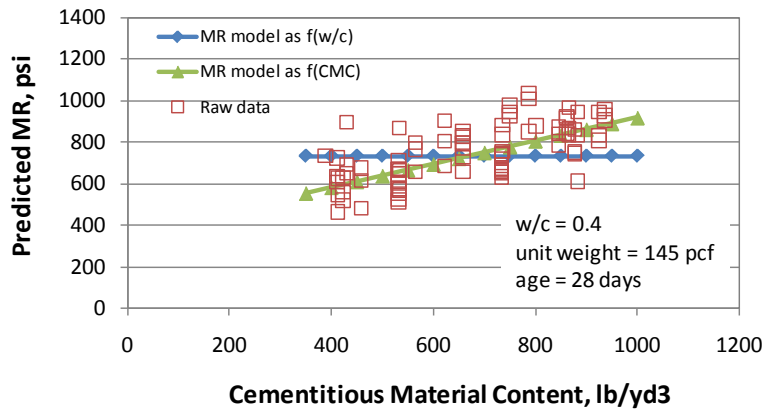
**Figure 49. Graph. Predicted versus measured values for flexural strength model based on age, unit weight, and CMC.**



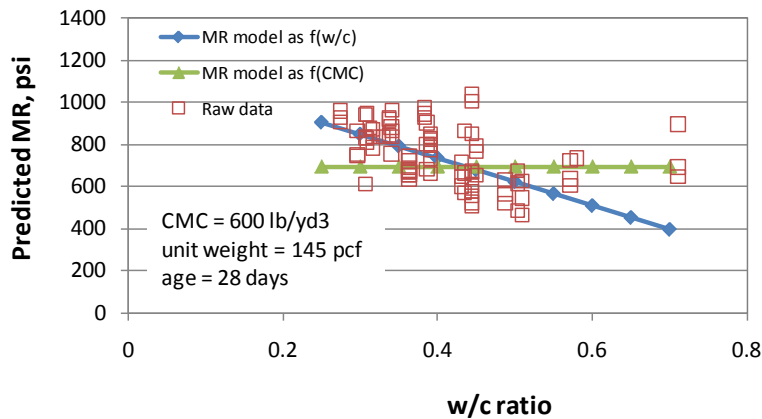
**Figure 50. Graph. Residual errors for flexural strength model based on age, unit weight, and CMC.**

Figure 51 through figure 54 present the sensitivity of the mix design-based flexural strength models to CMC, w/c ratio, unit weight, and age. Figure 51 and figure 52 show that prediction

models 7 and 8 do not show any sensitivity to CMC and w/c ratio (see figure 45 and figure 48). For typical values of these parameters, the flexural strength prediction from these two models could show a difference of about 200 psi for extreme values of w/c ratios. However, within a typical range of 0.35 to 0.45, the flexural strength prediction is within 50 psi. Similar trends are evident for the w/c ratio parameter. Therefore, if all details about a mix design are available, it is highly recommended that both models be used to predict flexural strength so that the user has a fair estimate of the flexural strength range. Figure 53 shows that the predictions are close from both models. Likewise, figure 54, which is more or less a flexural strength gain model for a typical mix design, shows very close predictions from both models.



**Figure 51. Graph. Sensitivity of flexural strength predictions to CMC.**



**Figure 52. Graph. Sensitivity of flexural strength predictions to w/c ratio.**

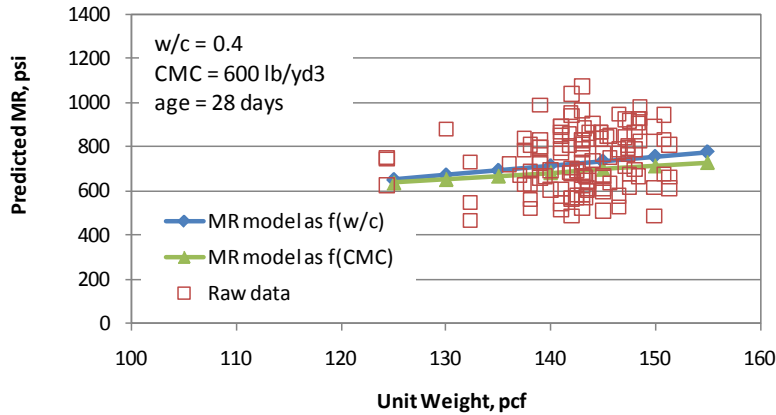


**Figure 53. Graph. Sensitivity of flexural strength predictions to unit weight.**

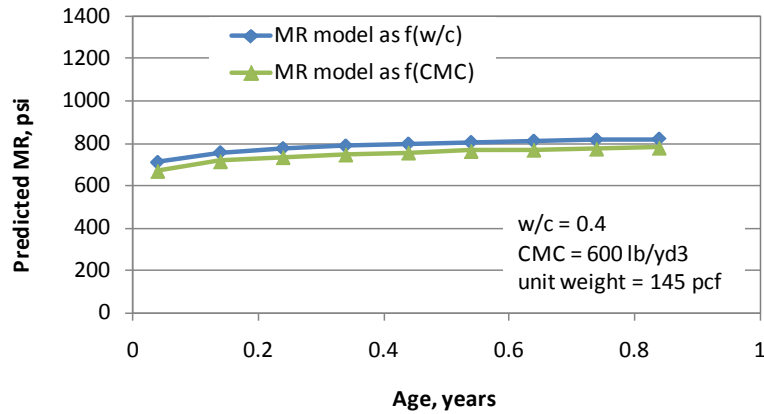


**Figure 54. Graph. Sensitivity of flexural strength predictions to age.**

## PCC ELASTIC MODULUS MODELS

### Validation of Existing Models

Existing models correlate elastic modulus to compressive strength and unit weight. The following represent the regressed models using LTPP data for existing model forms:

$$E_c = a * \sqrt{f'_c}$$

**Figure 55. Equation.  $E_c$  as a function of square root of compressive strength.**

Regressed coefficients for figure 55 are as follows:

- $a = 55,294$ .

Regression statistics for figure 55 are as follows:

- $N = 514$ .
- $R^2 = 11.8$  percent.

$$E = a * \sqrt{fc} + b$$

**Figure 56. Equation. Model form for  $E$  as a function of compressive strength with slope and intercept.**

Regressed coefficients for figure 56 are as follows:

- $a = 31,624.6$ .
- $b = 2,013,192$ .

Regression statistics for figure 56 are as follows:

- $N = 514$ .
- $R^2 = 11.8$  percent.

$$E_c = a * f_c^b$$

**Figure 57. Equation.  $E_c$ .**

Regressed coefficients for figure 57 are as follows:

- $a = 388,082$ .
- $b = 0.2809$ .

Regression statistics for figure 57 are as follows:

- $N = 514$ .
- $R^2 = 12.3$  percent.

$$E = a * (UW)^b * (fc)^c$$

**Figure 58. Equation.  $E$  as function of unit weight and compressive strength.**

Regressed coefficients for figure 58 are as follows:

- $a = 80,849.3$ .
- $b = 0.3648$ .
- $c = 0.2527$ .

Regression statistics for figure 58 are as follows:

- $N = 514$ .
- $R^2 = 10.8$  percent.

The quality of prediction in the validated models is poor, as indicated by the  $R^2$  values reported for figure 55 through figure 58. This trend is common with elastic modulus models, especially considering that the data used in this study were not generated from controlled laboratory experiments. Also, while compressive strength is the most commonly used strength parameter and correlations with the compressive strength can be implemented most easily, there is an inherent drawback in correlating modulus to compressive strength. Modulus does not test the material to its limits. Instead, it is more indicative of the elastic deformational characteristics of the material. The data contain modulus measured at a wide range of ages. Therefore, the new models developed utilized other mix parameters that impact modulus, including age.

### Elastic Modulus Model 1: Model Based on Aggregate Type

The PCC elastic modulus model can be expressed as follows:

$$E_c = (4.499 * (UW)^{2.3481} * (f_c)^{0.2429}) * D_{agg}$$

**Figure 59. Equation. Prediction model 9 for  $E_c$ .**

Where:

$E_c$  = PCC elastic modulus, psi.

$UW$  = Unit weight, lb/ft<sup>3</sup>.

$f_c$  = Compressive strength.

$D_{agg}$  = Regressed constant depending on aggregate type as follows:

- = 1.0 for andesite, limestone, and sandstone.
- = 0.9286 for basalt.
- = 1.0079 for chert.
- = 0.9215 for diabase.
- = 1.0254 for dolomite.
- = 0.8333 for granite.
- = 0.9511 for quartzite.

The development of the model required the use of a model form that accommodates aggregate type as categorical variables (assigned values of 1, 0). The values for  $D_{agg}$  were initialized to 1.0 at the start of the analyses and allowed to iteratively determine individual values for each aggregate type. The model had 71 observations, an  $R^2$  value of 35.8 percent, and an RMSE of approximately 500,000 psi.

The model indicates that the factor that accounts for the aggregate type,  $D_{agg}$ , has a value of 1.0 for andesite, limestone, and sandstone. Basalt, diabase, granite, and quartzite have lower  $D_{agg}$  values and therefore lower modulus values than mixes using andesite, limestone, and sandstone

aggregates. Likewise, chert and dolomite have higher values. Table 18 provides details of the range of data used to develop the model.

**Table 18. Range of data used for elastic modulus model based on aggregate type.**

Parameter	Minimum	Maximum	Average
Compressive strength	1,990	11,310	7,550
Unit weight	137	156	146
Elastic modulus	1,450,000	6,800,000	4,629,646

Figure 60 and figure 61 show the predicted versus measured plot and the residual plot, respectively. The  $R^2$  value is reasonable and therefore presented as a feasible model.

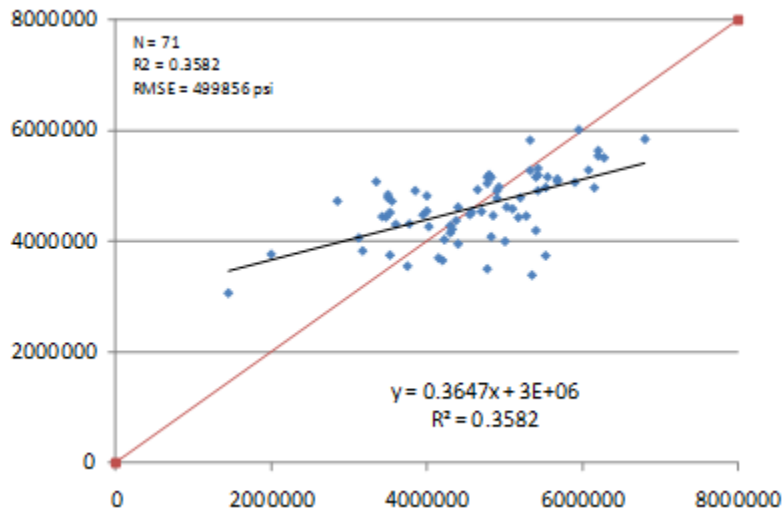


**Figure 60. Graph. Predicted versus measured for elastic modulus model based on aggregate type.**

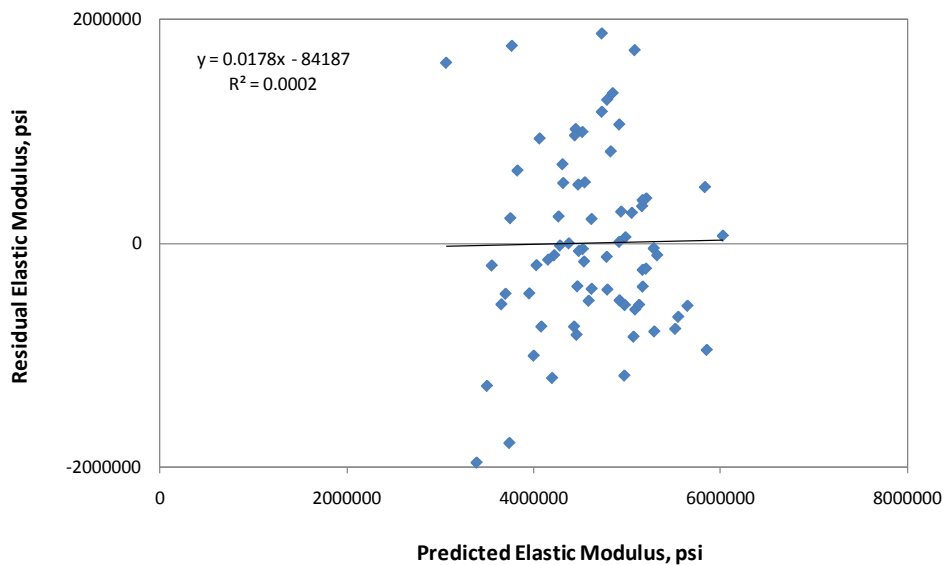


**Figure 61. Graph. Residual errors for elastic modulus model based on aggregate type.**

## Elastic Modulus Model 2: Model Based on Age and Compressive Strength

The model can be expressed as follows:

$$E_{c,t} = 59.0287 * (f'c_t)^{1.3} * (\ln(\frac{t}{0.03}))^{-0.2118}$$

**Figure 62. Equation. Prediction model 10 for  $E_{c,t}$ .**

Where:

$E_{c,t}$  = Elastic modulus at age  $t$ , years.

$f'c_t$  = Compressive strength at age  $t$ , years.

$t$  = Age at which modulus is determined, years.

The model uses 371 data points, has an  $R^2$  value of 26.14 percent, and an RMSE of about 900,000 psi. Table 19 shows the results of the nonlinear analysis, and table 20 provides details of the range of data used to develop the model.

**Table 19. Regression statistics for elastic modulus model based on age and compressive strength.**

Parameter Constants	Estimate	Standard Error	Approximate 95 Percent Confidence Limits
$a$	59.0287	2.8881	53.3495 to 64.7079
$b$	-0.2118	0.0284	-0.2677 to -0.1559

**Table 20. Range of data used for elastic modulus model based on age and compressive strength.**

Parameter	Minimum	Maximum	Average
Compressive strength	1,990	12,360	7,361
Pavement age	0.0384	45.3836	14.0900
Elastic modulus	1,450,000	6,800,000	4,586,545

The measured versus predicted plot and the residuals plot for this model are shown in figure 63 and figure 64, respectively.

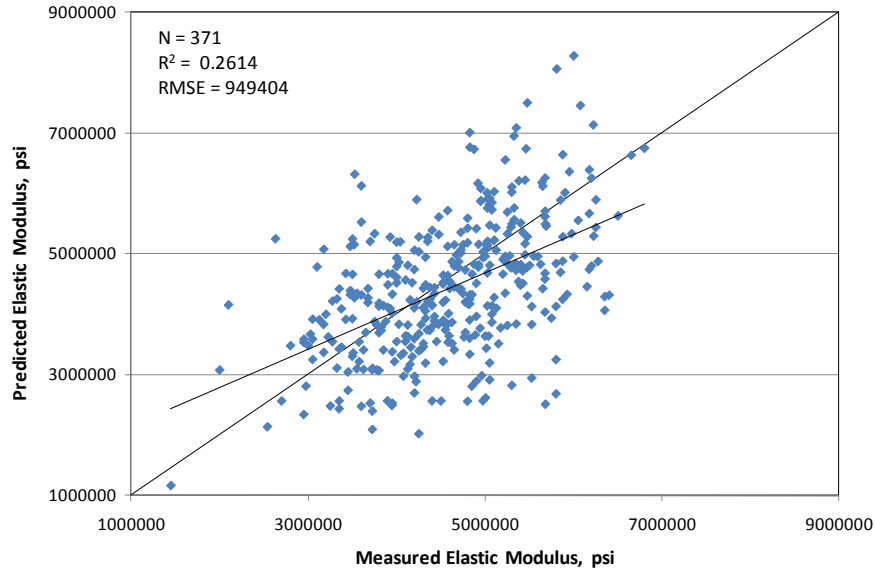


**Figure 63. Graph. Predicted versus measured for elastic modulus model based on age and compressive strength.**

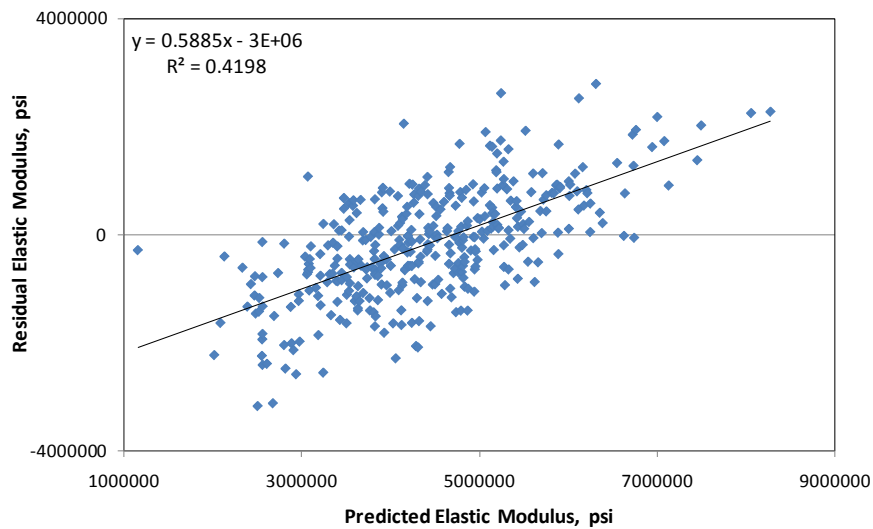


**Figure 64. Graph. Residual errors for elastic modulus model based on age and compressive strength.**

### Elastic Modulus Model 3: Model Based on Age and 28-Day Compressive Strength

Since the 28-day compressive strength is usually available for PCC materials, a predictive model based on age and the 28-day compressive strength can be useful in many situations. The relationship developed for these variables can be expressed as follows:

$$E_{c,t} = 375.6 * (f'_{c_{28\text{-day}}})^{1.1} * (\ln(\frac{t}{0.03}))^{0.00524}$$

**Figure 65. Equation. Prediction model 11 for  $E_{c,t}$ .**

Where:

$E_{c,t}$  = Elastic modulus at age  $t$ , years.

$f'c_{28-day}$  = 28-day compressive strength.

$t$  = Age at which modulus is determined, years.

The model used 46 data points, had an  $R^2$  value of 16.32 percent, and an RMSE of about 1,183,400 psi. Table 21 shows the results of the nonlinear analysis, and table 22 provides details of the range of data used to develop the model.

**Table 21. Regression statistics for elastic modulus model based on age and 28-day compressive strength.**

Parameter Constants	Estimate	Standard Error	Approximate 95 Percent Confidence Limits	
$a$	375.6	31.4592	312.5	439.3
$b$	0.00524	0.0714	-0.1388	-0.1492

**Table 22. Range of data used for elastic modulus model based on age and 28-day compressive strength.**

Parameter	Minimum	Maximum	Average
28-day compressive strength	3,034	7,912	5,022
Pavement age	0.0384	4.5288	0.9153
Elastic modulus	1,450,000	6,221,000	4,732,101

The measured versus predicted plot and the residuals plot for this model are shown in figure 66 and figure 67, respectively. This model uses data up to an age of 1 year. It is more appropriate for estimating the short-term modulus of a project and for supplementing strength estimates used to determine opening time for traffic.

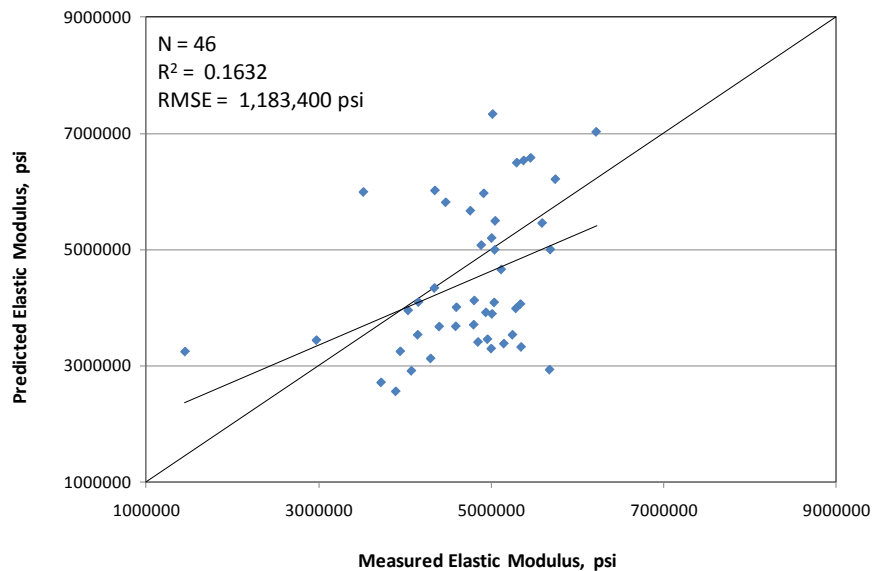


**Figure 66. Graph. Predicted versus measured for elastic modulus model based on age and 28-day compressive strength.**

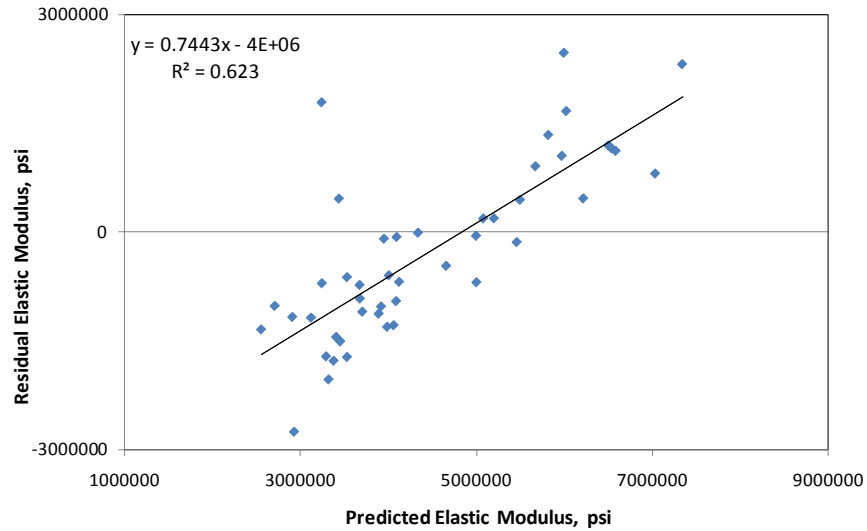


**Figure 67. Graph. Residual errors for elastic modulus model based on age and 28-day compressive strength.**

### Limitations of Elastic Modulus Models

An examination of the statistics proposed for determining elastic modulus suggests that they do not possess the predictive ability of the other material parameters presented in this study. The models are considered fair but not excellent. They provide users with an option of moderate estimates when no information about the elastic modulus is available. Therefore, it is recommended that users exercise caution when using the predicted elastic modulus values for analyses.

### PCC TENSILE STRENGTH MODELS

#### PCC Tensile Strength Model Based on Compressive Strength

This model development served as both a validation and development of a new correlation using the LTPP database. The model form used was a power equation and can be expressed as follows:

$$f_t = 8.9068 * (f'_c)^{0.4785}$$

**Figure 68. Equation. Prediction model 12 for  $f_t$ .**

Where:

$f_t$  = Indirect tensile strength of the PCC material.

$f'_c$  = Compressive strength of the mix determined at the same age.

The model statistics are presented in table 23. The model was developed using 541 data points with an  $R^2$  value of 42.09 percent and an RMSE of 61 psi. Table 24 provides details of the range of data used to develop the model.

**Table 23. Model statistics for tensile strength prediction model.**

Parameter	Estimate	Standard Error	95 Percent Confidence Limits
Coefficient	8.9068	2.0204	4.9381 to 12.8756
Power	0.4785	0.0256	0.4282 to 0.5288

**Table 24. Range of data used for tensile strength prediction model.**

Parameter	Minimum	Maximum	Average
Compressive strength	1,990	12,360	6,763
Tensile strength	316	1,012	600

Figure 69 and figure 70 show the predicted versus measured plot and the residual errors plot, respectively. Figure 71 shows the sensitivity of the model to compressive strength. The relationship developed shows that for typical ranges of compressive strength (i.e., 3,000 to 6,000 psi), the PCC tensile strength varies from about 400 to 570 psi, which is a reasonable range for this strength parameter.

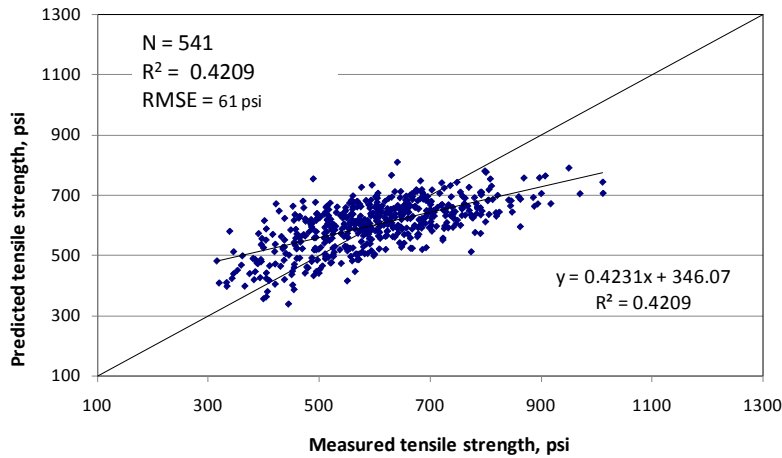


**Figure 69. Graph. Predicted versus measured for tensile strength model.**

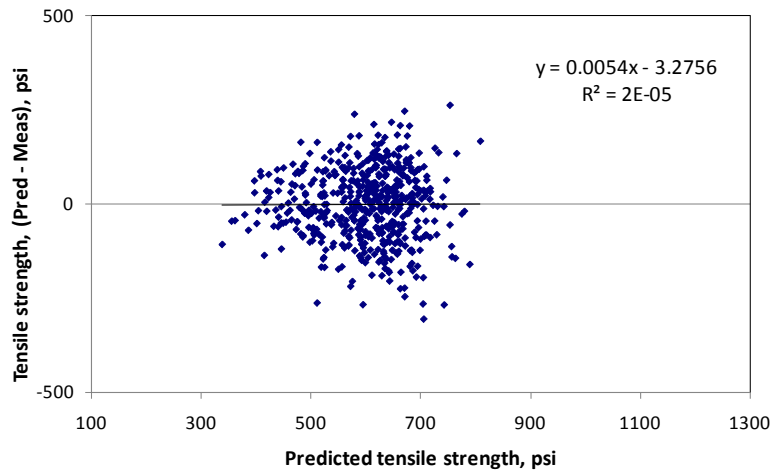


**Figure 70. Graph. Residual errors plot for tensile strength model.**

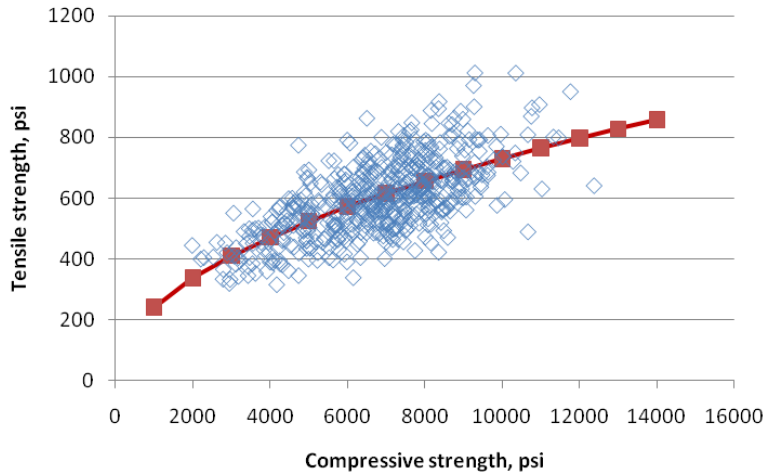


**Figure 71. Graph. Sensitivity of tensile strength prediction model to change compressive strength.**

## PCC CTE MODELS

### Current Issue with CTE Overestimation in LTPP Data

CTE tests of the PCC specimens from LTPP sections were performed by FHWA’s Turner-Fairbank Highway Research Center (TFHRC) using the AASHTO TP 60 protocol.<sup>(11)</sup> TFHRC initiated an inter-laboratory study during which an error was discovered with the protocol and procedure used to measure concrete CTE. The source of the error was in the assumption of a single CTE value for the calibration specimen. Testing performed at independent laboratories revealed that a CTE value must be determined for each calibration specimen, and the calibration specimen should be tested over the same range of temperature over which the concrete CTE is determined—50 to 122 °F. Not meeting these two conditions caused an overestimation of the reported CTE by approximately 0.83 inch/inch/°F. Since all of the initial LTPP testing for CTE had been done in one laboratory with one calibration specimen, the calibration offset can be corrected in the database, and it has been corrected in *Long-Term Pavement Performance Standard Data Release 24.0*.<sup>(12)</sup>

This overestimation of the CTE has significant ramifications, especially in light of the fact that the TFHRC has tested over 2,100 specimens for the LTPP program and the fact that the LTPP database was the primary source for the national calibration of the AASHTO MEPDG rigid pavement performance models. The national calibration coefficients for all JPCP and CRCP performance models may be invalid, and the models may need to be recalibrated. As a result, local implementation efforts may be delayed.

The impact of this error in the CTE values on the current study was described in an internal status report submitted to LTPP. *LTPP Standard Data Release Version 23.0* contained the uncorrected CTE values; therefore, the CTE models developed in this study are not applicable for the corrected data.<sup>(10)</sup> However, the models demonstrate the ability to develop correlations, and the procedures herein may be repeated for the corrected data.

**CTE Model 1: CTE Based on Aggregate Type (Level 3 Equation for MEPDG)**

CTE test data were averaged for each aggregate type, which constitutes level 3 inputs for MEPDG. Table 25 lists the average PCC CTE for each aggregate type as found in the literature. The data are in general agreement, providing a degree of confidence in the level 3 MEPDG input recommendations. The average CTE values determined from the data subset are recommended by this study.

**Table 25. Prediction model 13 for PCC CTE based on aggregate type, x 10<sup>-6</sup> inch/inch/°F.**

<b>Aggregate Type</b>	<b>Average From Literature</b>	<b>Average From All LTPP Data</b>	<b>Average From Data Used in Model (Recommended)</b>
Basalt	4.85	5.11	4.86
Chert	6.55	6.24	6.90
Diabase	4.85	5.33	5.13
Dolomite	5.75	5.79	5.79
Gabbro	4.85	5.28	5.28*
Granite	4.55	5.62	5.71
Limestone	4.25	5.35	5.25
Quartzite	6.85	6.07	6.18
Andesite	4.85	4.99	5.33
Sandstone	6.05	5.98	6.33
<i>N</i>		228	91

\*There were no samples with a Gabbro aggregate type in the data used in the model. Hence, the average from the entire dataset is recommended.

Figure 72 shows a plot of recommended CTE values versus average CTE values obtained from other sources. While they are in fairly good agreement, the values recommended from this study are slightly higher for most cases. This can be explained by the overestimation of CTE during testing.

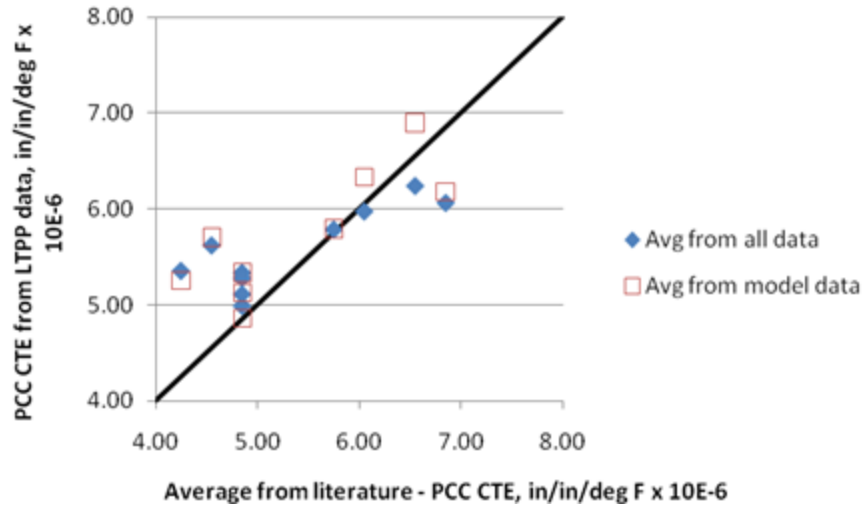


**Figure 72. Graph. Comparison of average values from other sources and recommended CTE values based on aggregate type from LTPP data.**

**CTE Model 2: CTE Based on Mix Volumetrics (Level 2 Equation for MEPDG)**

The PCC CTE model based on mix volumetrics was established as follows:

$$CTE_{PCC} = CTE_{CA} * V_{CA} + 6.4514 * (1 - V_{CA})$$

**Figure 73. Equation. Prediction model 14 for  $CTE_{PCC}$ .**

Where:

$CTE_{CA}$  = Constant determined for each aggregate type as shown in table 26.

The model statistics are presented in table 26, and details of the range of data used to develop the model are presented in table 27. The model has 89 data points, an  $R^2$  value of 44.15 percent, and an RMSE of 0.35006 psi.

**Table 26. Statistical analysis results for CTE model based on mix volumetrics.**

Parameter	Comment	Estimate	Standard Error	95 Percent Confidence Limits	
<i>c</i>	N/A	6.4514	0.1889	6.0758	6.827
<i>d</i>	$CTE_{CA}$ for basalt	3	0	3	3
<i>e</i>	$CTE_{CA}$ for chert	6.4	0	6.4	6.4
<i>f</i>	$CTE_{CA}$ for diabase	3.4835	1.2824	0.9337	6.0333
<i>g</i>	$CTE_{CA}$ for dolomite	5.1184	0.408	4.3071	5.9297
<i>h</i>	$CTE_{CA}$ for gabbro	3.75	N/A	N/A	N/A
<i>i</i>	$CTE_{CA}$ for granite	4.7423	0.4188	3.9096	5.5749
<i>j</i>	$CTE_{CA}$ for limestone	3.2886	0.3579	2.5771	4.0001
<i>k</i>	$CTE_{CA}$ for quartzite	6.1	0	6.1	6.1
<i>l</i>	$CTE_{CA}$ for andesite	3.6243	1.4539	0.7336	6.515
<i>m</i>	$CTE_{CA}$ for sandstone	4.5	0	4.5	4.5

N/A = Not applicable.

**Table 27. Range of data used for CTE model based on mix volumetrics.**

Parameter	Minimum	Maximum	Average
Coarse aggregate content	582	2,730	1,811
Coarse aggregate specific gravity	2.42	2.86	2.65
w/c ratio	0	0.71	0.45
Coarse aggregate volume fraction	0.13	0.62	0.41
Mortar volume	0.38	0.87	0.59

The predicted versus measured plot and the residual error plots are presented in figure 74 and figure 75, respectively.

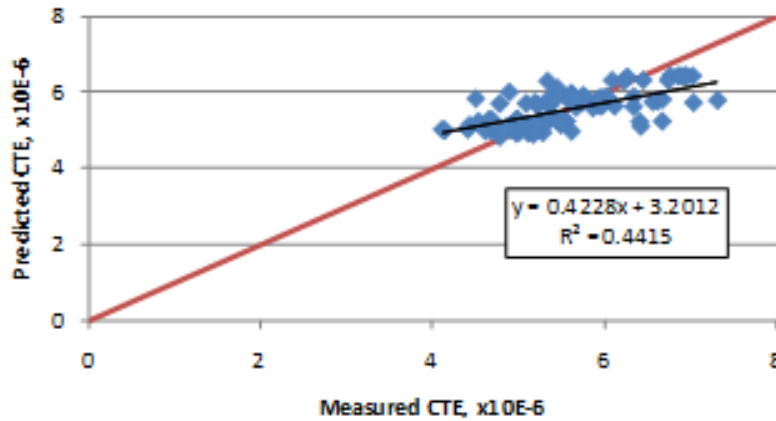


**Figure 74. Graph. Predicted versus measured for CTE model based on mix volumetrics.**

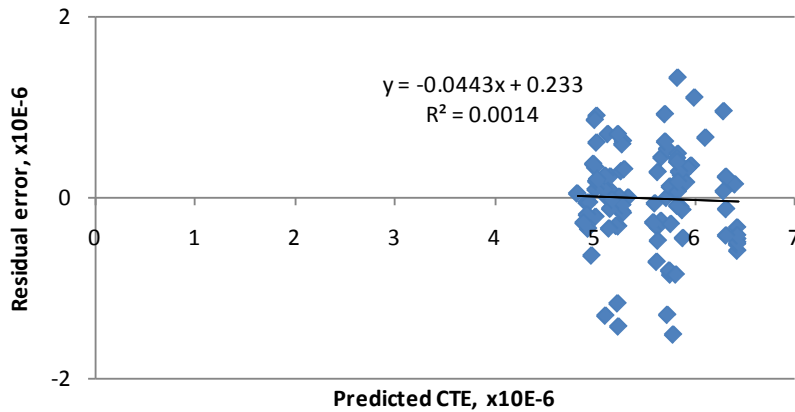


**Figure 75. Graph. Residual errors for CTE model based on mix volumetrics.**

The constant,  $C$ , determined as 6.4514, is equivalent to the CTE of the mortar. (At TFHRC, using the AASHTO TP 60 uncorrected values, a CTE value of 6.2 for mortar containing silica sand was determined, validating this equation.<sup>(12)</sup>) Since the mortar (all components of the mix design except the coarse aggregate) occupies a large volume of the matrix, it was necessary for the model to predict higher CTE for increased mortar proportions (or decreasing coarse aggregate proportions). In optimizing the model and selecting the representative CTE for each aggregate type, it was ensured that the CTE of the aggregate was not above 6.4514.

Figure 76 and figure 77 show a comparison of the predicted CTE values with average values reported in literature for each aggregate type. Figure 78 shows the sensitivity of the model to coarse aggregate content. As expected, CTE decreases as the coarse aggregate content increases (or mortar volume decreases). While this is true for most cases, it was also observed that for aggregates with high CTE values, such as chert and quartzite, the CTE of the aggregate approaches the CTE of the mortar, thereby showing little or no sensitivity to coarse aggregate content. As with all other models, the user is advised to verify model predictions with other sources of information. If possible, both CTE models should be evaluated simultaneously to obtain a range.

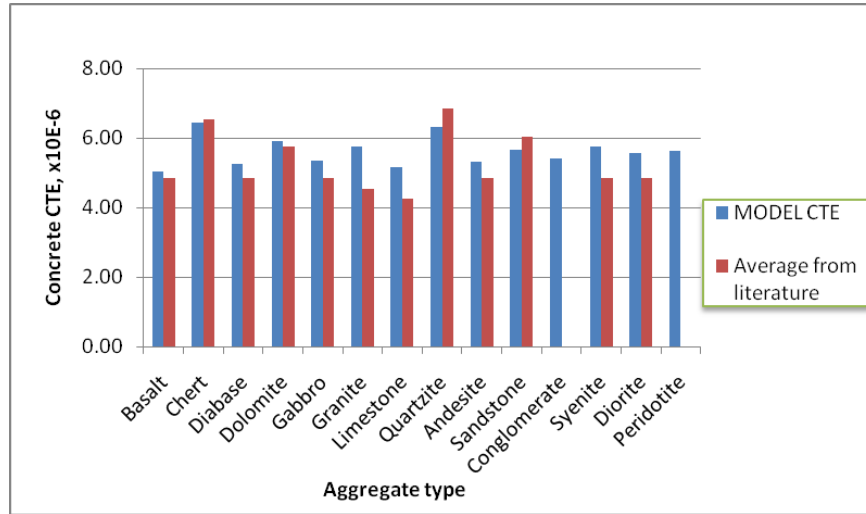


**Figure 76. Graph. Comparison of CTE model prediction with average values reported in literature for each aggregate rock type.**

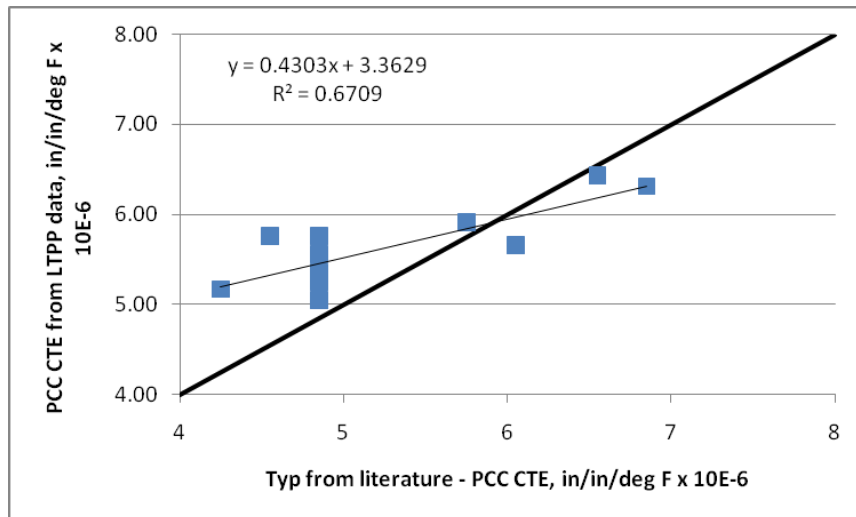


**Figure 77. Graph. CTE model prediction versus average values reported in literature for each aggregate rock type.**

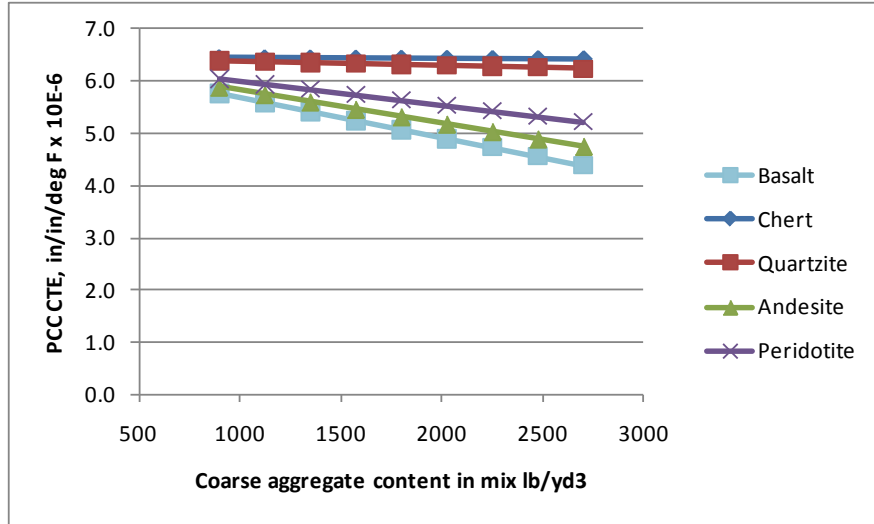


**Figure 78. Graph. Sensitivity of the CTE model to coarse aggregate content.**

## CHAPTER 4. RIGID PAVEMENT DESIGN FEATURES MODELS

The models developed for the prediction of MEPDG-specific inputs fall under the design features category. In developing these models, the dependent variable (e.g.,  $\Delta T$  for JPCP design) was determined through performing several trial and error runs of the MEPDG and establishing the optimum value that minimizes the error prediction. The independent variables were obtained from the LTPP database or MEPDG calibration files.

The MEPDG design files used to generate the dependent variable data were obtained from the model calibration performed under NCHRP 1-40D, which produced the MEPDG software program version 1.0 in 2007.<sup>(4)</sup> However, minor changes and software bug fixes have been performed since then, and the official version available at the time of this study was the MEPDG software version 1.1. Therefore, these models presented under this section are valid only for use with the distress calibration model of version 1.1 of the MEPDG software. The prediction models presented here for the estimation of design feature inputs therefore may not be valid once the products of future MEPDG updates and revisions are released.

### $\Delta T$ —JPCP DESIGN

The equation developed to estimate the  $\Delta T$  gradient variable can be expressed as follows:

$$\begin{aligned} \Delta T / \text{inch} = & -5.27805 - 0.00794 * TR - 0.0826 * SW + 0.18632 * PCCTHK \\ & + 0.01677 * uw + 1.14008 * w/c + 0.01784 * latitude \end{aligned}$$

**Figure 79. Equation. Prediction model 15 for  $\Delta T$ /inch.**

Where:

$\Delta T / \text{inch}$  = Predicted average gradient through JPCP slab, °F/inch.

$TR$  = Difference between maximum and minimum temperature for the month of construction, °F.

$SW$  = Slab width, ft.

$PCCTHK$  = JPCP slab thickness, inch.

$uw$  = Unit weight of PCC used in JPCP slab, lb/ft<sup>3</sup>.

$w/c$  = Water to cement ratio.

$latitude$  = Latitude of the project location, degrees.

The model considers climate ( $TR$ ,  $latitude$ ), design ( $SW$ ,  $PCCTHK$ ), and material ( $uw$ ,  $w/c$ ) parameters. The model statistics are presented in table 28. The model was developed with 147 data points, has an  $R^2$  value of 49.67 percent, and an RMSE of 0.3199 psi. Table 29 provides details of the range of data used to develop the model.

**Table 28. Regression statistics for JPCP  $\Delta T$  model.**

Variable	DF	Estimate	Standard Error	t-value	$P_r >  t $	VIF
Intercept	1	-5.27805	1.06943	-4.94	< 0.0001	0
<i>TR</i>	1	-0.00794	0.00396	-2	0.047	1.86047
<i>SW</i>	1	-0.0826	0.03432	-2.41	0.0174	1.07141
<i>PCCTHK</i>	1	0.18632	0.0195	9.55	< 0.0001	1.0642
<i>uw</i>	1	0.01677	0.00669	2.51	0.0133	1.22792
<i>w/c</i>	1	1.14008	0.2914	3.91	0.0001	1.14857
<i>latitude</i>	1	0.01784	0.0072	2.48	0.0144	1.85265

**Table 29. Range of data used for JPCP  $\Delta T$  model.**

Parameter	Minimum	Maximum	Average
Temperature range	21.2	64.5	47.4
Slab width	12.0	14.0	12.5
PCC thickness	6.4	14.3	9.6
Unit weight	134	156	147
w/c ratio	0.27	0.72	0.46
Latitude	27.93	49.60	39.58

Figure 80 shows the predicted versus measured for the proposed JPCP  $\Delta T$  gradient model, while figure 81 shows the residual errors. Note that the measured data here refers to the  $\Delta T$  gradient determined by matching MEPDG prediction to field performance. Figure 82 shows the predicted versus measured  $\Delta T$  for the model.

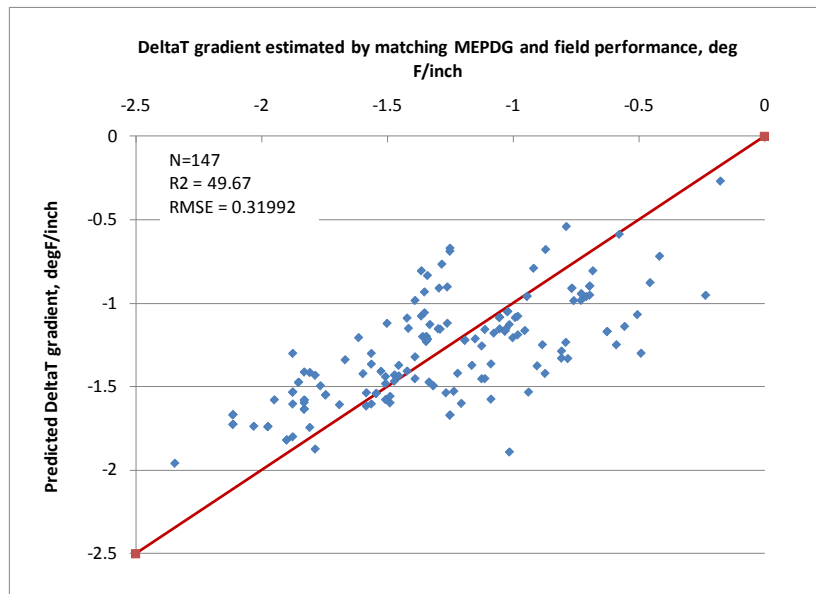


**Figure 80. Graph. Predicted versus measured for JPCP  $\Delta T$  gradient model.**

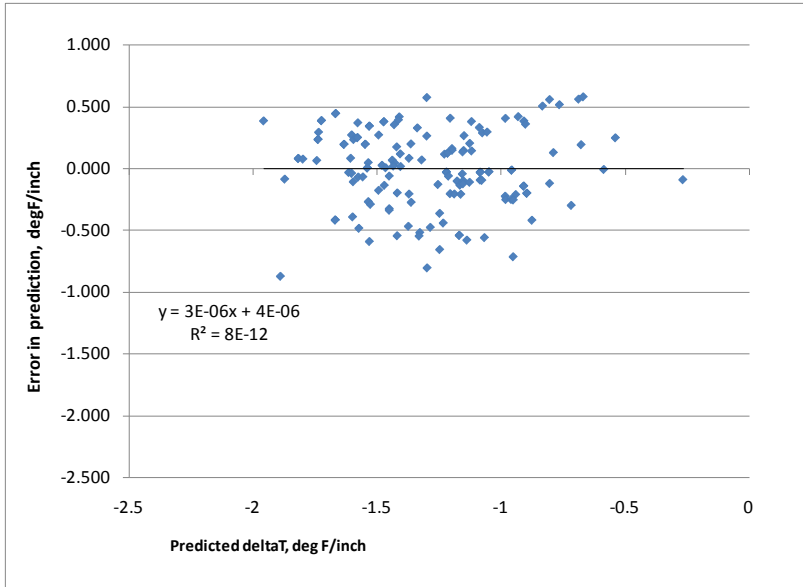


**Figure 81. Graph. Residual errors for JPCP *deltaT* gradient model.**

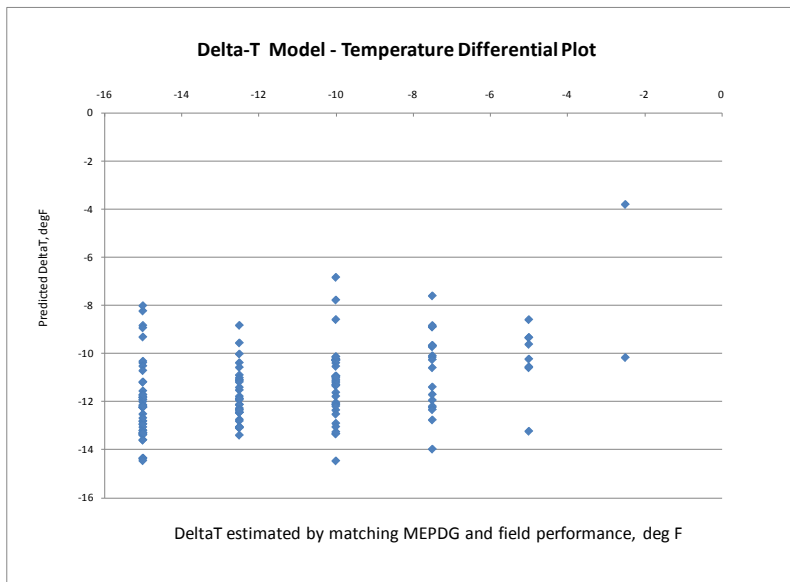


**Figure 82. Graph. Predicted versus measured *deltaT* based on the JPCP *deltaT* gradient model.**

Figure 83 through figure 89 present the sensitivity analysis performed to examine the impact of varying the model parameters on its prediction. The parameters included are temperature range, slab width, slab thickness, unit weight, w/c ratio, and latitude. For each sensitivity analysis, the variable of interest was varied while holding all other variables constant at their typical values. Typical values used in this analysis were 24 °F temperature range, 12-ft slab width, 10-inch slab thickness, 145 lb/ft<sup>3</sup> unit weight, 0.40 w/c ratio, and 40 degrees latitude.

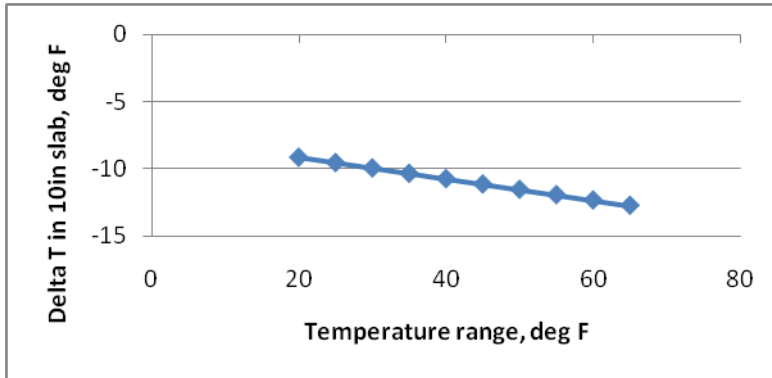


Figure 83. Graph. Sensitivity of predicted  $\Delta T$  to temperature range during month of construction.

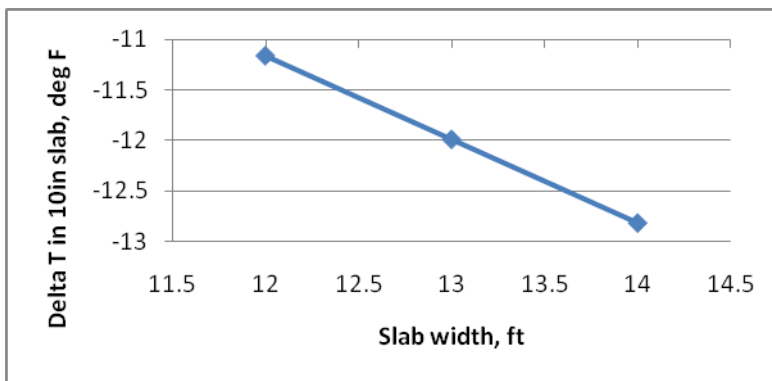


Figure 84. Graph. Sensitivity of predicted  $\Delta T$  to slab width.

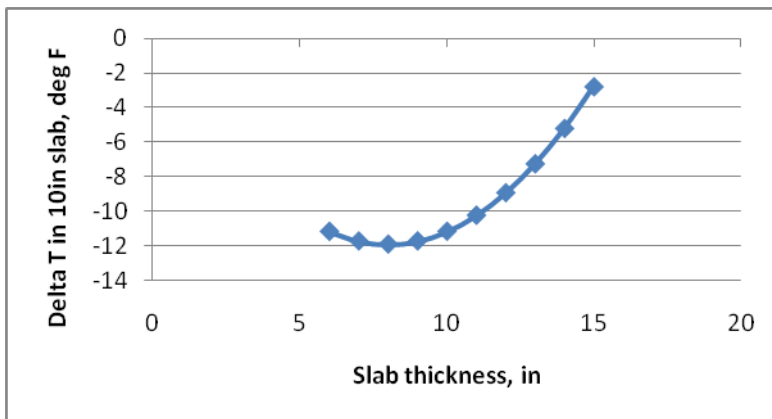


Figure 85. Graph. Sensitivity of predicted  $\Delta T$  to slab thickness.

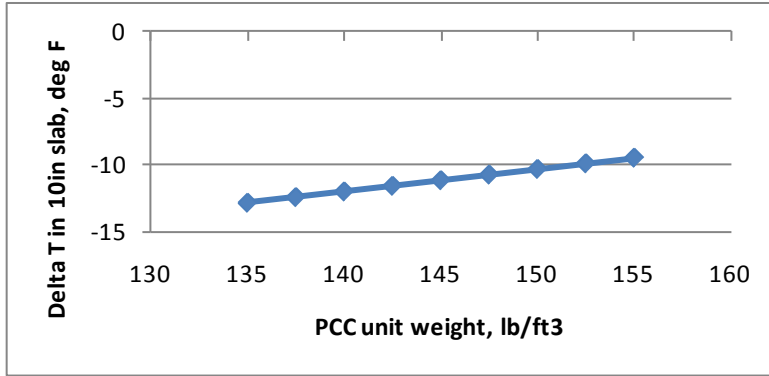


Figure 86. Graph. Sensitivity of predicted *deltaT* to PCC slab unit weight.

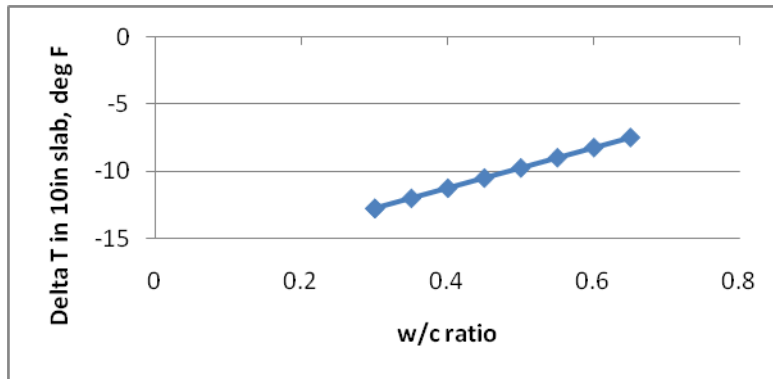


Figure 87. Graph. Sensitivity of predicted *deltaT* to PCC w/c ratio.

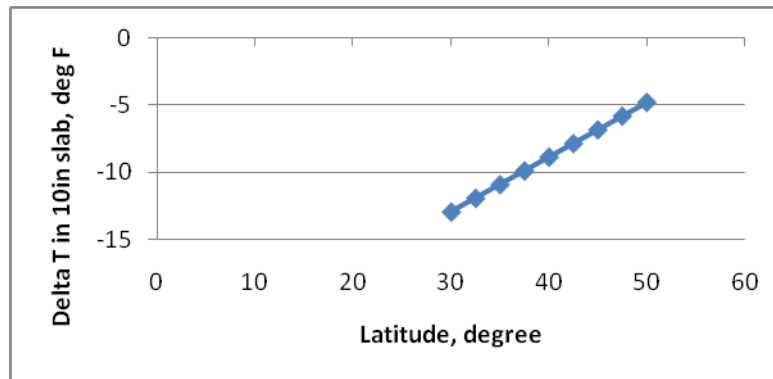
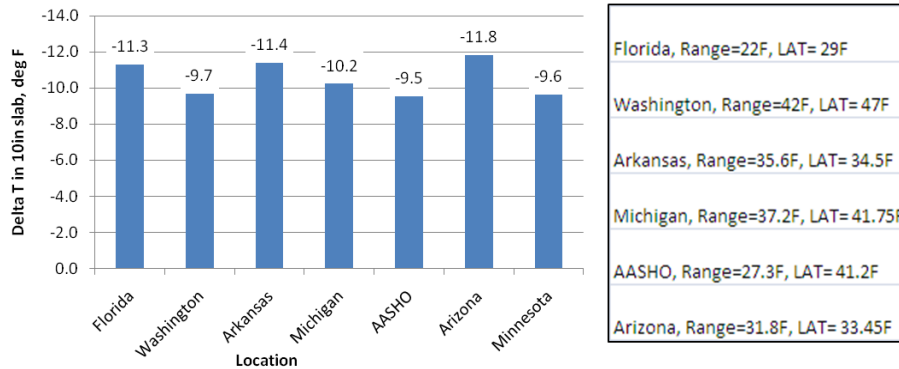


Figure 88. Graph. Sensitivity of predicted *deltaT* to latitude of the project location.



**Figure 89. Graph. Predicted  $\delta T$  for different locations in the United States.**

The following are brief observations from these sensitivity analyses:

- For the typical values used for each of these variables, the  $\delta T$  gradients estimated are in a reasonable range.
- An increase in local climate temperature range increases the temperature gradient (see figure 83). The local climate temperature range is indicative of the level of temperature drop the project location can experience. The larger the difference in the temperature between day and night (assuming paving is performed in the daytime), the larger the negative temperature gradient locked into the slab as the slab hardens within a 24-h period.
- Wider slabs produce a larger built-in gradient (see figure 84), as has been validated in several field studies. The total thermal expansion is larger for a longer/wider slab; therefore, the resulting curvature of the slab induces a greater lift-up at the slab corners. The data did not show a significant effect of the slab length or joint spacing parameter.
- Thicker slabs reduce the  $\delta T$  gradient, as shown in figure 85. This is the expected trend, as thicker slabs (due to a greater weight) tend to restrain the corners from curling up as the concrete hardens. This figure also shows that for very thin slabs (< 8 inches), the effect is reversed. The physical significance of this cannot be fully explained or supported with data. Therefore, it is necessary to evaluate the sensitivity to each parameter while selecting  $\delta T$  for each project.
- The larger unit weight of the PCC material used in the JPCP slab also reduces the magnitude of built-in gradient (see figure 86) primarily because of the restraint provided by the heavier slab during hardening.
- Lower w/c ratios have a higher rate of hydration; therefore, the PCC slab remains plastic for a shorter duration of time. Strength gain offers the slab the rigidity necessary to bear against the base and does not allow the slab corners to curl up. Therefore, lower w/c ratios tend to have higher built-in gradients, as seen in figure 87. Furthermore, at very low w/c ratios, the PCC mix undergoes autogenous shrinkage, which increases the potential for higher gradients in the slab.

- Figure 88 and figure 89 show the effect of latitude on predicted *deltaT* gradients. The United States lies between 30 and 50 degrees latitude in the Northern Hemisphere. The full range of latitudes is covered in figure 88. While this plot might appear to show *deltaT*'s high degree of sensitivity to the latitude parameter, for routine predictions using this model, the temperature range is a critical input. In other words, a given maximum temperature in the southern United States could have a much different temperature range relative to a location in the northern United States with the same maximum temperature. Therefore, the latitude parameter has to be evaluated combined with the temperature range parameter as shown in figure 89. The predicted *deltaT* for several locations in the United States are presented.

### Using the JPCP *deltaT* Model

This section provides an example for the use of the JPCP *deltaT* model developed under this study. The section used to describe the process is the LTPP Specific Pavement Studies 2 section 04\_0213 located in Maricopa County, AZ, and constructed in July 1993. The following latitude, design, and material inputs required for the *deltaT* prediction model can be obtained from the MEPDG inputs:

- Latitude: 33.45 degrees north.
- PCC thickness: 8.3 inches.
- Slab width: 14 ft.
- PCC unit weight: 145.3 lb/ft<sup>3</sup>.
- PCC w/c ratio: 0.365.

The temperature range input to this model is the difference between the mean monthly maximum and minimum temperatures for the month of July from historical climate data records (as climate data included in the MEPDG). If the user does not have this information readily available, the data to compute the temperature range can be determined from the output file of the MEPDG analysis of this section. The output file (i.e., titled "04\_0213.xls") contains a worksheet titled "Climate" with key climate data for the specific location (or the virtual climate station created). This worksheet includes the monthly climate summary with minimum and maximum temperature by month for all years of data used under the headings "Min. Temp. (°F)" and "Max. Temp. (°F)," respectively. (Note that this summary also includes "Average Temp. (°F)," "Max. Range (°F)," "Precip. (in.)," "Average Wind (mph)," "Average Sun (%)," "Number Wet Days," and "Max. Frost (in.)." However, these data are not of relevance to the *deltaT* model.

For the month of July, the average minimum and maximum temperatures are 73 and 111.7 °F, respectively. The difference between these temperatures is 38.7 °F.

Using these inputs, the *deltaT* gradient can be calculated as -1.7457138 °F/inch. For the slab thickness of 8.3 inches, this is equivalent to a *deltaT* of -14.5 °F. This value is significantly

higher than the default -10 °F/inch. This input can be revised in an MEPDG file and reanalyzed to evaluate the predicted transverse cracking performance.

***deltaT*—CRCP DESIGN**

The equation developed to estimate the CRCP *deltaT* gradient variable is as follows:

$$\begin{aligned} \text{deltaT / inch} = & 12.93007 - 0.15101 * \text{MaxTemp} - 0.10241 * \text{MaxTempRange} + 3.279 * \text{Chert} \\ & + 1.55013 * \text{Granite} + 1.40009 * \text{Limestone} + 2.01838 * \text{Quartzite} \\ & + 0.11299 * \text{PCCTHK} \end{aligned}$$

**Figure 90. Equation. Prediction model 16 for *deltaT*/inch.**

Where:

*deltaT/inch* = Predicted gradient in CRCP slab, °F/inch.

*MaxTemp* = Maximum temperature for the month of construction, °F.

*MaxTempRange* = Maximum temperature range for the month of construction, °F.

*PCCTHK* = JPCP slab thickness, inch.

*Chert* = 1 if PCC mix coarse aggregate is chert, or 0 if otherwise.

*Granite* = 1 if PCC mix coarse aggregate is granite, or 0 if otherwise.

*Limestone* = 1 if PCC mix coarse aggregate is limestone, or 0 if otherwise.

*Quartzite* = 1 if PCC mix coarse aggregate is quartzite, or 0 if otherwise.

The model considers climate (*MaxTemp* and *MaxTempRange*), design parameters (*PCCTHK*), and material (*Aggregate type*) parameters. The model statistics are presented in table 30. The model was developed with 35 data points, has an *R*<sup>2</sup> value of 82.5 percent, and an RMSE of 0.27932 psi. Table 31 provides details of the range of data used to develop the model.

**Table 30. Regression statistics for CRCP *deltaT* model.**

Variable	DF	Estimate	Standard Error	t-Value	<i>P<sub>r</sub></i> >  t	VIF
Intercept	1	12.93007	1.98459	6.52	< 0.0001	0
<i>MaxTemp</i>	1	-0.15101	0.01793	-8.42	< 0.0001	3.46347
<i>MaxTempRange</i>	1	-0.10241	0.01869	-5.48	< 0.0001	2.00933
<i>Chert</i>	1	3.279	0.30508	10.75	< 0.0001	2.24965
<i>Granite</i>	1	1.55013	0.22656	6.84	< 0.0001	4.96262
<i>Limestone</i>	1	1.40009	0.18956	7.39	< 0.0001	4.00053
<i>Quartzite</i>	1	2.01838	0.39449	5.12	< 0.0001	1.93773
<i>PCCTHK</i>	1	0.11299	0.0705	1.6	0.1207	1.68624

**Table 31. Range of data used for CRCP *deltaT* model.**

Parameter	Minimum	Maximum	Average
Maximum temperature	78.4	99.2	90.3
Temperature range	24.8	40.4	30.4
Chert	0	1	0.06
Granite	0	1	0.31
Limestone	0	1	0.46
Quartzite	0	1	0.03
PCC thickness	5.6	9.5	8.4

Figure 91 shows the predicted versus measured for the proposed CRCP *deltaT* gradient model, while figure 92 shows the residual errors. Note that the measured data here refers to the *deltaT* gradient determined by matching MEPDG prediction to field performance.

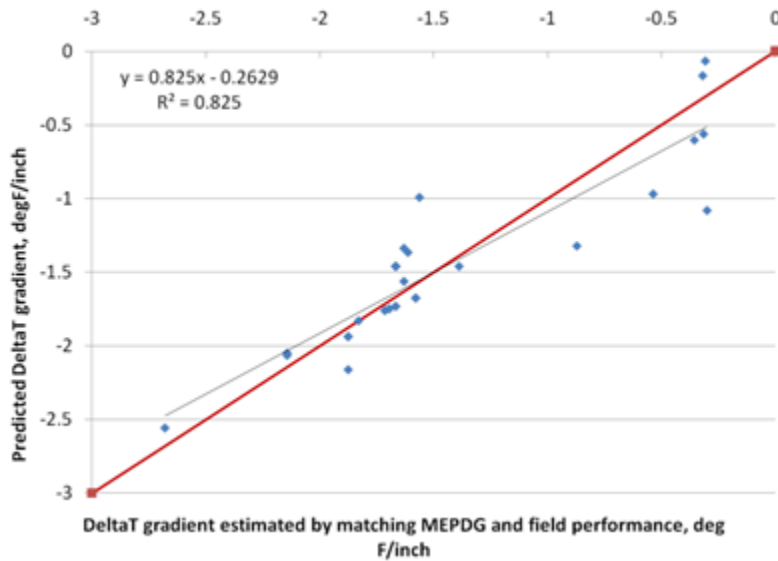


**Figure 91. Graph. Predicted versus measured for CRCP *deltaT* model.**

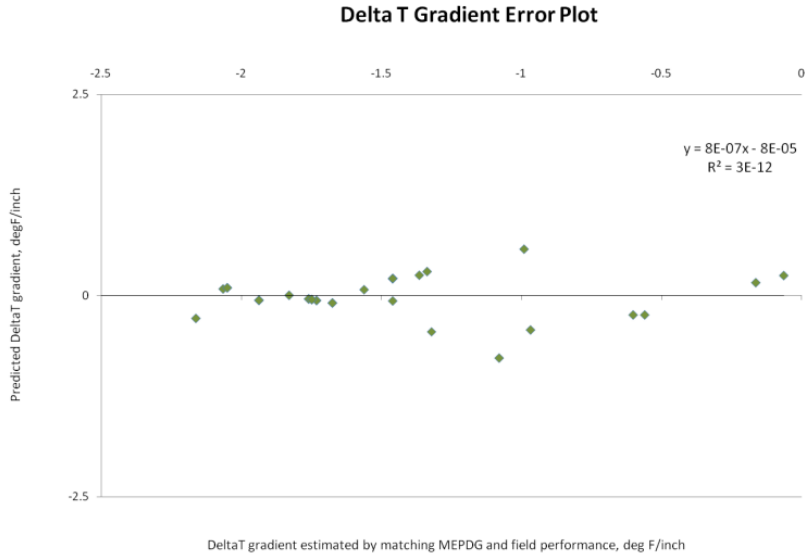


**Figure 92. Graph. Residual errors for CRCP *deltaT* model.**

Figure 93 through figure 96 show the sensitivity of the *deltaT* differential calculation to the parameters maximum temperature of the project location, maximum temperature range, CRCP slab thickness, and geographic location, respectively. The trends observed in the model—CRCP *deltaT* increasing with increasing maximum temperature and increasing temperature range—are reasonable. While the effect of slab thickness shows a linear relationship with the *deltaT* gradient, the magnitude of the coefficient for this variable results causes the *deltaT* differential (CRCP *deltaT* gradient  $\times$  thickness) to assume a nonlinear relationship with the *deltaT* differential, peaking at about 10 inches. Figure 96 shows the *deltaT* predictions for projects selected from LTPP sites in Texas, Illinois, Virginia, Mississippi, Oregon, and Georgia.

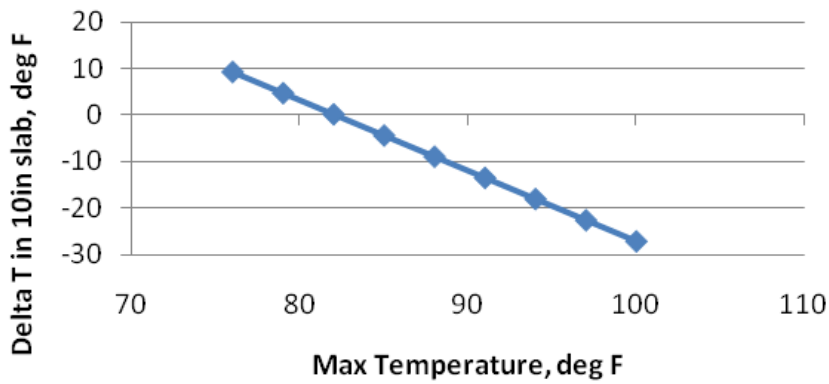


**Figure 93. Graph. Effect of maximum temperature on CRCP *deltaT* prediction model.**

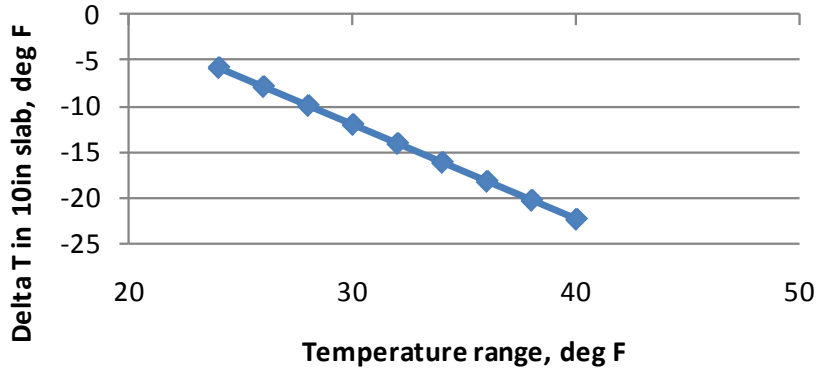


Figure 94. Graph. Effect of temperature range on CRCP *deltaT* prediction model.

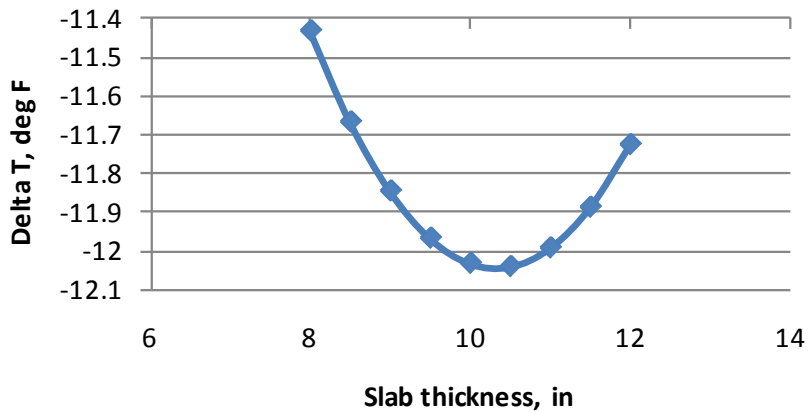


Figure 95. Graph. Effect of slab thickness on CRCP *deltaT* prediction model.

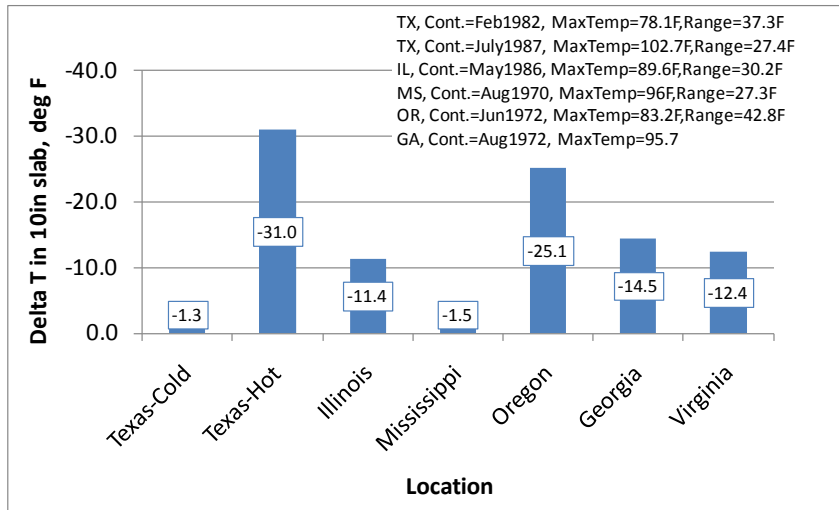


Figure 96. Graph. Effect of geographic location on CRCP *deltaT* prediction model.

The sensitivity analyses show reasonable trends but do not demonstrate that the model is robust. It is not clear, from an engineering standpoint, if the range of predicted values and their magnitudes are practical and realistic. The wide range of *deltaT* has a significant effect on design thickness. The data used to develop the model show very strong correlations, and it is likely that the predictions are valid, at least within a certain range of inputs. The current analyses and the data available are not adequate to determine these ranges. It is therefore recommended that this model be used with extreme caution.

### **Using the CRCP *deltaT* Model**

The CRCP *deltaT* model shares similarities with the JPCP *deltaT* model. The section used to describe the process is the LTPP General Pavement Studies section in Illinois, 17\_5020, which was constructed in May 1986. The CRCP thickness is 8.6 inches, and the PCC mix used a limestone aggregate. The following inputs can be directly obtained from the MEPDG input file:

- PCCTHK: 8.6 inches.
- *Chert*: 0.
- Granite: 0.
- Limestone: 1.
- Quartzite: 0.

The maximum temperature and maximum temperature range can be obtained by running the design file and deriving this input from the worksheet titled “Climate.” For the month of May, the maximum temperature and maximum temperature range for this location were 89.6 and 39.2 °F, respectively. Using these inputs, the CRCP *deltaT* gradient can be calculated as -1.3214 °F/inch. For the slab thickness of 8.6 inches, this is equivalent to a *deltaT* of -11.36 °F. This value is comparable to the -10-°F default. This input can be revised in an MEPDG file and reanalyzed to predict punchout development over time.

## CHAPTER 5. STABILIZED MATERIALS MODELS

As the LTPP database contains limited data on modulus values and index properties of stabilized materials, the only prediction model that can be developed for modulus prediction is that for LCB materials, which is included in this section.

### LCB ELASTIC MODULUS MODEL

The model developed can be expressed as follows:

$$E_{LCB} = 58156\sqrt{f'_{c,28d}} + 716886$$

**Figure 97. Equation. Prediction model 17 for  $E_{LCB}$ .**

Where:

$E_{LCB}$  = Elastic modulus of the LCB layer.

$f'_{c,28d}$  = 28-day compressive strength of the LCB material.

The predicted versus measured and the residual errors plots for this relationship are presented in figure 98 and figure 99, respectively. The model has an  $R^2$  value of 41.24 percent, an RMSE of 541,600 psi, and uses 11 data points. The compressive strength values range from 770 to 2,800 psi with an average value of 1,400 psi.

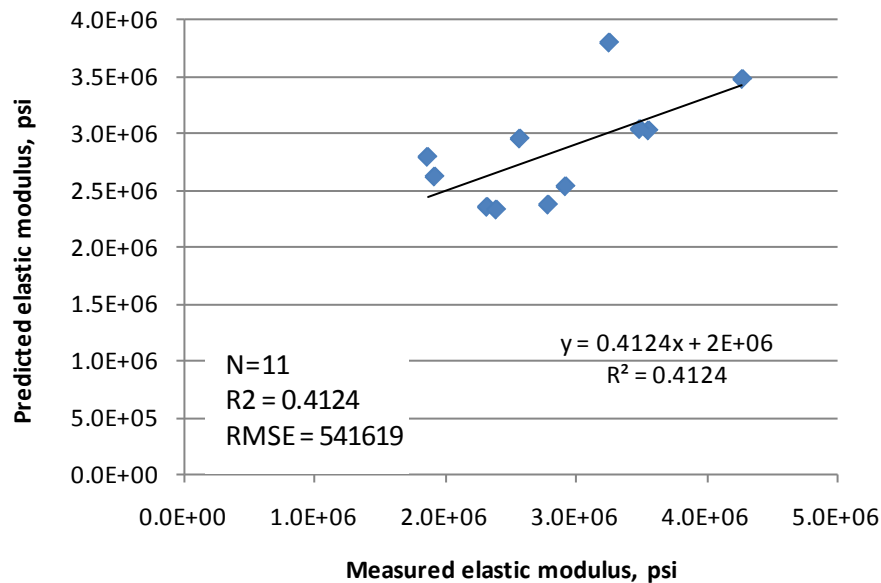


**Figure 98. Graph. Predicted versus measured for the LCB elastic modulus model.**

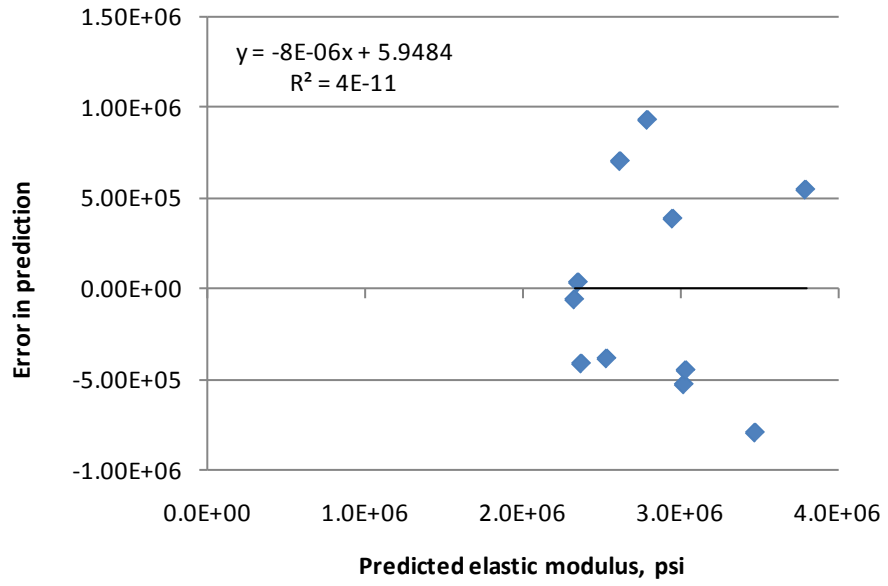


**Figure 99. Graph. Residual errors for the LCB elastic modulus model.**

## CHAPTER 6. UNBOUND MATERIALS MODELS

### RESILIENT MODULUS OF UNBOUND MATERIALS

The following model recommended for predicting the resilient modulus of unbound materials is based on the constitutive equation for modeling resilient modulus behavior when subjected to various stress states:

$$M_r = k_1 P_a \left( \frac{\theta}{P_a} \right)^{k_2} \left( \frac{\tau_{oct}}{P_a} \right)^{k_3}$$

**Figure 100. Equation.  $M_r$ .**

Where:

$\theta$  = Bulk stress =  $\sigma_1 + \sigma_2 + \sigma_3$ .

$\sigma_1$  = Principal stress.

$\sigma_2, \sigma_3$  = Confining pressure.

$P_a$  = Atmospheric pressure.

$\tau_{oct}$  = Octahedral normal stress =  $1/3 (\sigma_1 + 2 \sigma_3)$ .

$k_1, k_2, k_3$  = regression constants that are a function of soil properties, as defined in figure 101 through figure 103 of this report.

This model can be used for various soil types, and the model attributes ( $k_1, k_2$ , and  $k_3$ ) for a given soil type remain the same regardless of stress state. Furthermore, models used to predict constitutive model attributes for a given set of soil properties are recommended to characterize resilient modulus behavior rather than developing models individually for each possible combination of expected stress states.

#### Constitutive Model Parameter $k_1$

$$k_1 = 1446.2 - 4.56764 * PCTHALF + 4.92 * LL - 27.73 * OPTMOIST$$

**Figure 101. Equation. Prediction model 18 for  $k_1$ .**

Model statistics for  $k_1$  are as follows:

- $R^2 = 0.16$  percent.
- Standard error of estimate (SEE) = 237.4.
- $N = 1,029$ .

#### Constitutive Model Parameter $k_2$

$$k_2 = 0.45679 - 0.00073376 * PCTNO80 - 0.00269 * LL + 0.00060555 * PCTGRVL + 12.97 * D_{10}$$

**Figure 102. Equation. Prediction model 19 for  $k_2$ .**

Model statistics for  $k_2$  are as follows:

- $R^2 = 0.67$  percent.
- $SEE = 0.0934$ .
- $N = 1,032$ .

**Constitutive Model Parameter  $k_3$**

$$k_3 = -0.188 \text{ (for fine grained soils)}$$

$$k_3 = -0.153 \text{ (for coarse grained materials)}$$

**Figure 103. Equation. Prediction model 20 for  $k_3$ .**

Where:

$PCTHALF$  = Percent passing  $\frac{1}{2}$ -inch sieve.

$LL$  = Liquid limit, percent.

$OPTMOIST$  = Optimum moisture content, percent.

$PCTNO80$  = Percent passing No. 80 sieve.

$PCTGRVL$  = Percent gravel fraction (0.078- to 2.36-inch size).

$D_{10}$  = Maximum particle size of the smallest 10 percent of soil sample.

In the development of these models, a wide range of  $k_1$ ,  $k_2$ , and  $k_3$  parameters were used, which varied by soil class. Histograms showing the distribution of  $k_1$ ,  $k_2$ , and  $k_3$  values by soil class are shown in figure 104 through figure 106, respectively.

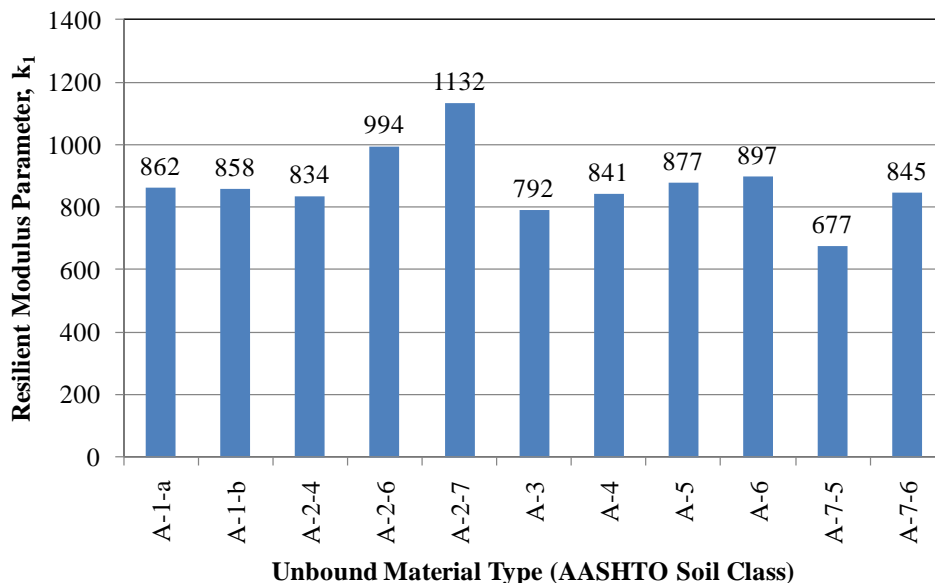


**Figure 104. Graph. Resilient modulus parameter  $k_1$  for unbound material types included in the model development database.**

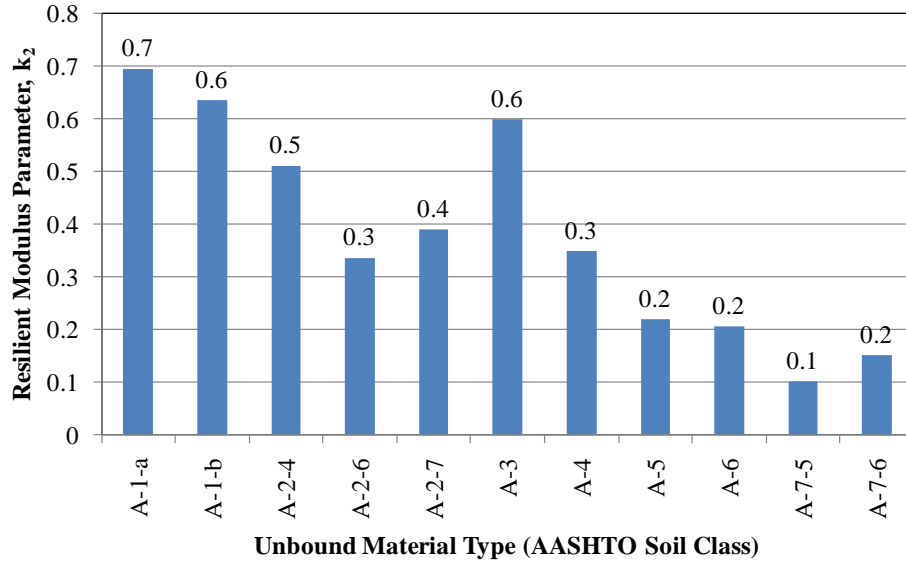


**Figure 105. Graph. Resilient modulus parameter  $k_2$  for unbound material types included in the model development database.**

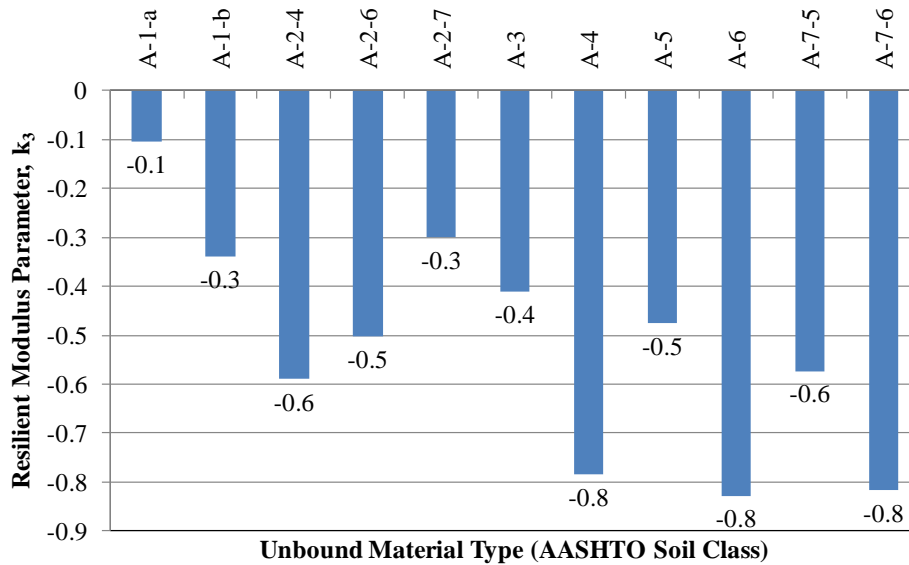


**Figure 106. Graph. Resilient modulus parameter  $k_3$  for unbound material types included in the model development database.**

Model prediction accuracy and reasonableness were evaluated by reviewing the plot of predicted and measured resilient modulus for all individual resilient modulus test values used in model development as presented in figure 107. Figure 108 presents a plot of measured and predicted resilient modulus versus bulk stress for all fine- and coarse-grained materials included in the model development database.

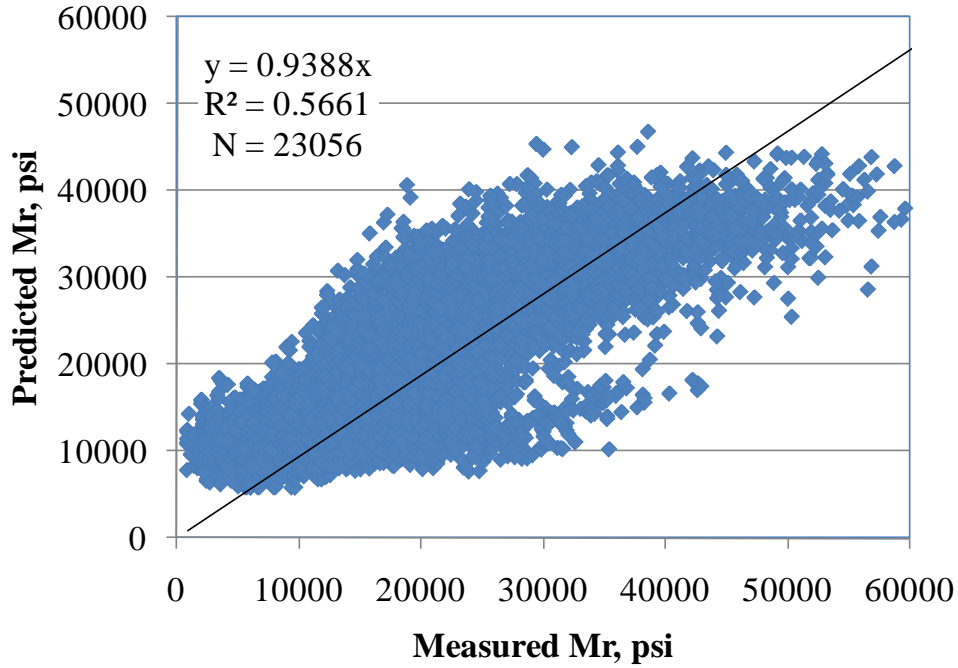


**Figure 107. Graph. Plot of measured versus predicted resilient modulus (using  $k_1$ ,  $k_2$ , and  $k_3$  derived from figure 101 through figure 103).**

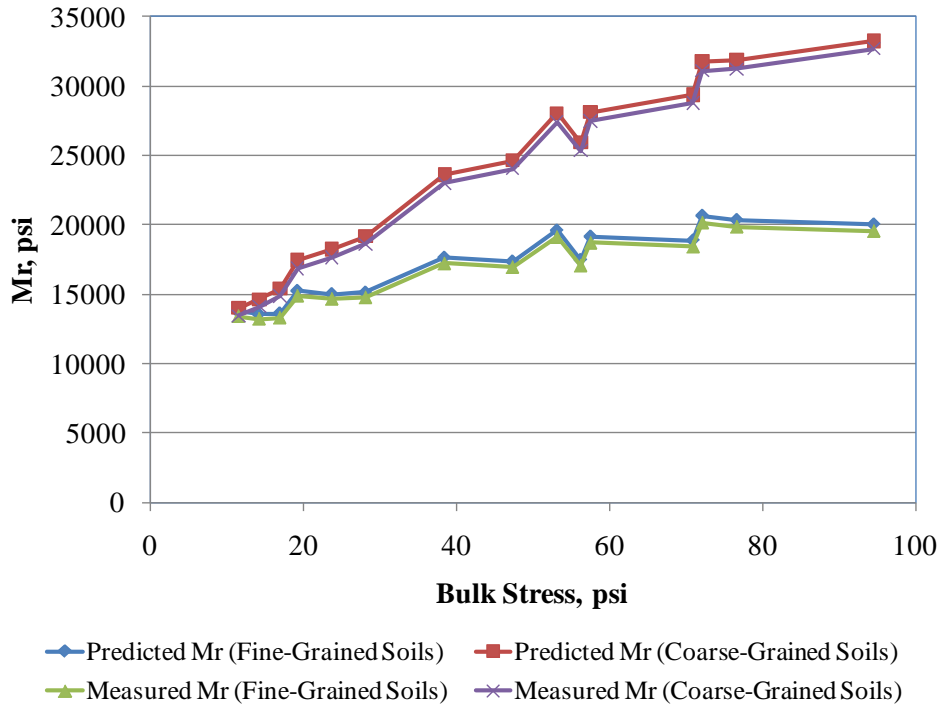


**Figure 108. Graph. Plot showing predicted and measured resilient modulus versus bulk stress for fine- and coarse-grained soils.**

Sensitivity analysis results are presented in figure 109 through figure 115. The results of the sensitivity analysis are summarized as follows:

- Increasing bulk stress results in significantly higher level of resilient modulus for coarse-grained materials. Soil type has a significant impact on predicted resilient modulus.
- Increasing the amount of finer materials results in a decrease in resilient modulus.
- Increasing the amount of gravel results in an increase in resilient modulus.
- Increasing effective size results in an increase in resilient modulus.
- Increasing optimum moisture content results in a decreased in resilient modulus.
- Increasing liquid limit results in an increase in resilient modulus.

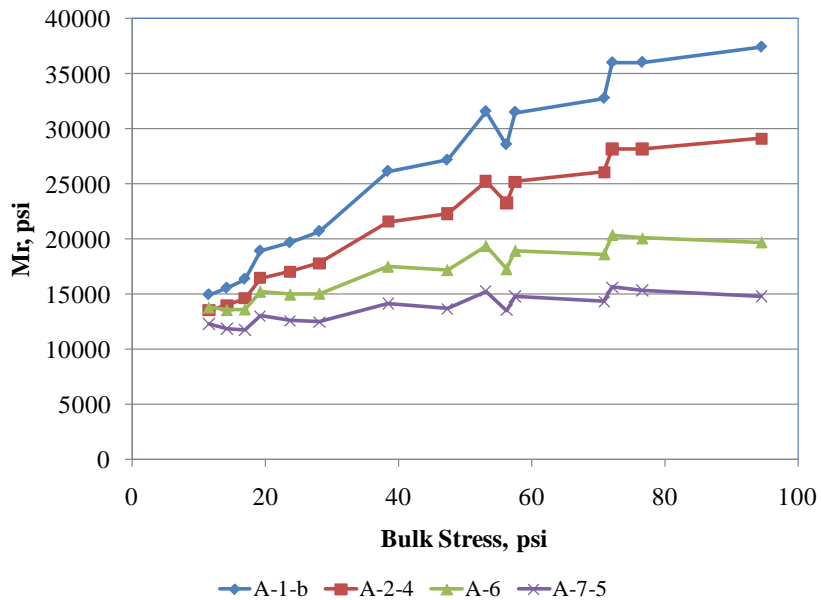


**Figure 109. Graph. Effect of material type (AASHTO soil class) on predicted resilient modulus.**

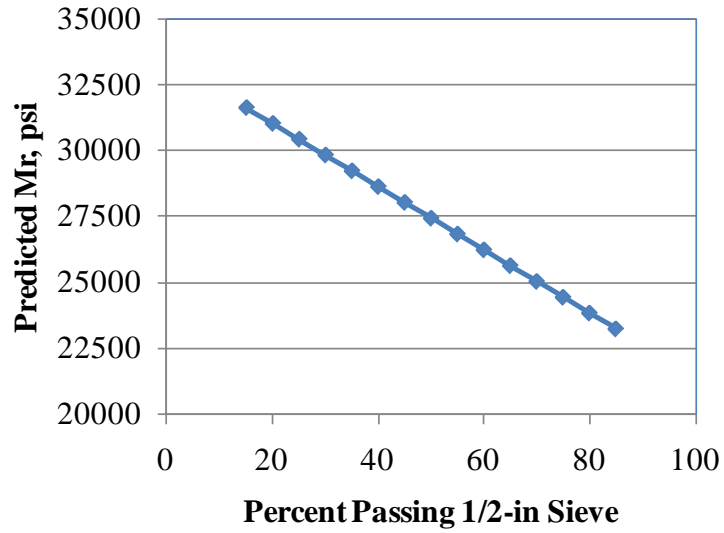


**Figure 110. Graph. Effect of percent passing 1/2-inch sieve on predicted resilient modulus.**

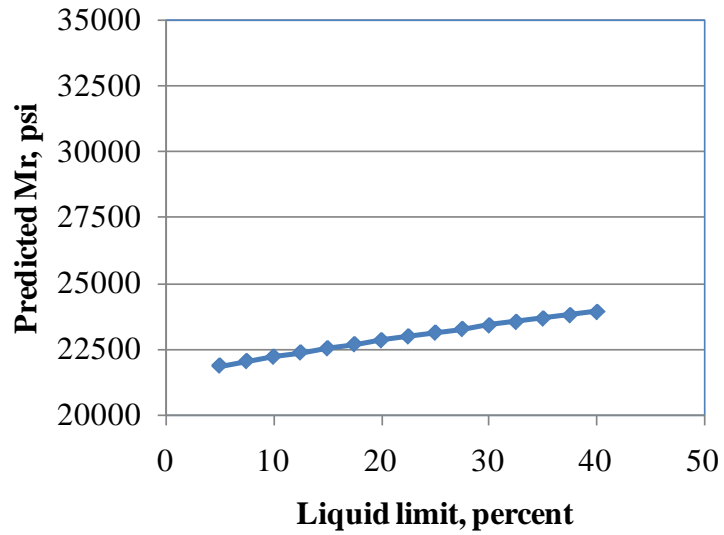


**Figure 111. Graph. Effect of liquid limit on predicted resilient modulus.**

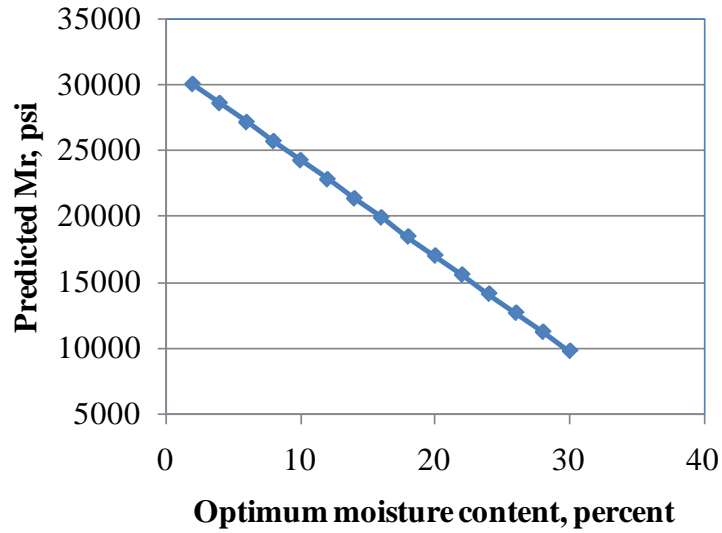


Figure 112. Graph. Effect of optimum moisture content on predicted resilient modulus.

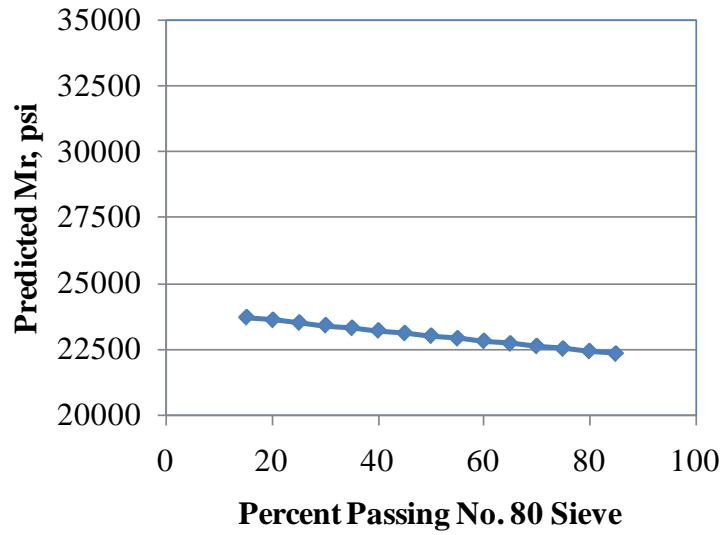
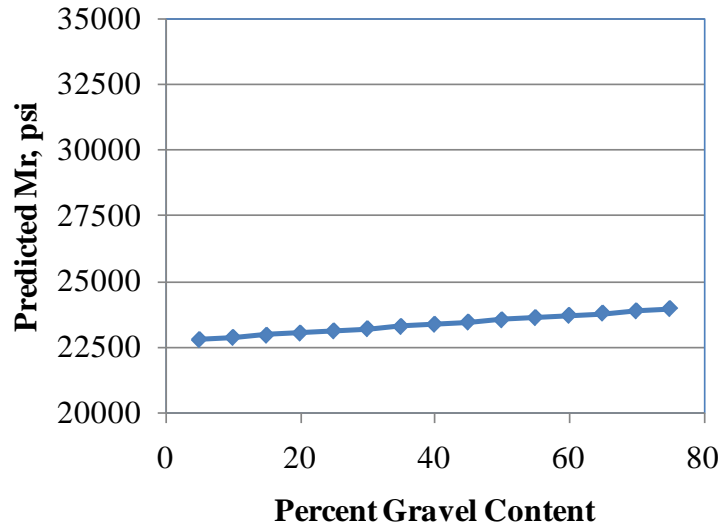
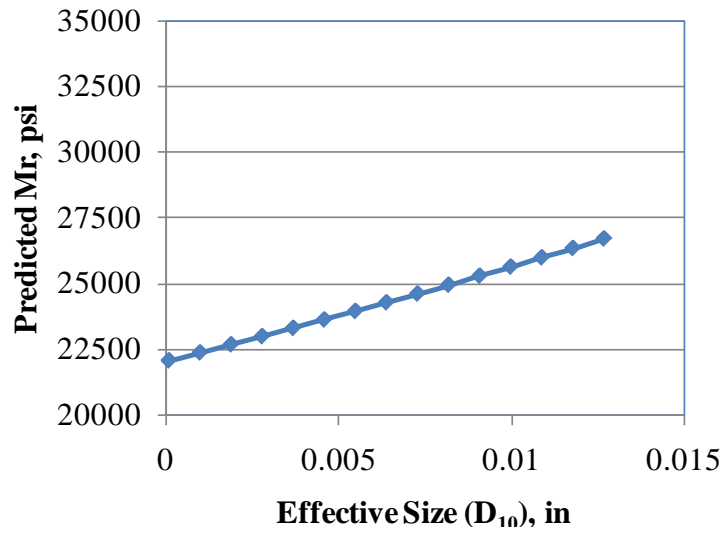


Figure 113. Graph. Effect of No. 80 sieve on predicted resilient modulus.



**Figure 114. Graph. Effect of gravel content on predicted resilient modulus.**



**Figure 115. Graph. Effect of effective size on predicted resilient modulus.**

## REFERENCES

1. American Association of State Highway and Transportation Officials. (2008). *Mechanistic-Empirical Pavement Design Guide, Interim Edition: A Manual of Practice*, American Association of State Highway and Transportation Officials, Washington, DC.
2. Turner-Fairbank Highway Research Center. *How to Get LTPP Data*, Federal Highway Administration, Washington, DC. Obtained from: <http://www.fhwa.dot.gov/research/tfhrc/programs/infrastructure/pavements/ltp/getdata.cfm>.
3. National Cooperative Highway Research Program. (2004). *Mechanistic-Empirical Pavement Design Guide*, NCHRP Project 1-37A, Transportation Research Board, Washington, DC. Obtained from: <http://www.trb.org/mepdg/guide.htm>. Site last accessed April 2010.
4. National Cooperative Highway Research Program. (2006). *Research Results Digest 308: Changes to the Mechanistic Empirical Pavement Design Guide Software Through Version 0.900*, NCHRP Project 1-40D, Transportation Research Board, Washington, DC.
5. National Cooperative Highway Research Program. (2009). *User Manual and Local Calibration Guide for the Mechanistic-Empirical Pavement Design Guide and Software*, Final Report, Project NCHRP 1-40B, Transportation Research Board, Washington, DC.
6. Irick, P.E., Seeds, S.B., Myers, M.G., and Moody, E.D. (1990). *Development of Performance-Related Specifications for Portland Cement Concrete Pavement Construction*, Final Report, Report No. FHWA-RD-89-211, Federal Highway Administration, Washington, DC.
7. Okamoto, P., Wu, C.L., Tarr, S.M., Darter, M.I., and Smith, K.D. (1993). *Performance Related Specifications for Concrete Pavements*, Report No. FHWA-RD-93-044, Federal Highway Administration, Washington, DC.
8. Hoerner, T.E., Darter, M.I., Khazanovich, L., Titus-Glover, L., and Smith, K.L. (2000). *Improved Prediction Models for PCC Pavement Performance-Related Specifications, Volume I: Final Report*, Report No. FHWA-RD-00-130, Federal Highway Administration, Washington, DC.
9. Rao, C., et al. (2012). *Estimation of Key PCC, Base, Subbase, and Pavement Engineering Properties from Routine Tests and Physical Characteristics*, Report No. HRT-12-030, Federal Highway Administration, Washington, DC.
10. Federal Highway Administration. (2009). *Long-Term Pavement Performance Program Standard Data Release 23.0*, VR2009.01, DVD Version, Federal Highway Administration, Washington, DC.
11. AASHTO TP 60. (2000). *Standard Test Method for the Coefficient of Thermal Expansion of Hydraulic Cement Concrete*, American Association of State Highway and Transportation Officials, Washington, DC.

12. Federal Highway Administration. (2010). *Long-Term Pavement Performance Program Standard Data Release 24.0*, VR2010.0, DVD Version, Federal Highway Administration, Washington, DC.



